Universidade do Algarve

Faculdade de Ciências e Tecnologia

Supramolecular biomimetic binding of the DNA-dye Hoechst 33258 by a synthetic macrocycle

Cátia Diana Parente Caldeira Carvalho

Biomedical Sciences Master

2010

Universidade do Algarve

Faculdade de Ciências e Tecnologia

Supramolecular biomimetic binding of the DNA-dye Hoechst 33258 by a synthetic macrocycle

Cátia Diana Parente Caldeira Carvalho

Dissertation guided by: Dr. Uwe Pischel and Dr. José Paulo da Silva

Biomedical Sciences Master

2010

If we knew what it was we were doing, it would not be called research, would it?

Albert Einstein

Acknowledgments

My deep appreciation goes to my thesis advisors Dr. Uwe Pischel and Dr. José Paulo da Silva for the constant help, guidance and the countless hours of attention devoted throughout the course of this work. Theirs priceless suggestions made this work interesting and learning for me. I am also very thankful to Dr. Werner Nau and Vanya Uzunova for their collaboration and contributions that were very helpful for the development of this study.

I am gratified to University of Huelva, University of Algarve, Jacobs University, and RISE for the facilities and financial support to this research work.

I am particularly thankful to Vânia Pais, Patricia Remón, and all my friends who helped during my study, contributing with good disposition and back up.

I wish to express my heartfelt gratitude to my family for their encouragement, constant prayers and continuous support. I owe a lot of thanks to my boyfriend for his extra patience, motivation and help in the preparation of this manuscript.

Abstract

The supramolecular interaction between the well-known DNA-binder Hoechst 33258 dye (guest) and cucurbit[7]uril (CB[7], host) was investigated in detail. The formation of the 1:1 complexes was verified by various methodologies such as Job's plot method and electrospray ionization mass spectrometry. The binding is characterized by a high association constant, $K = 3.5 \times 10^6$ M^{-1}, which was determined by UV-Vis and fluorescence titrations. The formation of supramolecular 1:1 complexes is accompanied by drastic changes in the fluorescence quantum yield (Φ_f) of the dye. While the free dye is barely fluorescent in water at pH 7 ($\Phi_f = 0.01$), the emission is considerably increased in the host-guest assembly ($\Phi_f = 0.74$). The binding characteristics at pH 4.5 are similar to the ones at pH 7. However, the fluorescence enhancement at the former pH is less dramatic, because the free dye has here already its highest emission ($\Phi_f = 0.29$). Proton magnetic resonance spectroscopy clearly demonstrated that CB[7] is accommodated around the piperazine-benzimidazole unit. A mechanism that explains this peculiar fluorescence behavior, which involves intramolecular proton transfer and charge transfer, internal rotation of the free and complexed dye is proposed.

The competitive binding to CB[7] of several polyamines (putrescine, cadaverine, spermidine, spermine, and histamine) towards Hoechst 33258 was evaluated as well. For some of these polyamines the CB[7] binding constant has been determined the first time to the best of my knowledge.

Finally, the well-characterized binding of the dye with calf-thymus DNA was used in competition experiments. It was found that the known unspecific binding of the dye to DNA leads to strong fluorescence quenching, which becomes appreciable through the initially high fluorescence of the dye in its CB[7] complex. Hence, the strongly emissive Hoechst 33258/CB[7] platform may be further used for the characterization of unspecific DNA binding through fluorescence.

Resumo

Os cucurbit[*n*]urilos são uma família de compostos macrocíclicos obtidos apenas por síntese e constituídos por *n* unidades glicolurílicas. Possuem uma estrutura simétrica em forma de barril, com uma cavidade central hidrofóbica e dois anéis de grupos carbonilo orientados para fora da cavidade, formando dois portais idênticos. Esta estrutura permite-lhes formar complexos de inclusão com diferentes moléculas e com constantes de acoplamento várias ordens de grandeza superiores às encontradas para as correspondentes ciclodextrinas. As espécies alojadas na cavidade destes macrociclos ficam relativamente imobilizadas e têm uma interacção com o solvente bastante diminuída ou mesmo nula. É possível assim avaliar o efeito do solvente e também da liberdade rotacional nas propriedades das moléculas que formam complexos de inclusão. Uma das propriedades mais interessantes é a fluorescência, que normalmente aumenta com a inclusão, o que constitui um melhoramento muito importante para moléculas que se pretendam utilizar como sondas. Esta melhoria permite novas abordagens experimentais que envolvam, por exemplo, a utilização de interruptores moléculares para medir actividades enzimáticas ou novas formas de proteger o ADN, através da formação de complexos ternários com intercaladores de ADN. Neste contexto, um candidato muito interessante é o Hoechst 33258, um conhecido corante luminescente do núcleo de células. Esta molécula intercala-se normalmente numa região rica em adeninas e timinas do sulco menor do ADN, emitindo com um elevado rendimento quântico de fluorescência. Assim, o estudo da interacção supramolecular entre o corante Hoechst 33258 e os cucurbit[*n*]urilos pode ser muito importante para o desenvolvimento de um novo par macrociclo/corante com potencialidades como interruptor molécular e que poderá ser uma ferramenta extremamente útil para a investigação da interacção entre o corante e ADN, que não está totalmente esclarecida.

Dadas as potencialidades destes sistemas, definiu-se como primeiro objectivo deste trabalho o estudo da interacção supramolecular entre o corante Hoechst 33258 e o macrociclo cucurbit[7]urilo (CB[7]). A formação do complexo de inclusão corante/CB[7] levou a uma modulação de propriedades fotofísicas do Hoechst 33258, tais como a absorção UV-Vis e a fluorescência. Estas modulações permitiram a determinação das constantes de associação e das estequiometrias do complexo, assim como a total caracterização dos efeitos solvatocrómicos, das diferenças dos rendimentos

quânticos de fluorescência e tempos de vida, e da dependência do pH no processo de inclusão. De forma a complementar o trabalho, realizaram-se estudos de espectrometria de massa com ionização por electrospray e também ensaios de espectroscopia de ressonância magnética de protões.

Uma vez caracterizado o complexo supramolecular Hoechst 33258/CB[7], e utilizando o seu potencial como interruptor molecular (diminuição da fluorescência, *switch-off*), realizaram-se ensaios de competição com poliaminas biológicas e ADN do timo de borrego. As poliaminas (putrescina, cadaverina, espermidina, espermina e histamina) são competidores do corante pela ligação ao CB[7], o que permitiu a determinação de constantes de associação entre as diversas poliaminas e o macrociclo e também avaliar o mecanismo inerente da selectividade do CB[7] para cada uma delas.

O ADN é um competidor do macrociclo pela ligação ao corante, o que permitiu estabelecer o complexo Hoechst 33258/CB[7] como uma ferramenta na investigação da ligação entre o corante e o ADN. Os ensaios de competição foram efectuados por estudos de espectroscopia de absorção UV-Vis e fluorescência, bem como por estudos de dicroísmo circular.

Verificou-se a formação de complexos de inclusão entre o CB[7] e o Hoechst 33258 com estequiometria 1:1. A formação de complexos de inclusão 1:1 (estequiometria) foi determinada pelo método de variação contínua ("Job's plot") e também por espectrometria de massa com ionização por electrospray. A ligação é caracterizada por uma constante de associação elevada, $K = 3{,}5 \times 10^6\ M^{-1}$, obtida por titulação de absorção UV-Vis e também de fluorescência.

A complexação é acompanhada por mudanças drásticas no rendimento quântico de fluorescência (Φ_f) do corante. A pH 7 o corante praticamente não apresenta fluorescência quando livre em solução aquosa ($\Phi_f = 0{,}01$), enquanto que incluído em CB[7] o rendimento quântico aumenta para 0.74. No entanto, a pH 4,5, verifica-se um aumento de fluorescência menos acentuado ($\Phi_f = 0{,}29$), devido ao maior potencial do Hoechst 33258 para emitir a este pH. As restantes propriedades da interacção a pH 4,5 são semelhantes às verificadas a pH 7.

Através dos ensaios de espectroscopia de ressonância magnética de protões demonstrou-se que o CB[7] fica alojado entre a unidade piperazina e o benzimidazole1 do corante. É

apresentado e discutido neste trabalho um mencanismo envolvendo transferência intramolecular de protões, transferência de carga e rotação interna para explicar o peculiar comportamento da fluorescência do corante, nas diferentes situações estudadas.

A competição das poliaminas biológicas com o Hoechst 33258 pela ligação ao CB[7] foi estudada a partir da diminuição da fluorescência (*switch-off*) após sucessivas adições de poliamina. A poliamina que apresenta maior constante de associação é a espermina, $K = 2{,}6 \times 10^7\ M^{-1}$, seguida da cadaverina, $K = 2{,}0 \times 10^7\ M^{-1}$, da espermidina, $K = 1{,}2 \times 10^6\ M^{-1}$, da putrescina, $K = 1{,}1 \times 10^5\ M^{-1}$ e da histamina, $K = 1{,}7 \times 10^4\ M^{-1}$. As constantes obtidas para a espermidina e a espermina foram determinados pela primeira vez. As afinidades das diferentes poliaminas para o CB[7] variam com a quantidade de carbonos lineares entre os grupos amina da molécula, com o número de grupos amina e com a afinidade destes para os portais do macrociclo.

A partir dos ensaios de dicroísmo circular e da competição entre o CB[7] e ADN pelo Hoechst 33258, confirmou-se a existência de dois tipos de ligação ligação entre o corante e o ADN que dependem da razão de concentrações das duas espécies. A baixas concentrações de corante, o tipo de ligação é específico e envolve a região rica em adeninas e timinas do sulco menor do ADN ($\Phi_f = 0{,}62$); a concentrações mais elevadas há ligação não específica, o que causa na supressão da fluorescência. Esta forte supressão da fluorescência torna-se bastante evidente por comparação com a elevada fluorescência inicial associada à formação do complexo. Assim, o complexo supramolecular Hoechst 33258/CB[7], fortemente emissivo, pode servir de plataforma para a caracterização da fluorescência da ligação não específica ao ADN.

A realização deste trabalho vau permitir o desenvolvimento futuro de novas aplicações e metodologias para o complexo supramolecular Hoechst 33258/CB[7].

Keywords / Palavras chave

Supramolecular Chemistry / Química Supramolécular

Fluorescence / Fluorescência

Cucurbit[*n*]urils / Cucurbit[*n*]urilos

Minor groove binder / Ligante do sulco menor de ADN

Hoechst 33258 / Hoechst 33258

Polyamines / Poliaminas

Abbreviations

A – Adenine;

C – Cytosine;

CB[*n*] – Cucurbit[*n*]urils;

CD - Circular dichroism;

CT - Calf thymus;

ESP - Electrostatic surface potential

G – Guanine;

H33258 - Hoechst 33258 - 2'-(4-Hydroxyphenyl)-5-(4-methyl-1-piperazinyl)-2,5'-bi-1H-benzimidazole;

HCT - Ultra high capacity trap;

ICD - Induced circular dichroism;

I_f - Fluorescence intensity;

IRF - Instrumental response function;

IUPAC – International union of pure and applied chemistry;

K - Binding constant;

k_r - Radiative decay rate;

k_{nr} - Nonradiative decay rate;

NMR - Nuclear magnetic resonance;

PAs – Polyamines;

pK_a - Acid dissociation constant;

S – Solubility;

TCSPC - Time-correlated single-photon-counting;

T – Thymine;

ε – Molar extinction coefficient;

λ_{exc} - Excitation wavelength;

λ_{obs} – Observation wavelength;

λ_{abs} – Absorption wavelength;

λ_{f} – Fluorescence wavelength;

τ_{f} - Fluorescence lifetime;

Φ_{f} - Fluorescence quantum yield;

Contents

I – Introduction

I.1 – Cucurbit[*n*]urils

Cucurbit[*n*]urils (CB[*n*], Figure 1) are a recently rediscovered family of macrocyclic compounds readily assembled by an acid-catalyzed condensation reaction of urea and glyoxal, forming glycoluril and polymeric analogues in the presence of excess formaldehyde, comprising *n* glycoluril units. Although the synthesis of cucurbit[6]uril (CB[6]) was first reported by Behrend *et al*. in 1905 (Behrend's polymer), its chemical nature and structure had been unknown until 1981, when Mock and co-workers reinvestigated the report and disclosed the remarkable macrocyclic structure naming it cucurbituril. The name is attributed to the resemblance with the most prominent member of the *cucurbitaceae* family, the pumpkin.[1-6]

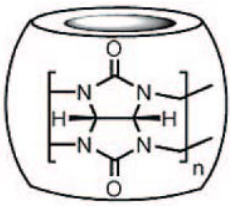

Figure 1 – Representation of the CB[*n*] structure. *Adapted from* [7]

According to IUPAC nomenclature, the systematic name of CB[6] is dodecahydro-1H, 4H, 14H, 17H-2, 16:3, 15-dimethano-5H, 6H, 7H, 8H, 9H, 10H, 11H, 12H, 13H, 18H, 19H,20H, 21H, 22H, 23H, 24H, 25H, 26H-2, 3, 4a, 5a, 6a, 7a, 8a, 9a, 10a, 11a, 12a, 13a, 15, 16, 17a, 18a, 19a, 20a, 21a, 22a, 23a, 24a, 25a, 26a-tetracosaazabispentaleno[1''', 6''':5'', 6'', 7'']cycloocty[1'', 2'', 3'':3',4']pentaleno (1', 6':5, 6, 7) -cycloocta (1, 2, 3-gh:1', 2', 3'-g'h') cycloocta (1, 2, 3-cd:5, 6, 7-c'd') dipentalene-1, 4,6, 8, 10, 12, 14, 17, 19, 21, 23, 25-dodecone. Cucurbit[6]uril (CB[6]) is considerably easier to remember.

In the turn of the millennium, the Kim, Day, and Nau research groups reported the discovery of other members of the CB[*n*] family (*n* = 5-10) and successful isolation of CB[*n*] (*n* = 5, 7, 8 and 10•5), see Figure 2, which has broadened the scope of CB[*n*] chemistry enormously.[3,5,8-10]

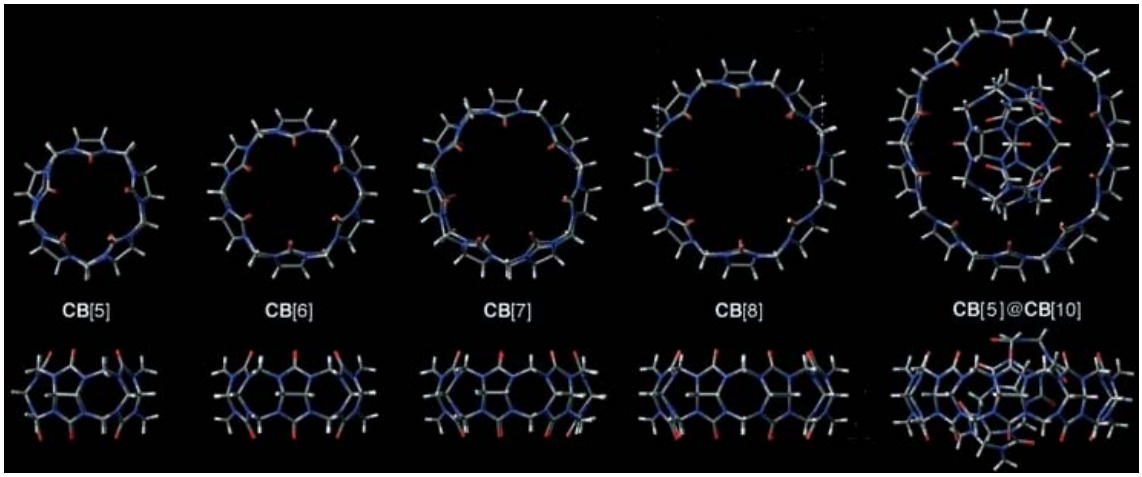

Figure 2 – Top and side views of the X-ray crystal structures of CB[*n*] (*n* = 5-8 and 10•5). The various compounds are drawn to scale. Color codes: carbon, grey; nitrogen, blue; oxygen, red. *Adapted from* [5]

I.1.1 – Fundamental properties

Cucurbit[*n*]urils are highly symmetrical and rigid macrocycles with a central hydrophobic cavity and two identical carbonyl-laced portals. While the hydrophobic interior is a potential inclusion site for several nonpolar molecules, the polar ureido carbonyl groups at the portals allow the binding of ions and molecules through charge-dipole and hydrogen bonding interactions. The electrostatic potential (ESP) map of CB[*n*] reveals that the regions around carbonyl oxygens and inner surface of the cavity are negatively charged, and at the same time the outer surface is somewhat positive, as shown in Figure 3. As a result, CB[*n*] ($pK_a \approx 3.02$) become protonated in strongly acidic media, and are capable of coordination to metal ions and other positively charged species. Nonetheless, a delicate match between the hydrophobicity, charge, shape, and size of the guest and the host is crucial for the formation of a stable inclusion complex.[3,4,11,12]

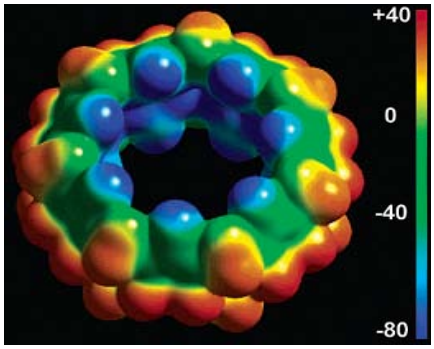

Figure 3 – Electrostatic surface potential map of CB[7]. Significantly negative ESP (blue colored) in the regions around the carbonyl groups at the portal; the inner surface of the cavity is also quite negative, while the outer surface is somewhat positively charged. *Adapted from* [6]

The various CB[*n*] have a common depth of 9.1 Å, and the portals guarding the entry are approximately 2 Å narrower than the cavity itself, which results in constrictive binding that produces significant steric barriers for guest association and dissociation. Depending on the number of glycoluril units of the CB[*n*] homologues, on going from CB[5] to CB[10], the outer diameter, internal cavity, volume, and the molecular weight increases progressively (Table 1).[4,5,13]

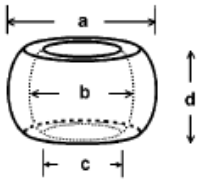

Table 1 – Dimensions and physical properties of CB[*n*].[5,14-16]

		CB[5]	CB[6]	CB[7]	CB[8]	CB[10][b]
Outer diameter (Å)	**a**[a]	13.1	14.4	16.0	17.5	-
Cavity (Å)	**b**[a]	4.4	5.8	7.3	8.8	~11.7
	c[a]	2.4	3.9	5.4	6.9	~10.0
Height (Å)	**d**[a]	9.1	9.1	9.1	9.1	9.1
Cavity volume (Å^3)		82	164	279	479	870
MW		830	996	1163	1329	1661
S_{H2O} [mM]		20-30	0.018	20-30	<0.01	-
S_{acids} [mM]		60 (HCl 3M)	61 (1:1 HCO_2H/H_2O)	700 (HCl 3M)	1.5 (HCl 3M)	-
Stability [ºC]		>420	425	370	>420	-

[a] The values quoted for a, b, c and d for CB[*n*] take into account the van der Waals radii of the relevant atoms.
[b] Determined from the X-ray structure of the CB[5]@CB[10] complex.

The solubility of CB[*n*] in common solvents constitutes a potential limitation. Particularly, CB[6] and CB[8] are essentially insoluble ($<10^{-5}$ M) in water, whereas CB[5] and CB[7] have a modest, but appreciable solubility (~ $2\text{-}3\text{x}10^{-2}$ M) in water. On the other hand, the solubility of this family increases dramatically in concentrated aqueous acid solutions. *In vitro* tests revealed that most CB[*n*] are non-toxic.[3,5,6]

One of the outstanding features of the CB[*n*] family is the high thermal stability. No decomposition is observed up to 420 ºC for CB[*n*] (*n* = 5, 6, and 8), although CB[7] starts decomposing at a lower temperature (370 ºC).[3,5,6]

The stability of CB[*n*] can be estimated from the relative strain energy upon cyclization (Table 2). The most stable CB[*n*] (*n* = 4-12) is CB[6], closely followed by CB[7] with a relative strain energy of *ca.* 1 kcal/mol.[6]

Table 2 – Relative Strain Energies of CB[*n*].

	CB[4]	CB[5]	CB[6]	CB[7]	CB[8]	CB[9]	CB[10]	CB[11]	CB[12]
ΔE (kcal/mol)	23.03	5.06	0	1.14	5.86	12.87	21.41	31.03	41.43

Although CB[*n*] are commonly regarded as being rigid hosts, they are subjected to deformation in the transition states during ingression and egression of the guests. Overall, the binding ability of cucurbit[*n*]urils generally equals or exceeds that of well-known host molecules such as cyclodextrins and crown ethers.[5,17]

I.1.2 – Applications

Cucurbit[*n*]urils have a high hydrogen-bonding and ion-dipole interaction ability at the portals and a hydrophobic interior. This and the fact that they have variable cavity and portal sizes leads to remarkable molecular recognition properties (Figure 4). These distinct binding and restriction environments have profound implications in the formation of stable host-guest complexes, offering inumerous applications in many different areas.[3-5,18]

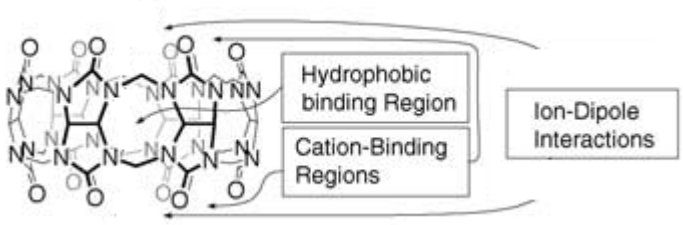

Figure 4 – Representation of the different binding regions of CB[6]. *Adapted from* [5]

Based on the crystallographic data, Blatov and coworkers recently developed a computational technique that identifies suitable guests for each member of the CB[*n*] family, taking into account not only the charge, but also the size and shape of the guest.[19]

Meanwhile, the studies related to redox control of guest binding,[5,14] stabilization of charge-transfer complexes inside the host cavity,[4,14] inclusion of two identical or different guest molecules,[20,21] inclusion of macrocyclic guests,[22] encapsulation of drug molecules,[6] formation of redox-controllable vesicles,[23] control of chemical reactions inside the host cavity,[24] CB[7] as an hydrogel,[25] and so on, allowed numerous applications such as:

- Recognition and separation: the ability of certain CB[*n*] to effectively remove heavy metals (chromates and dichromate), aromatic substances, acid dyes, and reactive dyes from textile waste streams, being able to function as pollutants sequestering agent.[26-28]

- Improvement of dye properties: complexation of dyes with CB[*n*] can not only dramatically improve their fluorescence intensity but also prevent its aggregation in solutions, and reduce surface adsorption and photobleaching, which can be applied in biological imaging and screening.[12,29]

- Catalysis: the unique structure of CB[*n*] is ideal to promote and accelerate some chemical reactions in their cavities, mimicking some enzyme-substrate interactions, a broad new field in catalysis.[17,30,31]

- DNA binding and gene transfection: it is known that CB[*n*] can encapsulate some DNA intercalators, mixing with DNA could yield a ternary complex

(DNA•CB[*n*]•DNA-intercalator molecule) that partially protects supercoiled DNA against cleavage by restriction enzymes. Another surprising feature of CB[*n*] is that through complexation with specific molecules it can function as a gene-delivery carrier as demonstrated by Kim and coworkers.[32,33]

- Controlled drug delivery: CB[7] is a viable host for drugs. The high stability of some complexes suggests the potential use of CB[7] in controlled drug release, mainly applied in the treatment of cancer.[6,34,35]

- Molecular switches, logic devices, and machines: External stimuli-dependent host-guest behavior of CB[*n*] has provided operating principles of molecular switches, logic devices, and machines.

  Some complex pairs between a dye and CB[*n*] can be followed by a binary fluorescence response (switch-on or switch-off type) becoming a molecular switch. One interesting application for these molecular switches is the ability to follow enzymatic reactions through the appearance of the product or disappearance of the substrate (Figure 5).[36-38]

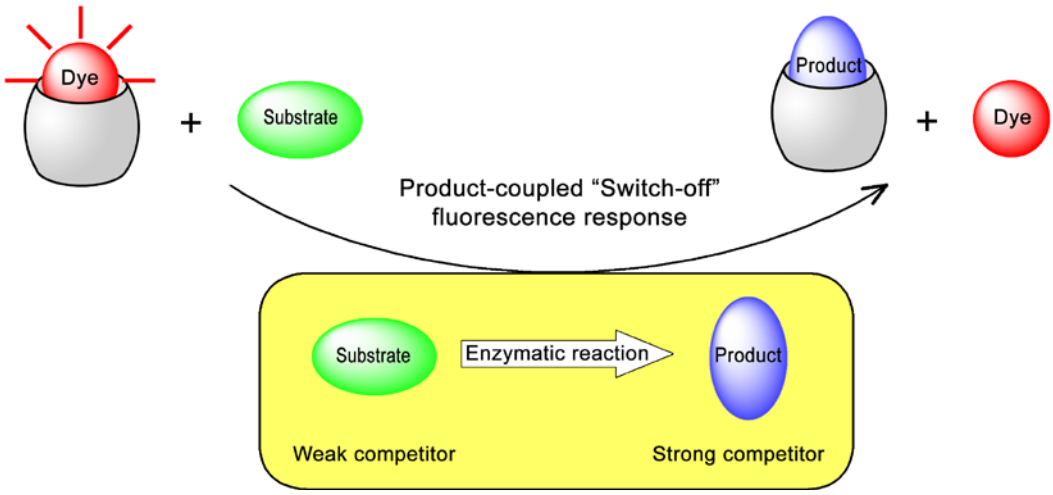

Figure 5 – Illustration of a switch-off fluorescence response of a macrocycle-dye pair in the course of an enzymatic reaction. *Adapted from* [39]

Molecular logic devices based in variations of fluorescence are of interest for further miniaturization in information technology, and the complexation of a molecule with cucurbit[*n*]turils allows the realization of logic functions that may overcome problems with silicon-circuitry based on electrical signals.[40,41]

Self-assembly of photoswitchable molecular machines based on cucurbit[*n*]urils, such as pseudorotaxane complexes, are promising prototypes for a variety of molecular machines because of their ability to undergo controlled motions in response to external stimuli.[42,43]

The CB[*n*] family is the first class of synthetic hosts with sufficient affinity and selectivity to serve as components of complex self-sorting systems that mimic partially the complexity seen in natural systems.[20]

Despite the amazing properties of CB[*n*], their applications are still limited due to the poor solubility. One way to solve this problem is introducing functional groups on their surfaces, which has been quite challenging. Functionalized cucurbit[*n*]urils have allowed further new applications for these macrocyclic hosts, such as formation of vesicles, and 2D polymers, immobilization of CB[*n*] on solid surfaces, CB[*n*]-anchored silica gel for chromatography, ion selective electrodes, new scaffold for antibiotics, and ion channels. [3]

I.1.3 - Supramolecular photochemistry

The incorporation of a fluorescence molecule into a cucurbituril host can alter the radiative properties of the included guest. Wagner and coworkers were the first to report fluorescence enhancement phenomena upon complexation by cucurbit[*n*]urils.[44-46] However, the broad field of photophysical engineering of dye properties upon inclusion in CB[*n*] was opened by Nau *et al*.[29] The possibility to form complexes with chromophoric guests and thereby improve their fluorescence properties is of much interest. The changes verified in the inclusion complexes are due to polarity effects (positioning of the fluorophore into the more hydrophobic and nonpolar environment of the host cavity), polarizability inside CB[*n*], and confinement effects (geometrical

confinement of the chromophore within the host), that lead to a decrease in nonradiative decay rates. The most characteristic consequence of the low polarizability experienced by guest molecules encapsulated inside cucurbit[*n*]urils is the lower radiative decay rate ($k_r = \Phi_f / \tau_f$). In other words, the fluorescence of dyes is emitted "slower" from CB[*n*] (increased τ_f). The cavity of cucurbit[*n*]urils can also efficiently suppress photochemical reactions of fluorescent dyes and therefore protect the guest against photodecomposition, resulting in an improved photostability. In addition, encapsulation by CB[*n*] should also enhance the chemical stability of chromophores that are sensitive to oxidation or hydrolysis. These properties combined with the suppression of dye adsorption and aggregation turn out to be useful for the production of fluorescent dye solutions of unprecedented storage capacity and working stability.[12]

Complexation within CB[*n*] may also have the potential to increase the solubility of insoluble or poorly water-soluble guest molecules. These host molecules also reduce or completely suppress the fluorescence quenching of dyes by external additives, because they provide a protective shield.[12]

Fluorescent dyes encapsulated in cucurbit[*n*]urils have a higher propensity to become protonated than the free dyes in aqueous solution (host-assisted guest protonation). The protonation can be spectroscopically followed by pH-dependent changes of the UV-Vis absorption or fluorescence spectra of complexed and uncomplexed dyes.[12]

For the development of this project it was desired to "tune" the fluorescence properties of an organic fluorescent dye (Hoechst 33258) in aqueous solution, using CB[7] as a host. CB[7] is the most attractive host, because it fulfills the requirement of sufficient water solubility and has a favorable size to form 1:1 complexes with a wide range of organic guest molecules.

I.2 – The Hoechst 33258 Dye

I.2.1 – General remarks

2'-(4-Hydroxyphenyl)-5-(4-methyl-1-piperazinyl)-2,5'-bi-1H-benzimidazole, usually named Hoechst 33258 (H33258) is a heterocyclic compound containing two benzimidazole rings along with a phenol and a piperazine moiety as terminal units (Figure 6). This synthetic ligand can have more than one conformer in solution due to various rotation sites along the benzimidazole axis.[47-49]

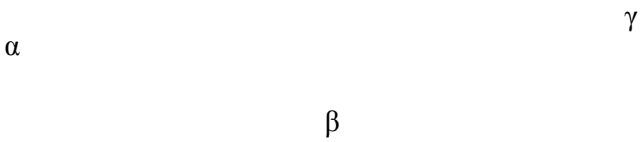

Figure 6 – Molecular structure of H33258. The dye is composed of four structural units: a piperazine ring, two benzimidazole rings (bz1 and bz2), and a phenol ring. The inter ring torsional angles are indicated by α, β, and γ.

H33258 is commercially available and water-soluble, widely used as a luminescent probe. It is relatively non toxic, has membrane permeability, and contains several proton donating and accepting groups, which take part in its protonation equilibria.[48-50]

I.2.2 – Photophysical properties

The photophysical properties of H33258 are much dependent on the protonation state of the dye. Therefore the different protonated forms will be discussed first in this

subchapter. Surprisingly, the protonation states of H33258 dye in aqueous solution are relatively few understood. The reported pK_a values of the dye are approximately 3.5 (nitrogen atom of the bz2 ring), 5.5 (nitrogen atom of the bz1 ring), 8.5 (hydroxyl group of the phenol ring) and 9.8 (aliphatic nitrogen atom of the piperazine ring). In Figure 7 the resulting distribution of H33258 according to its different protonation states as a function of pH is represented.[47,49,51,52]

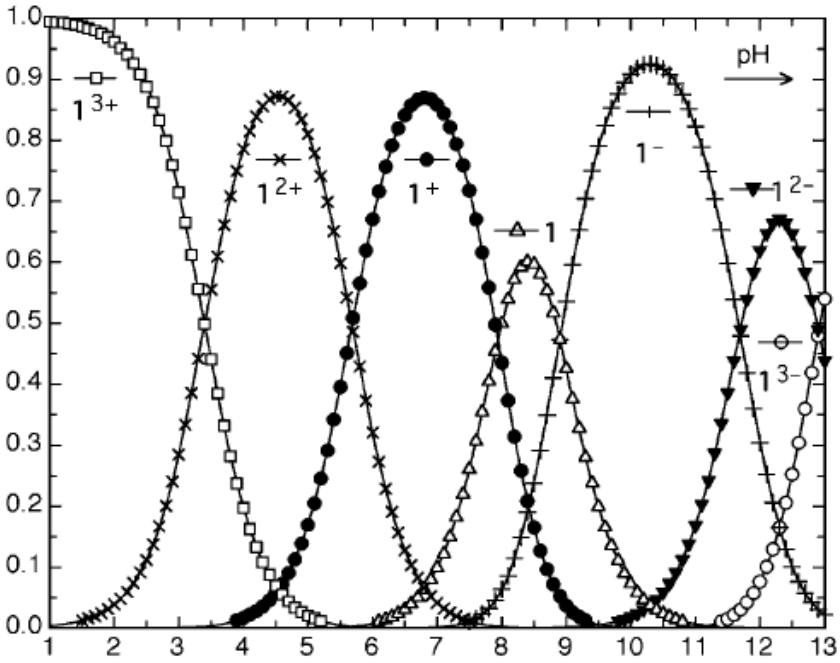

Figure 7 – Distribution of H33258 dye species (represented as 1). The total concentration is arbitrarily set to 1M.[49]

At most pH, several forms of protonated H33258 dye coexist. However, at pH 4.5 the diprotonated form is prevalent (> 90% of all species) and at pH 7 mainly monoprotonated dye is observed. These two pH values have been also considered in this work, in order to facilitate according interpretations of the photophysical properties of the dye.

At pH values below 2 the triple protonated dye prevails. The tetraprotonated dye only exists at pH < 0. The mono-, double and triple deprotonated dye forms are existent at basic pH.[49]

The unprotonated dye has its distribution peak at *ca.* pH 8.5. In Scheme 1 the related equilibria and the respective protonation/deprotonation sites are summarized.

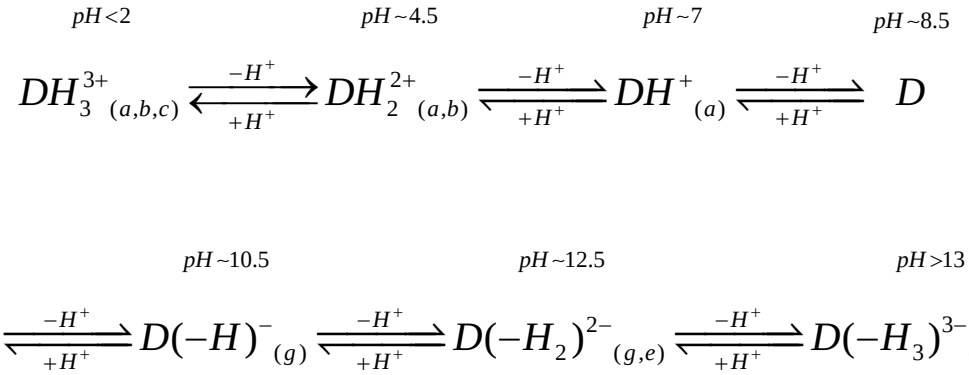

Scheme 1 - Protonation equilibria of H33258, where D represents the dye.

The H33258 dye exhibits a relatively large Stokes shifts (excitation/emission *ca.* 340/460 nm, see Table 3) that is probably due to excited state intramolecular proton or charge transfer. Therefore the Stokes shifts depends on the polarity of the medium (increases with an increase of polarity), but is largely unaffected by the ionic strength (NaCl, 1-6 M) of the solution.[48,51,53]

The fluorescence spectrum of H33258 dye varies with the pH and the solvent (Figure 8 and Table 3). For instance, comparing with the fluorescence intensity in water at pH 6.86 it increases about 70 times when 2-propanol is the solvent.[51] A different case is when it is in water at pH 4.0; the fluorescence band shifts to a longer wavelength and

the intensity increases considerably. The fluorescence quantum yields at different pH are also summarized in Table 3.[48,53-55]

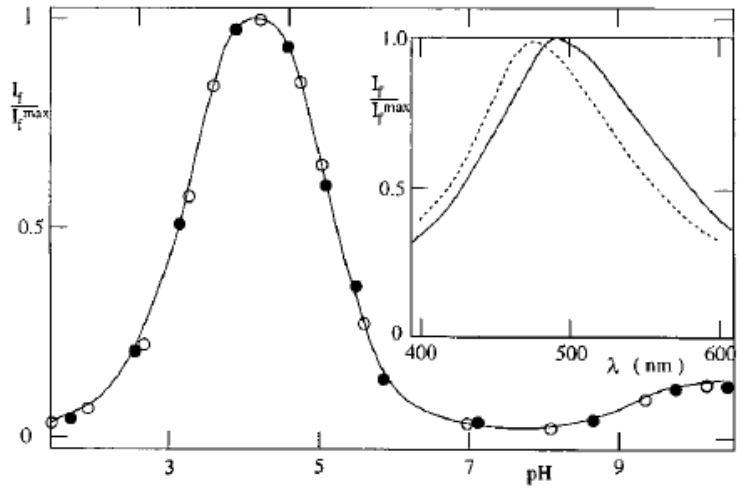

Figure 8 – Effect of pH on the fluorescence intensity (I_f) for the H33258 dye in aqueous solution at 25 ºC, λ_{exc} = 300 nm and λ_f = 480-520 nm. Inset: fluorescence spectra of the dye in aqueous solution at pH 7 (full) and in ethanol (dotted).[53]

Table 3 – Absorption and fluorescence maxima and quantum yield of fluorescence. *Adapted from [53]*

Medium	λ_{abs} **(nm)**	λ_f **(nm)**	Φ_f
DMF	344	480	0.4
Ethanol	340	475	0.5
Water (pH 2)	344	485	0.05
Water (pH 4)	340	485	0.4
Water (pH 7)	337	490	0.02
Water (pH 10)	348	485	0.03

The absorption spectra of H33258 dye also depend on the medium and pH (Figure 9).[51,53]

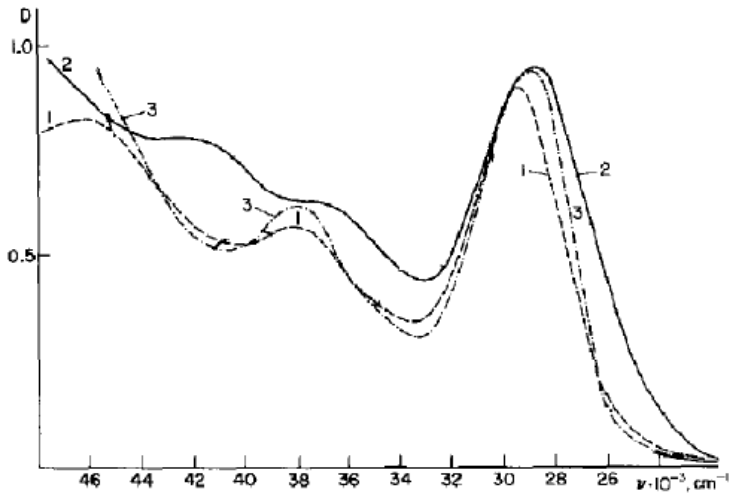

Figure 9 – Absorption spectra of H33258 dye. 1 - buffer at pH 6.86; 2 - buffer at pH 4.0; 3 - 2-propanol. *Adapted from* [51]

The concentration of the dye may contribute to the bandwidth of the absorption spectra, *i.e.* dimerization (aggregation) could play a role at higher dye concentrations.[53] In fact, several authors refer that H33258 self-aggregates but do not reveal clearly the critical concentration for this process. The extinction coefficient value of H33258 dye in aqueous solution at pH 7 is (4.1-4.2) x 10^4 M^{-1} cm^{-1} at 338 nm, and also varies with pH, being *ca.* 15% higher at pH 3 or 10.[52,53,56,57]

The H33258 dye shows a biexponential decay in aqueous solution, which was explained by an intramolecular proton transfer in the excited state or by the planar and non-planar structures that H33258 can have, [48,54] because fluorescence excited state lifetimes are very sensitive to the structure and dynamics of the fluorescent molecule.[48,54,58] With this, the dye has two fluorescence lifetimes at pH *ca.* 7, τ_1 = 0.3 ns and τ_2 3.6 ns. The relative contributions from these components were 60% and 40% respectively. On the other hand, at pH 4.5 the fluorescence lifetime is 3.54 ns.[58,59] However, aggregation may be another and simpler explanation for the short lifetime component.[60]

I.2.3 – Interaction with DNA

The H33258 dye is a well-known DNA-binding ligand with high affinity for B-DNA sequences containing solely adenine (A) and thymine (T) base pairs. Employing an array of different methods (optical spectrometry, footprinting studies, kinetics studies of the DNA-binding process, X-ray diffraction studies in single crystals, ^{1}H-NMR spectroscopy, and theoretical modelling), it was discovered that H33258 binds to the minor groove of DNA, covering about four repeated AT units and forming intermolecular H bonds between thymidine O atoms and the imido H atoms of both benzimidazole moieties (Figure 10).[48,55,57,61-88]

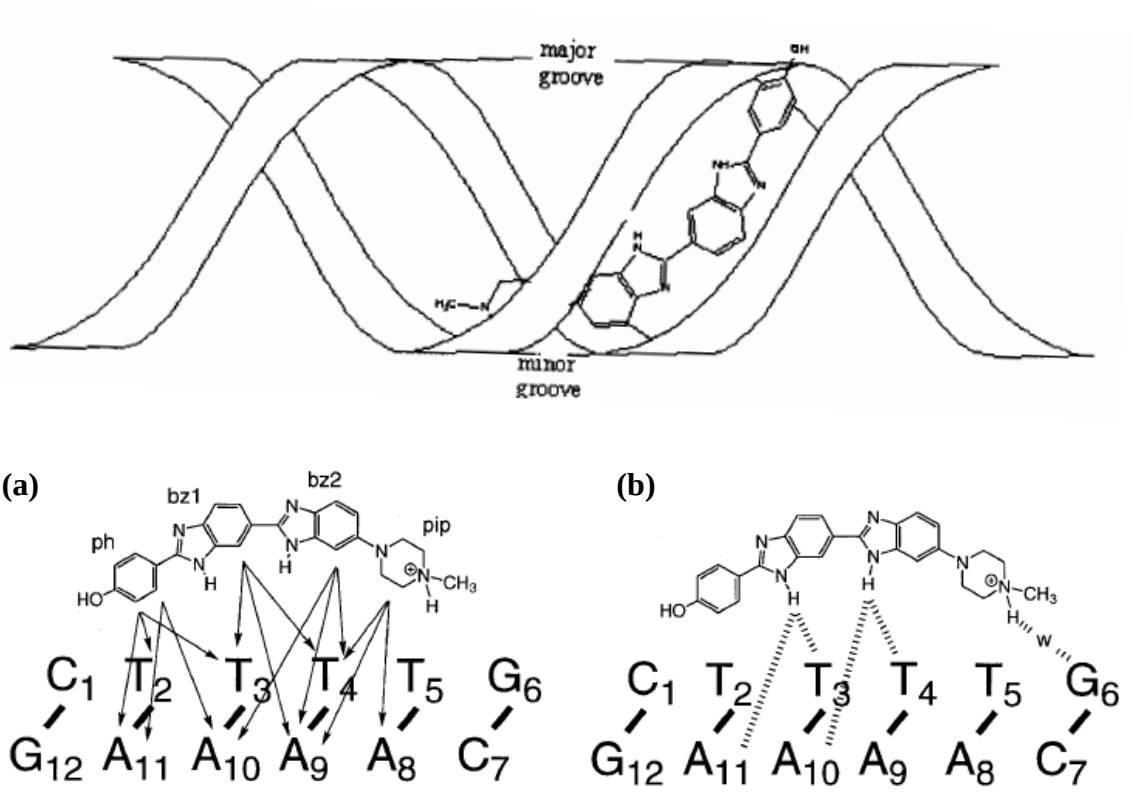

Figure 10 – The binding of the H33258 dye to DNA. (a) Non-exchangeable protons that define the position of H33258 within the minor groove. (b) Direct and solvent-mediated hydrogen bonding interactions with the floor of the minor groove (adenine N_3 and thymine O_2; w, water). *Adapted from [88,89]*

Despite the affinity to AT sequences, the guanine (G) and cytosine (C) regions adjacent to the AT tracts on the DNA sequence are important for the favorable accommodation

of the piperazine ring.[90-92] Accordingly, depending on the DNA sequence, the H33258 dye binds in slightly different modes, resulting in different associative binding constants (*K*), see Table 4. Moreover, the *K* of the H33258-DNA complex is dependent on pH and ionic strength.[59,93]

Table 4 – H33258-DNA binding constant and respective technique used.

Sequence	**Binding constant (M^{-1})**	**Technique**	**Reference**
Calf thymus (CT) DNA	6×10^8	van't Hoff plot	[57]
poly [d (A-T)]	3.8×10^8	van't Hoff plot	[57]
$d(CGCAAATTTGCG)_2$	3.2×10^8	Fluorescence titration	[93]
$d(CCGGAATTCCGG)_2$	3.2×10^8	van't Hoff plot	[57]
$d(CGCGAATTCGCG)_2$	4×10^8	van't Hoff plot	[57]
$d(CGCGAATTCGCG)_2$	1×10^7	^{1}H-NMR	[85]
$d(CTGAATTCAG)_2$	$(2\text{-}5) \times 10^8$	Fluorescence titration	[68]
$d(GCAAATTTGC)_2$	2.9×10^7	Circular dichroism	[90]
$d(GCAAATTTGC)_2$	3.6×10^8	Fluorescence titration	[94]
$d(GCAAAATTTTGC)_2$	1×10^8	Fluorescence titration	[91]

Because the photophysical properties of the H33258 dye depend on the polarity of the environment, and the minor groove of the DNA is relatively non-polar (with a dielectric constant of *ca.* 20), the supramolecular dye-DNA interaction leads to increased fluorescence intensity (*ca.* 30 times) and a blue-shift of the fluorescence maximum. The bright fluorescence of the H33258-DNA complex is reflected by a fluorescence quantum yield of *ca.* 0.42 to 0.58.[54,56,79,95]

Differences in the absorption spectrum are also noticed when going from the free dye to dye complexed to DNA (bathochromic shift). The absorption band starts decreasing and shifts gradually to a longer wavelength (red-shift) (Figure 11).[57]

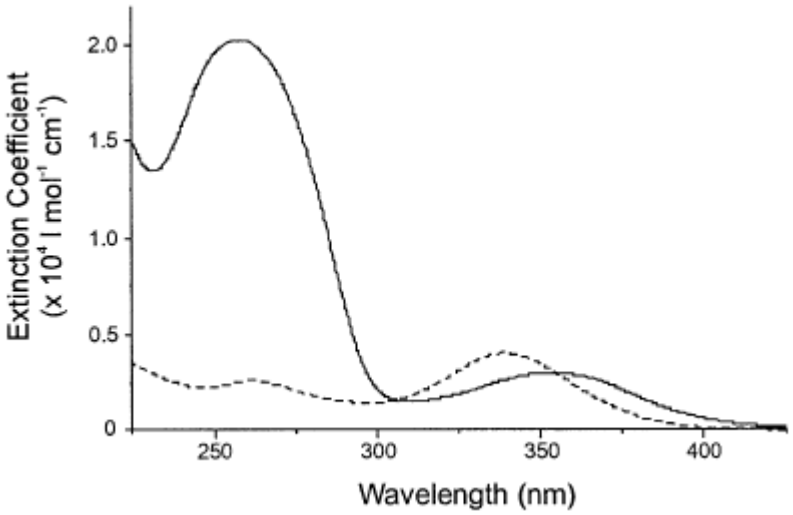

Figure 11 – Relative absorption spectra of H33258 dye (--) and upon binding to double strand DNA (—). *Adapted from* [79]

The magnitude of these shifts is also dependent on the location of the dye in the DNA structure.[54]

It was also observed that the fluorescence properties of the H33258-DNA complex were different at pH 4.5, where the strong fluorescence of the dye was significantly quenched upon the addition of nucleic acids (Figure 12).[59]

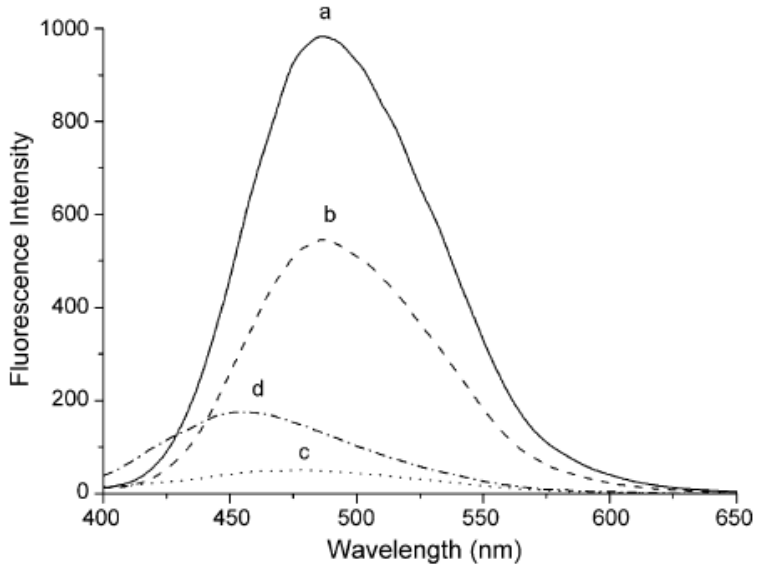

Figure 12 – Fluorescence emission spectra of (a) free H33258 at pH 4.5, (b) H33258-DNA at pH 4.5, (c) free H33258 at pH 7.2 and (d) H33258-DNA at pH 7.2.[59]

Nowadays it is known that the pH influences the fluorescence quenching effect (Figure 13), and that is why the pH *ca.* 7 is normally chosen when the H33258-DNA complex is studied.[59]

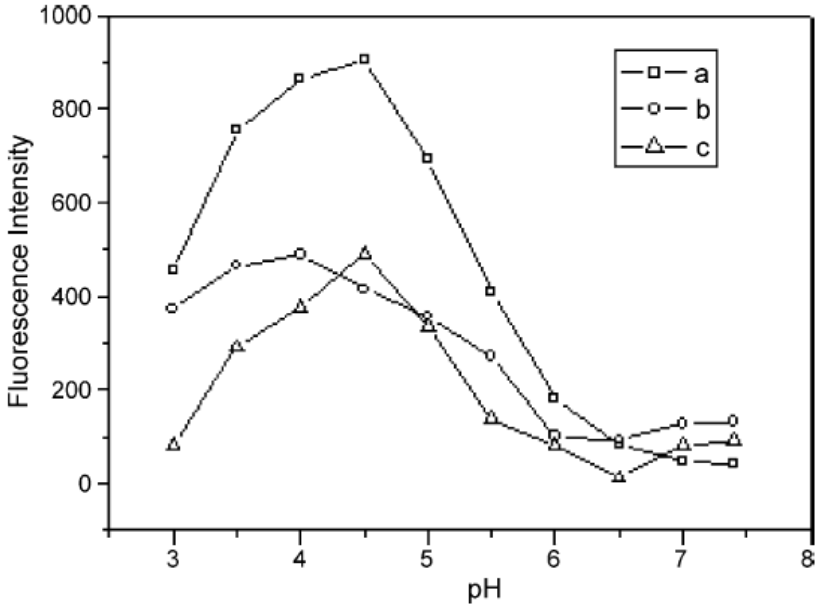

Figure 13 – Influence of pH on the fluorescence quenching effect in the pH range 3-7.5. The profiles represent the fluorescence of (a) H33258, (b) H33258-DNA, and (c) the intensity difference between them.[59]

Fluorescence lifetime measurements of complexes of H33258 dye with repetitive and heterogeneous sequences of DNA show two decay processes (0.2-0.5 and 2.5-3.9 ns). The relative amplitudes depend on the nucleic acid sequence and the ionic strength of the solution.[54,68,96,97] In fact, a double exponential fluorescence decay is evidence for at least two modes of binding: a strongly fluorescent complex formed at low binding densities (of high quantum yield) and a non-fluorescent complex at high binding densities (of lower quantum yield).[98]

The two modes of H33258-DNA interaction depend on the [dye] / [base pairs] ratio. When the dye concentration is lower, H33258 binds to the minor groove of the DNA duplex, and when the dye concentration is much higher an additional weaker binding mode appears. These unspecific binding interactions might be charge-mediated between the monocationic H33258 and the phosphate-charged backbone of DNA, a binding of

free dye to other H33258 molecules already bound to the DNA, or H33258 intercalation in GC rich sequences. This “non-specific” binding causes fluorescence quenching (often related to energy transfer from minor groove H33258), has no base pair preference, and causes an unwinding of the DNA duplex by *ca.* 1 degree. However, it is possible to dissociate the unspecific bound H33258, through an increase in the ionic strength of the solution or by adding a low amount of ethanol.[53,57,76,79,95,99-101]

I.2.4 – Applications

Since the early 1970s, H33258 has been widely used as a fluorescent DNA stain.[68,76,102] This application is possible because the dye has ready access into cells and becomes highly fluorescent after getting bound to the minor groove of double-stranded DNA. The bright fluorescence microscopic image of chromosomal DNA is very clear because it has a high contrast, due to minimal interference from the dye bound to other cell components.[57,61,76]

Nowadays, H33258 dye has become also attractive for several other important biochemical applications:

- Anthelmintic: the dye is active against infections by parasitic worms.[55,103-105]
- Multi-color-labeling experiments: due to the relatively large Stokes shifts of H33258, it can be used in multi-color-labeling experiments.[48]
- Displacement of DNA intercalators: The strong binding between the dye and the AT-rich sequences of DNA leads to a displacement of several DNA intercalators (such as ethidium bromide, quinacrine, acridine orange, daunomycin, adriamycin, and proflavin).[57]
- Inhibitor of the action of several enzymes: It was verified for free cell systems, that the presence of H33258 blocks helicase and topoisomerases I and II activity. It was also demonstrated that the transcription and translation of DNA is affected in the presence of the dye, although it is not known whether H33258 dye also interferes with other important proteins of these processes.[75,95,106-110]

- Radioprotector: H33258 can offer protection against radiation-induced strand breaks. The protection by this dye has two possible mechanistic components involved: scavenging of OH-radicals by the DNA-bound ligand and additional protection by quenching the OH-radical-induced DNA-radicals.[66,111-114]

- Anticancer activity: The fluorescence probe H33258 showed some activity against L1210 and P388 leukemias in mice, inducing cytotoxicity in the cancerous cells without causing serious side effects.[115-117]

The dye can be very useful for the design of new drugs able to interfere in gene regulation, and therefore, to modify chemotherapy or as a potential anticancer drug. In addition, the wide application as fluorescent dye makes the study of its photophysical properties in supramolecular assemblies a worthy objective.

I.3 – Biological polyamines

Biological polyamines (PAs) are organic molecules such as putrescine, cadaverine, histamine, spermidine, and spermine, that have two or more amino groups. These natural PAs are present in almost all living species.[118]

Leeuwenhoek first described PAs in 1678, however, active investigation did not begin until the last quarter of the 19th century, when spermine (1878), cadaverine (1886), putrescine (1889), and spermidine (1927) were identified.[118,119]

I.3.1 – Characteristics

PAs that are formed from the decarboxylation products of ornithine and S-adenosyl-methionine, are known classically by the names of putrescine, spermidine, and spermine.[120] Other amines, such as histamine and cadaverine also occur naturally but are not included under the general term of PAs,[121,122] although they are generally

considered biogenic amines. However, to make things easier, in this thesis all these amines will be called PAs.

The different PAs are ubiquitous low molecular weight aliphatic compounds (Table 5), and due to their ability to establish hydrogen bonds with protic solvents they are water soluble.[123] The linear PAs are recognized to have high conformational freedom,[120] and they are fully protonated at physiological pH (pK_s around 10), while histamine is only monoprotonated at pH 7 (pK_a 9.4 and 5.8).[124,125] It seems that the protonation influences the specific function of the different PAs, and it has been shown, that spermine is the most active in the control of various biological processes (such as the regulation of ornithine decarboxylase activity, stimulation of G-ptoteins, activation of nuclear factor kappaB in breast cancer cells, caspase activation in leukaemia cells, *etc*.).[126-129]

Table 5 – IUPAC name, chemical structure and molecular weight of several PAs.

Polyamine	**IUPAC name**	**Chemical structure**	**MW (g mol^{-1})**
Putrescine	butane-1,4-diamine	$H_2N(CH_2)_4NH_2$	88.152
Cadaverine	pentane-1,5-diamine	$H_2N(CH_2)_5NH_2$	102.178
Spermidine	N-(3-aminopropyl)butane-1,4-diamine	$H_2N(CH_2)_3NH(CH_2)_4NH_2$	145.246
Spermine	N,N'-bis(3-aminopropyl)butane-1,4-diamine	$H_2N(CH_2)_3NH(CH_2)_4NH(CH_2)_3NH_2$	202.340
Histamine	2-(1*H*-imidazol-4-yl)ethanamine	2-imid$(CH_2)_2NH_2$	111.150

imid = imidazolyl

PAs are synthesized in cells via highly-regulated pathways, however their actual function is not entirely clear. So far they have been implicated in cell growth,[124,130-133] cell attachment,[134,135] intestinal mucosa maturation,[136] cell migration,[115,130,137,138] cell cycle regulation,[139] chromatin structure,[121] nucleic acids packaging,[140] DNA replication,[140] apoptosis,[140] membrane stability,[115,141,142] transcription and

translation,[140,143-145] the intracellular distribution of F- and G-actin and thymosin β4,[146] ion channels, and cell signaling.[147-149] These activities are essential for normal embryonic development, differentiation, cellular maintenance, and wound healing.[150]

On the negative side high polyamine levels are toxic to cells and facilitate cell death mainly by oxidative mechanisms.[151,152] The elevated levels have been found in numerous relevant pathologies, such as cancer, infections,[153,154] psoriasis,[67,155,156] polycythemia rubra vera,[157] systemic lupus erythematosus,[158-162] uremia,[163,164] chronic nephritis,[165] liver cirrhosis,[166,167] cystic fibrosis,[168,169] muscular dystrophy,[170,171] and Alzheimer's disease.[172,173] Insufficient levels of PAs are also harmful, because suboptimal growth and ultimately cell death may result.

For a long time, the monitoring of polyamine concentrations in biological fluids has been employed as biochemical marker of tumor kinetics and was related to rapid cell growth, spontaneous cell death, or both.[174] Hence, it is of elevated interest to develop rapid and sensitive assay methods with the ability to quantify the different PAs.

I.3.2 – Host-guest assemblies with cucurbit[*n*]urils

Macrocyclic hosts are well-known to form complexes with biologically relevant cationic analytes. So it is no surprise that biological PAs are suited guests for different CB[*n*] (Figure 14). The dual hydrophilic-lipophilic character of the polyamine ligands, comprising cationic amine groups (both primary and secondary) and alkyl linkers of variable length, may lead to high association constants of the host-guest complexes (Table 6). This hydrophilic-lipophilic balance depends on the relationship between the length of the carbon bridging chains and the number of amine moieties.[120]

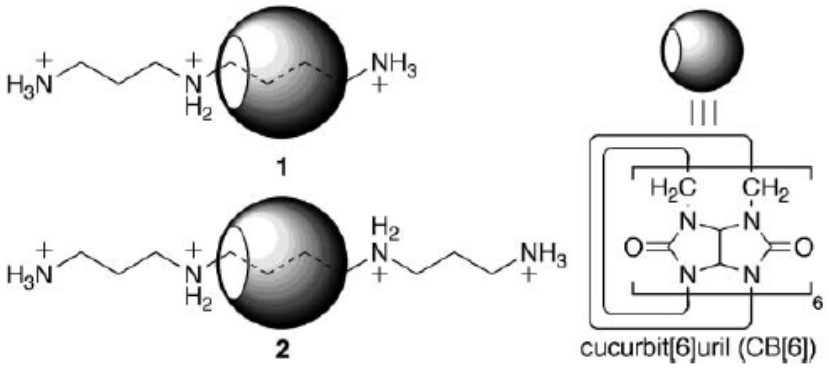

Figure 14 – Representation of the supramolecular complexes spermidine • CB[6] (1) and spermine • CB[6] (2).[175]

Table 6 – Selected binding constants (*K*) between CB[*n*]s and PAs.

Complex	*K* (M^{-1})	Reference
CB6 • Cadaverine	9.5×10^9	[38]
CB6 • Putrescine	2.0×10^7	[176]
CB6 • Spermidine	4.1×10^8	[176]
CB6 • Spermine	3.3×10^9	[176]
CB[7] • Cadaverine	4.5×10^6	[177]
CB[7] • Cadaverine	1.4×10^7	[39]
CB[7] • Histamine	3.2×10^4	[39]
CB[7] • Putrescine	3.7×10^5	[39]

The ability of PAs to form supramolecular assemblies with cucurbit[*n*]urils gives rise to new possibilities regarding polyamine detection, as well as new perspectives in terms of their application in the characterization of biological and chemical processes, such as monitoring specific enzymatic reactions, e.g., amine oxidase and several amino acid decarboxylases.[39]

II – Objective

The presented thesis has two main objectives, which will be briefly outlined below.

Objective 1: It is of interest to study the formation of supramolecular host-guest complexes between Hoechst 33258, a well-used DNA binder, and cucurbit[7]uril (CB[7]) as synthetic macrocyclic host. Based on earlier studies with other dyes, it is to be expected that the interaction between dye and CB[7] will lead to significant modulation of the photophysical properties of the dye (such as UV-Vis absorption and fluorescence). These modulations will be used to determine binding constants and complex stoichiometries. Nuclear magnetic resonance spectroscopy and electrospray ionization mass spectrometry are planned to complement the investigation. Furthermore, it is of interest to fully characterize corresponding solvatochromic effects, changes in fluorescence quantum yields and lifetimes, as well as the pH dependence of the supramolecular inclusion event.

Objective 2: Once the supramolecular and photophyscial properties (see objective 1) of the Hoechst 33258/CB[7] assembly are established, competitive binding with structures of biological interest will be studied. These experiments will be based on UV-Vis absorption and fluorescence spectroscopy as well as circular dichroism measurements. Biological polyamines and calf-thymus DNA will be play a predominant role in this objective. Polyamines are competing guests, while calf-thymus DNA plays the role of a competing host. It is expected to gain new insights into the binding affinities and selective binding of polyamines by CB[7] as well as to establish the Hoechst 33258/CB[7] complex as useful tool for the investigation of dye binding by calf-thymus DNA.

III – Materials and methods

III.1 – Equipment

Spectrophotometer UV-1603 (Shimadzu); Fluorescence Spectrophotometer Varian Cary Eclipse (Varian, Inc); Microprocessor pH Meter HI221 with calibration check (HANNA Instruments); Circular Dichroism (CD) Spectropolarimeter Jasco J-810 (Jasco); Water purifier Milli-Q Plus 185 (Millipore); Mass spectrometer HCT *ultra* (Bruker Daltonics Inc); Nuclear Magnetic Resonance (NMR) Spectrometer ECX 400 (JEOL); Time-correlated single photon counting (TCSPC) fluorimeter FLS 920 (Edinburgh Instruments).

III.2 – Reagents

1,4-Diaminobutane (Acros Organics); Cadaverine (Fluka); CT-DNA (Fluka); Cucurbit[7]uril was provided from Werner Nau group (synthesized according to[10]); Histamine dihydrochloride (Fluka); Hoechst 33258, pentahydrate (Invitrogen); Quinine hemisulfate salt monohydrate (Fluka); Spermidine (Sigma); Spermine (Sigma); Sodium phosphate dibasic (Acros Organics); Sodium phosphate monobasic monohydrate (Acros Organics); Sulfuric acid 0.05 mol/l (Merck).

III.3 – Experimental procedure

All measurements were performed at room temperature (22 - 25 ºC) in aerated water, except when CT-DNA was involved, which implied 1 mM phosphate buffer at pH 7.2.

The absorption, fluorescence, and CD measurements have been made with a quartz cell of 1 cm optical path length and analyzed in Origin 8 (Microcal Inc.) software package. The baselines were always recorded with the suitable solutions prior to each set of experiments and all emission spectra were corrected with a correction file specific for the instrument.

The pH of the solutions were adjusted by addition of NaOH or HCl.

The concentration of CT-DNA was determined by absorption spectroscopy, using the extinction coefficient of 6600 M^{-1} cm^{-1} at 260 nm.[178]

III.3.1 – Spectrophotometric titration

Several absorption and fluorescence titrations were performed to allow the determination of pK_a's and binding constants (K). A fixed concentration of H33258 (frequently 1 µM) was titrated at different pHs and against increasing CB[7], and CT-DNA concentrations. Competitive titrations were also performed with the H33258/CB[7] complex (usually 1 µM / 3 µM) with cadaverine, putrescine, spermine, spermidine, histamine, and CT-DNA. Finally, H33258/CB[7]/CT-DNA complexes were titrated with CB[7]. Excitation wavelengths (λ_{exc}) varied from 295 nm to 358 nm, depending on the specific experiment.

In order to obtain pK_a and K values the data were fitted using standard procedures for 1:1 binding, competitive binding, and pH titrations.

III.3.2 – Job's plot

The Job's continuous variation method was applied to determine the binding stoichiometry of H33258 dye when associated with CB[7].[179] The concentration of both reactants was varied, while the sum of their concentrations was constant (10 µM) at pH 4.5 and 7. The differences in the fluorescence intensity were plotted against the input mole fraction (χ) of the CB[7] at λ_{exc} = 295 nm.

III.3.3 – Fluorescence quantum yield

The fluorescence quantum yield of H33258, H33258/CB[7] complex, and H33258/CT-DNA complex were optically matched at the excitation wavelength of quinine sulfate, that was used as standard. Φ_f were calculated through the ratio of the fluorescence areas of the compound and quinine sulfate, multiplied with the Φ_f of quinine sulfate in 0.05 M

H_2SO_4 ($\Phi_{f,\ compound}$ = [area $_{compound}$ / area $_{quinine\ sulfate}$]*$\Phi_{f,\ quinine\ sulfate\ (0.05\ M\ H_2SO_4)}$), that is 0.546.[180]

III.3.4 – Fluorescence lifetimes

Lifetimes of H33258 (100 μM) in presence and absence of CB[7] (3 mM), at pH 4.5 and pH 7, were measured by time-correlated single photon counting (TCSPC) using a PicoQuant pulsed LED (PLS-280, λ_{ex} = 280 nm, λ_{obs} = 470 nm for pH 7, and 490 nm for pH 4.5, fwhm *ca.* 450 ps) as excitation source. Concentrations were chosen to obtain sufficient signal strength. The intensity fluorescence decays were fitted according to monoexponential and biexponetial (in case of the dye at pH 7) decay models and by employing instrument-specific software and reconvoluted with the instrument response function. The quality of the fitting was evaluated by χ^2.

III.3.5 – Mass spectrometry

Solutions of H33258, CB[7], and H33258/CB[7] complex (proportion 1:3, respectively) at pH 4.5 and 7, were infused at 240 μl/h directly into the mass spectrometer. The drying gas temperature was 300 ºC, spray voltage was -4.0 kV and nebulizer 20 psi. Data were collected for approximately 50 scans. MS/MS spectra were made in the same conditions.

III.3.6 – NMR

The ^{1}H NMR spectra were recorded in D_2O (99.9%) and the resonance assignments were confirmed using 2D-COSY. The pD values of the solutions were adjusted by addition of DCl (99 %). ^{1}H NMR spectra (400 MHz) were recorded by using the chemical shift of HOD in D_2O, preset at 4.67 ppm as reference. Concentrations of H33258 dye (3 and 5 mM) and CB[7] (3 mM) were chosen to obtain sufficient signal strength. The NMR spectra of guest only were measured in very acidic solution (50 mM

DCl) to allow efficient peak resolution; while the NMR spectra of complex were done in less acidic solution (10 mM) due to the better signal resolution obtained with CB[7].

III.3.7 – Circular dichroism

All ICD spectra were recorded from 250 to 450 nm with a Jasco J-810 circular dichrograph (0.2 nm resolution, 6 accumulations, 1 cm cell) by using the buffer solution for background correction. All measurements were made in 10 mM sodium phosphate buffer (pH 7.0). The respective concentrations of H33258, DNA and CB[7] were extrapolated from the fluorescence titration results such that the case of nonspecific and specific DNA binding in presence of CB[7] is examined.

IV – Results

IV.1 – Aggregation

The aggregation experiments of H33258, at pH 7 and 4.5, were performed in order to select the optimal work concentrations for this study. The assay consists in a Lambert-Beer-plot of the dye and the verification of non-aggregation is performed by the linearity of the absorption spectra at a selected wavelength.

The in Figure 15 shown aggregation assay was performed at pH 7 at an observation wavelength of 418 nm and a concentration maximum of 1 mM.

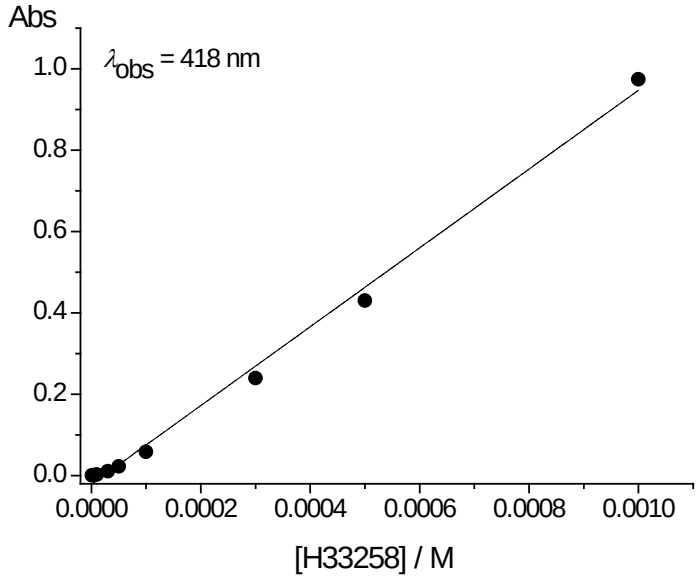

Figure 15 – Aggregation assay of H33258 at pH 7 with concentration maximum of 1 mM. The selected λ_{obs} was 418 nm to guarantee that the absorption does not exceed 1. The data are the result of an average of three assays.

The in Figure 16 shown aggregation assay was performed at pH 7 at an observation wavelength of 339 nm and a concentration maximum of 30 µM. The obtained slope, which corresponds to the molar extinction coefficient (ε), was 42300 M^{-1} cm^{-1}.

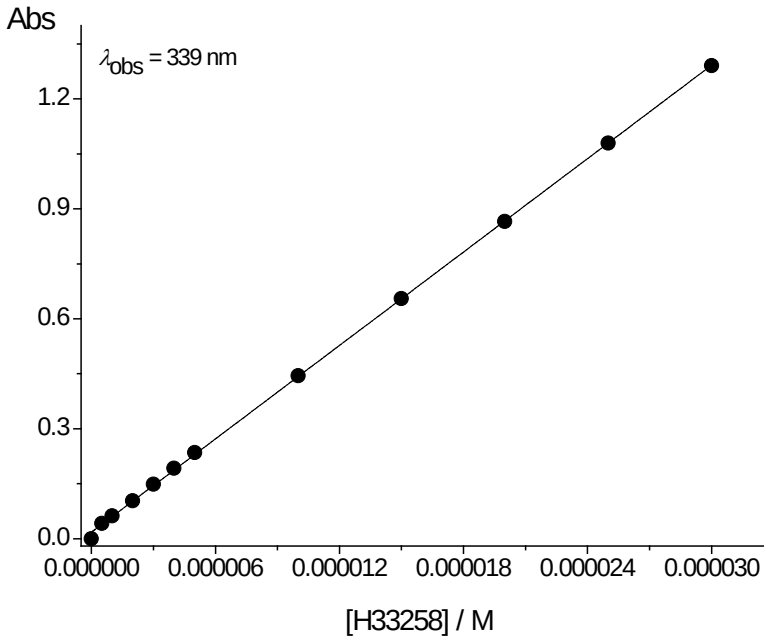

Figure 16 – Aggregation assay of H33258 at pH 7 with a concentration maximum of 30 µM. The selected λ_{obs} was the absorption maximum (339 nm). The data are the result of an average of three assays.

The in Figure 17 shown aggregation assay was performed at pH 4.5 at an observation wavelength of 432 nm and a concentration maximum of 1 mM.

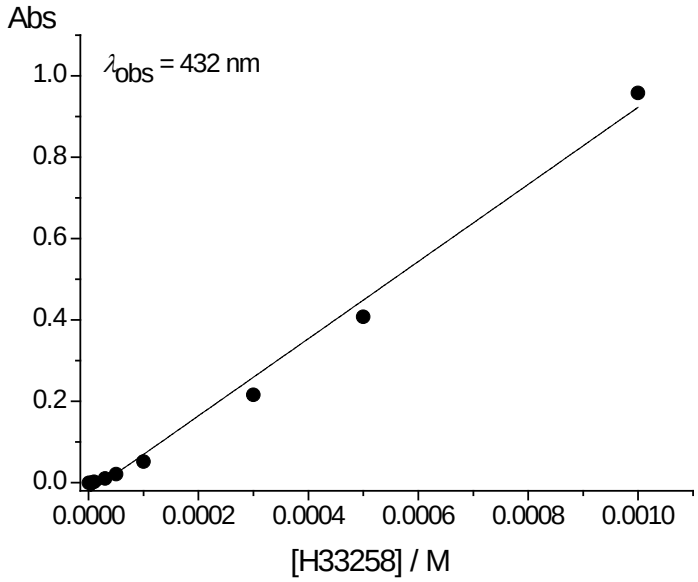

Figure 17 – Aggregation assay of H33258 at pH 4.5 with a concentration maximum of 1 mM. The selected λ_{obs} was 432 nm to guarantee that the absorption does not exceed 1. The data are the result of an average of three assays.

The in Figure 18 shown aggregation assay was performed at pH 4.5 at an observation wavelength of 382 nm and a concentration maximum of 50 µM. The obtained slope, which corresponds to the ε, was 20100 M^{-1} cm^{-1}.

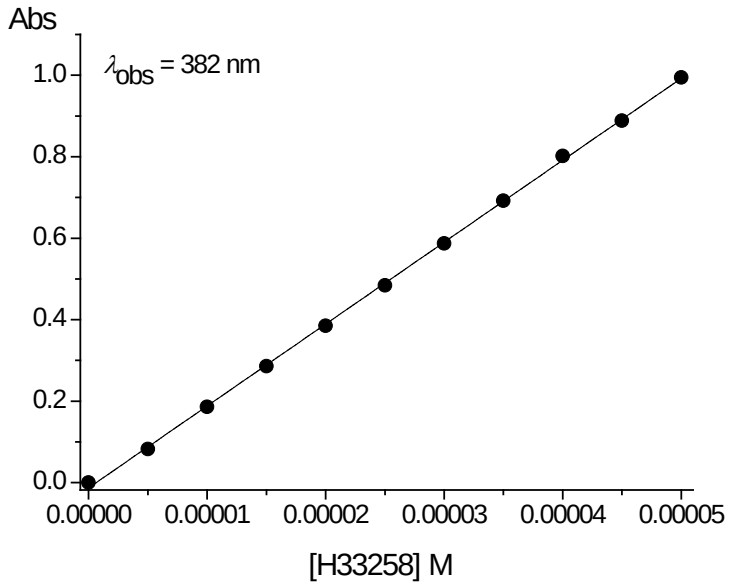

Figure 18 – Aggregation assay of H33258 at pH 4.5 with a concentration maximum of 50 µM. The selected λ_{obs} was 382 nm to guarantee that the absorption does not exceed 1. The data are the result of an average of three assays.

IV.2 - pH Titration of Hoechst 33258 and its complex with CB[7]

pH Titration experiments of the H33258 dye and its complex with CB[7] were performed in order to verify the fluorescence properties of the dye and the changes when complexed by cucurbituril. The experiments were done by UV-Vis absorption and fluorescence spectroscopy and performed in the same day to allow comparisons between the spectra.

In Figure 19 the influence of the pH on the absorption spectra of 1 µM H33258 is shown. The assay was performed by varying the pH from 2.5 to 11.0 in intervals of 0.5. However, the figure shows only selected pHs, because it is easier to realize the corresponding spectral alterations.

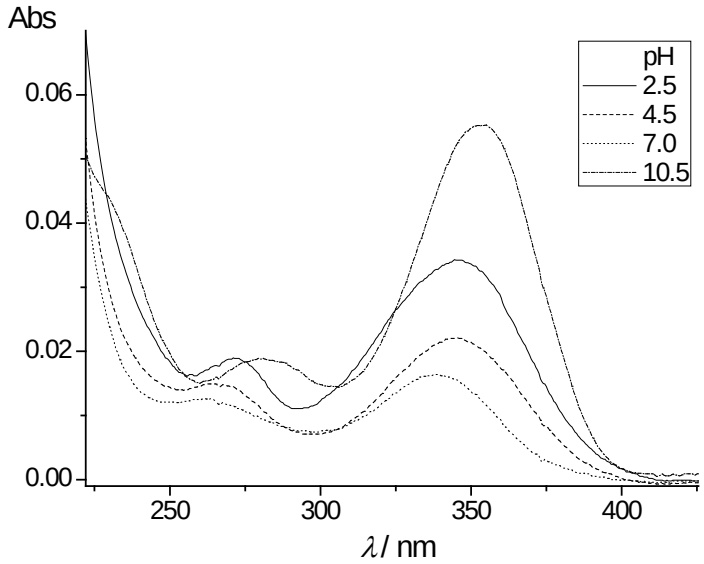

Figure 19 – Absorption spectra of H33258 dye in water. H33258 concentration was kept fixed at 1μM and pH was varied from 2.5 to 10.5.

From pH 2.5 to 7 the maximum absorption decreases and suffers an hypsochromic shift (345 to 339 nm, respectively), while from pH 7 to 11 the absorption maxima intensity increases and undergoes a bathochromic shift (339 to 354 nm, respectively).

Figure 20 shows the same study executed with the emission spectra. From pH 2.5 to 4.5 the fluorescence intensity increases, while from pH 4.5 to 8 the fluorescence intensity decreases and suffers a blue-shift (492 to 480 nm). From pH 8 to 10.5 the fluorescence intensity increases and suffers a red-shift (480 to 503 nm).

Through the absorption and fluorescence spectra it was possible to calculate the different pK_a's of the dye. The plot of a selected wavelength from the pH titration *versus* the pH originates sigmoidal curves whose geometric center (equivalence point) corresponds to the pK_a, for example Figure 21.

With this, the calculated pK_a values from the UV-Vis absorption pH titration were 4.1 and 8.8 and from the fluorescence measurements three pK_a values of 3.4, 5.0, and 9.1 were obtained.

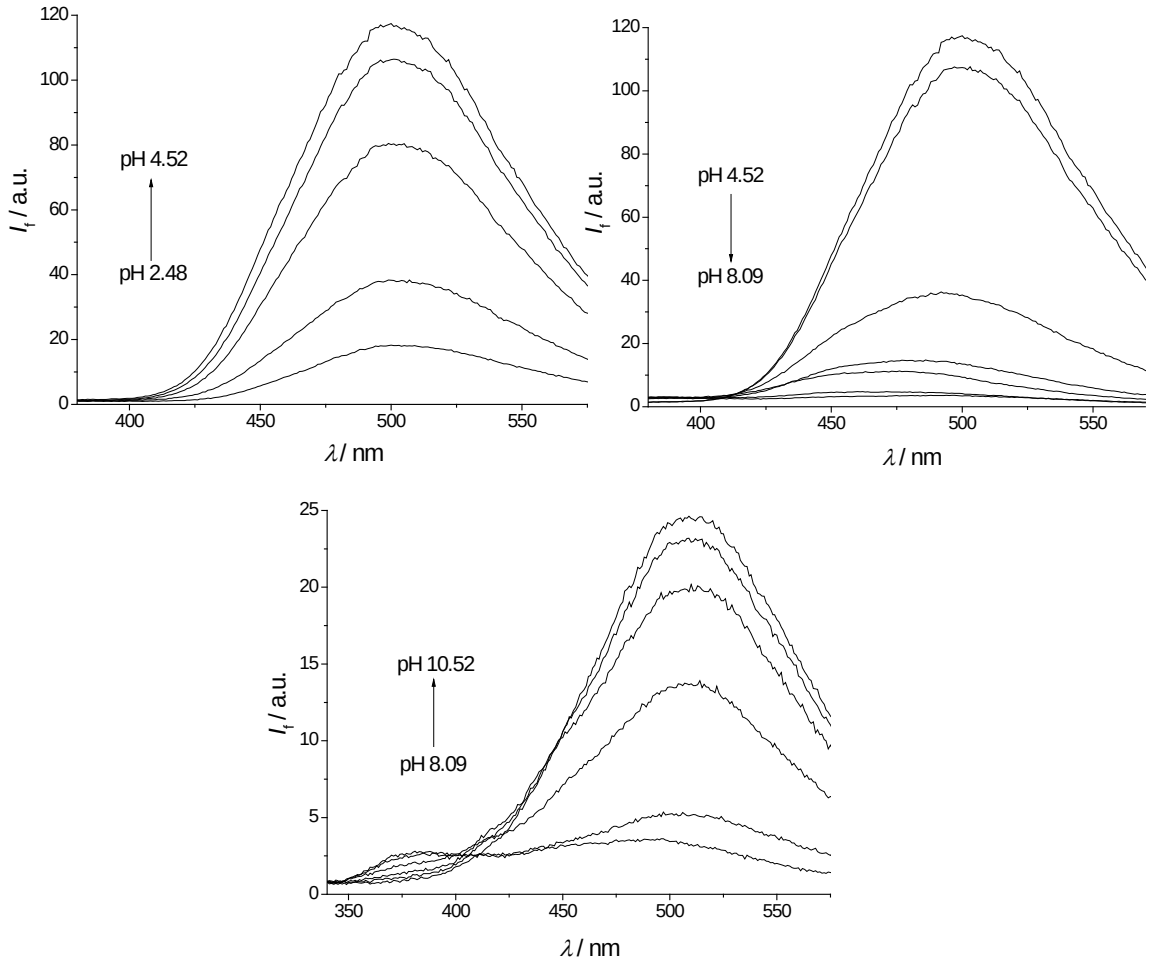

Figure 20 – Fluorescence spectra of H33258 dye in water. The concentration of the H33258 was kept fixed at 1µM and pH was varied from 2.5 to 10.5. The measurement conditions were: λ_{exc} = 295 nm.

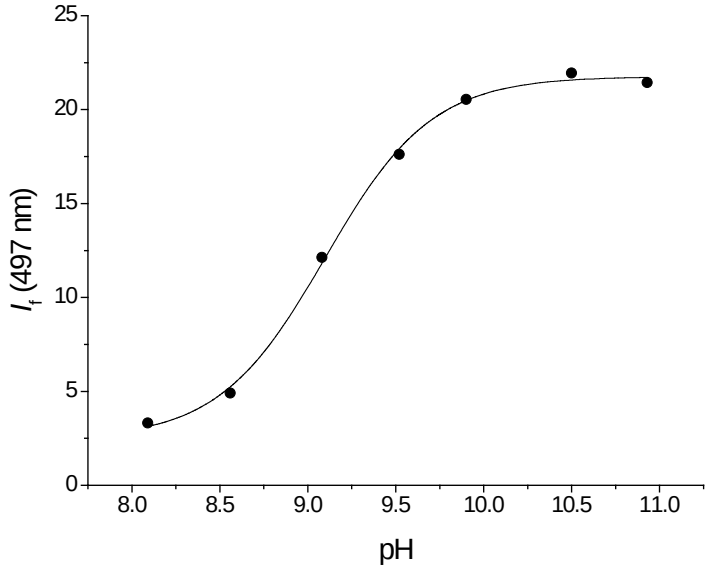

Figure 21 – pH Titration of 1 µM H33258 dye. The pH range was from 8 to 11.

In Figure 22 the influence of pH on the H33258/CB[7] complex (1 µM / 30 µM, respectively) absorption spectra is represented.

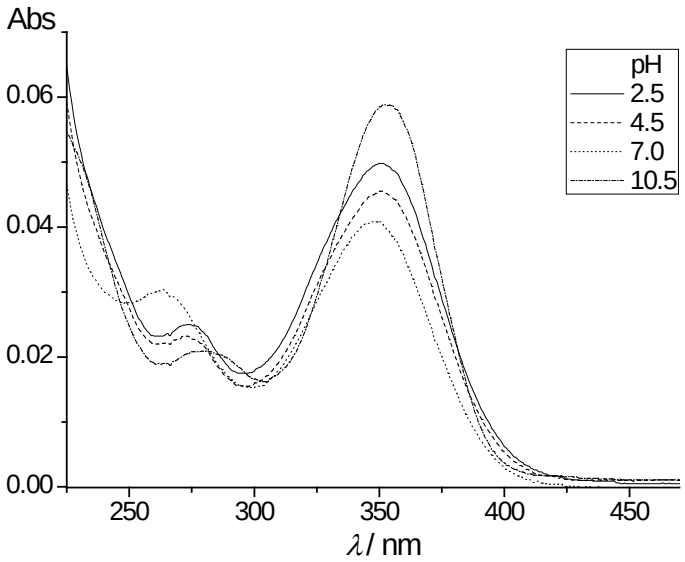

Figure 22 – Absorption spectra of H33258/CB[7] in water. The concentrations were kept at 1µM H33258 / 30 µM CB[7] and the pH was varied from 2.5 to 10.5.

The assay was performed by varying the pH from 2.5 to 11.0 in intervals of 0.5, but Figure 22 presents only selected pHs. From pH 2.5 to 7.5 the absorbance at the maximum wavelength decreases and suffers a small hypsochromic shift (351 to 349 nm), while from pH 7.5 to 11 the same increases and undergoes a small bathochromic shift (349 to 352 nm).

Figure 23 shows the same study executed with emission spectra. From pH 2.5 to 6.5 the fluorescence intensity increases, and the band suffers a hypsochromic shift (485 to 471 nm), while from pH 6.5 to 11 the fluorescence intensity decreases and undergoes a further hypsochromic shift (471 to 465 nm).

The only safely calculated pK_a value for the complex was 9.0 from UV-Vis pH titration, while the fluorescence titration allowed the extraction of two values: 5.7 and 8.0.

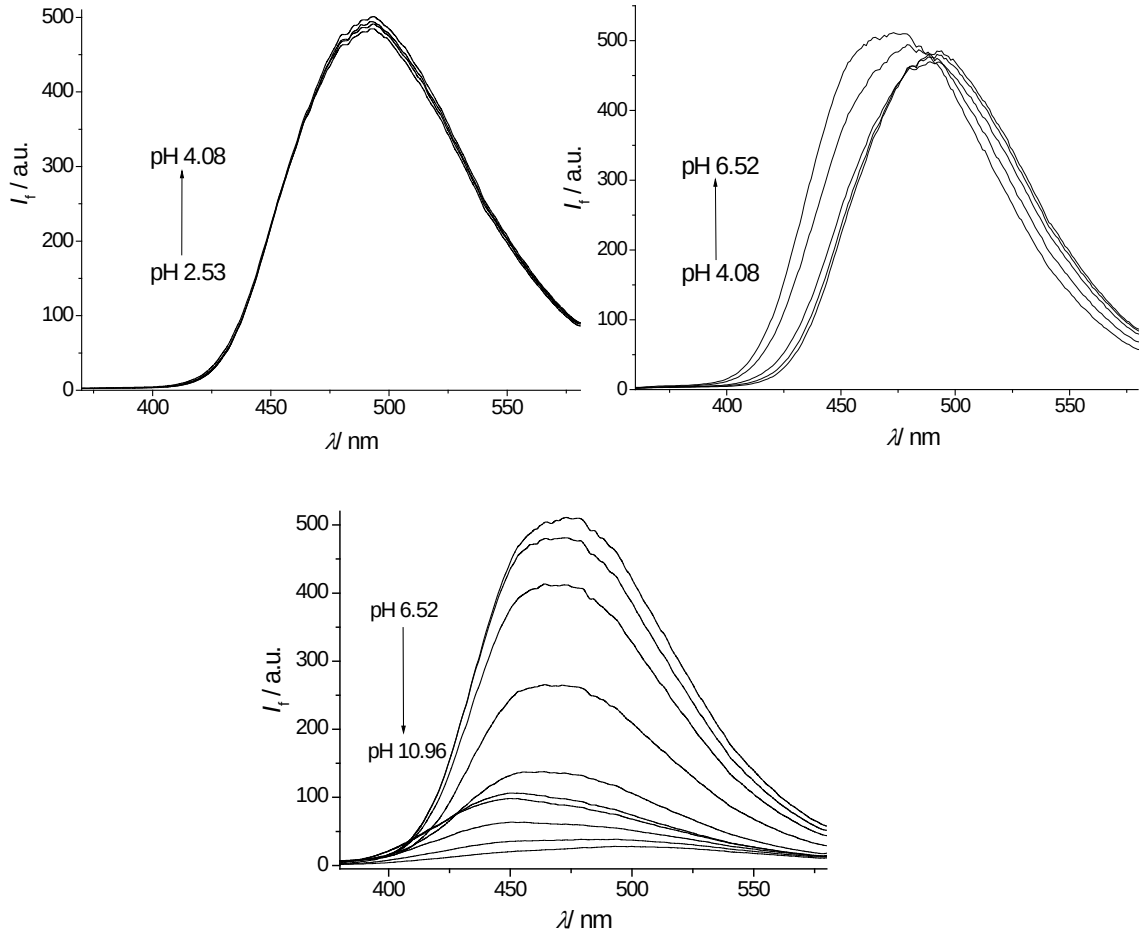

Figure 23 – Fluorescence spectra of H33258/CB[7] complex in water. The concentrations were kept at 1μM H33258 to 30μM CB[7] and the pH was varied from 2.5 to 11. The measurement conditions were: λ_{exc} = 295 nm.

In Figures 24 and 25 the pH titration profiles related to UV-Vis absorption and fluorescence, respectively, are shown. In Figure 26 the fluorescence enhancement factor upon the addition of CB[7] with respect to the free H33258 dye is shown as well.

Thus, the enhancement factor upon the formation of the complex at pH 7 is 43 times, while at pH 4.5 it is 5 times. At a pH of 7.5 this factor can reach a value even as high as 90.

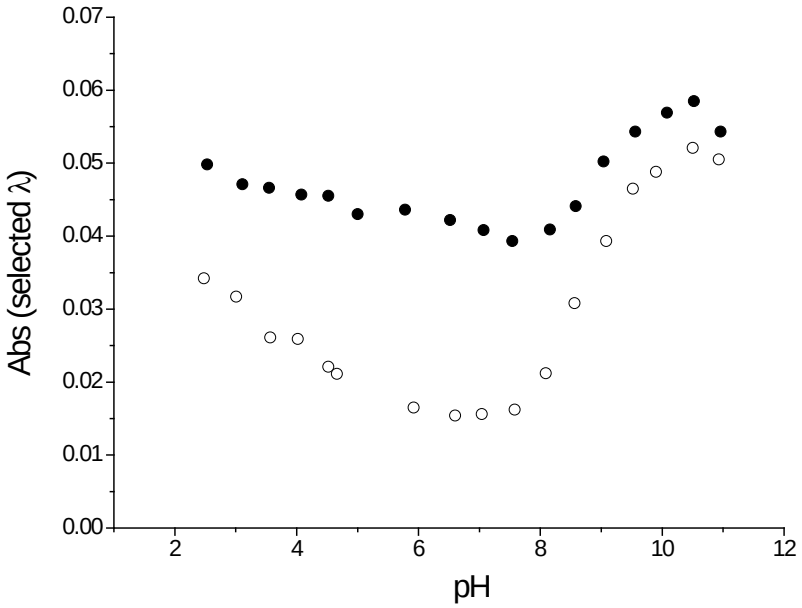

Figure 23 – pH Titration of free H33258 dye and with CB[7] at selected wavelengths. ○ H33258 (1 µM) at λ_{obs} = 345 nm. ● H33258/CB[7] (1 µM / 30 µM) at λ_{obs} = 350 nm.

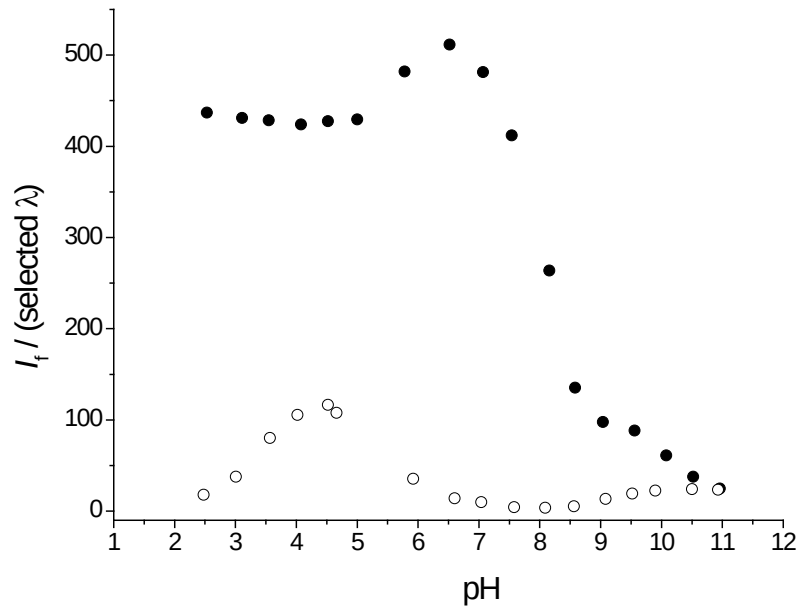

Figure 25 – pH Titration of free H33258 and with CB[7] at selected wavelengths. ○ H33258 (1 µM) at λ_{obs} = 497 nm. ● H33258/CB[7] (1 µM / 30 µM) at λ_{obs} = 473 nm.

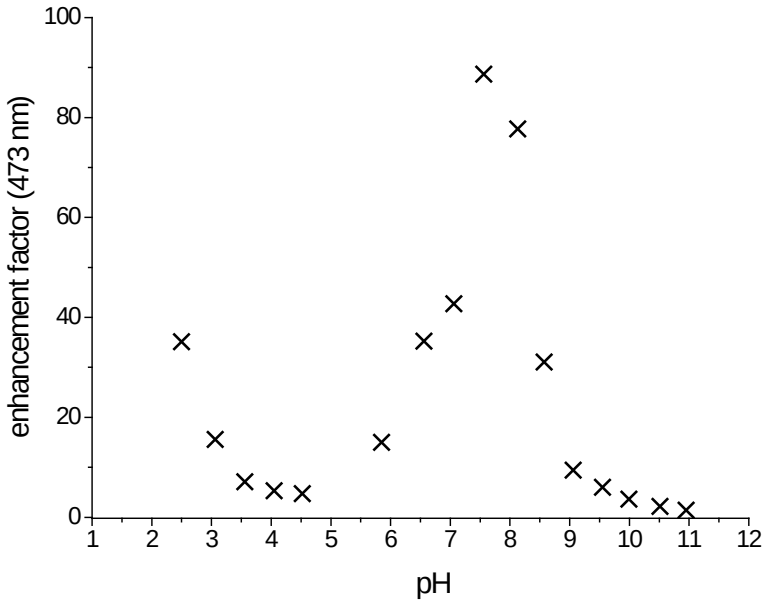

Figure 26 – Enhancement factor upon addition of CB[7] (at a concentration of 30 μM) to a solution of 1μM H33258 at λ_{obs} = 473 nm at different pH values.

IV.3 – CB[7] titration at pH 7 and 4.5, and in 1 mM phosphate buffer (pH 7.2)

The CB[7] titrations at pH 7 and 4.5, and in 1 mM phosphate buffer (pH = 7.2) were performed in order establish the binding affinity between the H33258 dye and CB[7] under different conditions. Note that at pH 7 the dye is mainly present as monoprotonated form, while at pH 4.5 it exists as diprotonated form.

The Figures 27 and 28 show the fluorescence titration curves upon successive addition of CB[7] to 1 μM of H33258 at pH 7 and 4.5, respectively. The calculated binding constants (*K*), according to a 1:1 complexation model, are $(3.5 \pm 0.8) \times 10^6$ M^{-1} at pH 7 and $(3.4 \pm 1.4) \times 10^6$ M^{-1} at pH 4.5.

The CB[7] titration curve in 1 mM phosphate buffer at pH 7.2 is represented in Figure 29 and allowed to calculate a 1:1 binding constant *K* of $(3.7 \pm 0.05) \times 10^6$ M^{-1}.

In Figure 30 the CB[7] UV-Vis titration curve of 2 μM of H33258 at pH 7, is shown. The 1:1 fitting led to a binding constant *K* of $(3.4 \pm 0.5) \times 10^6$ M^{-1}. This is in absolute agreement with the value obtained from the fluorescence titration.

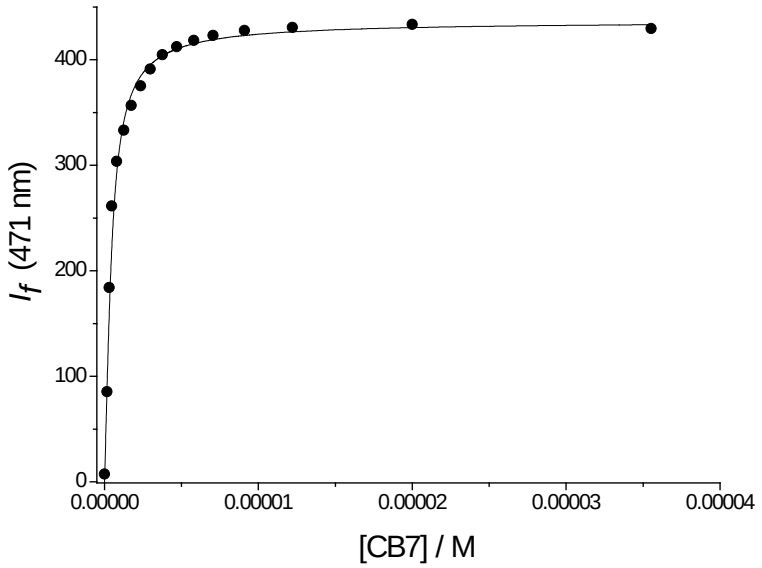

Figure 27 – Fluorescence titration of H33258 dye with CB[7] at pH 7. The fluorescence amplitude, in arbitrary units, at 471 nm is plotted *versus* the concentration of CB[7]. The fluorescence measurements were made at λ_{exc} = 295 nm.

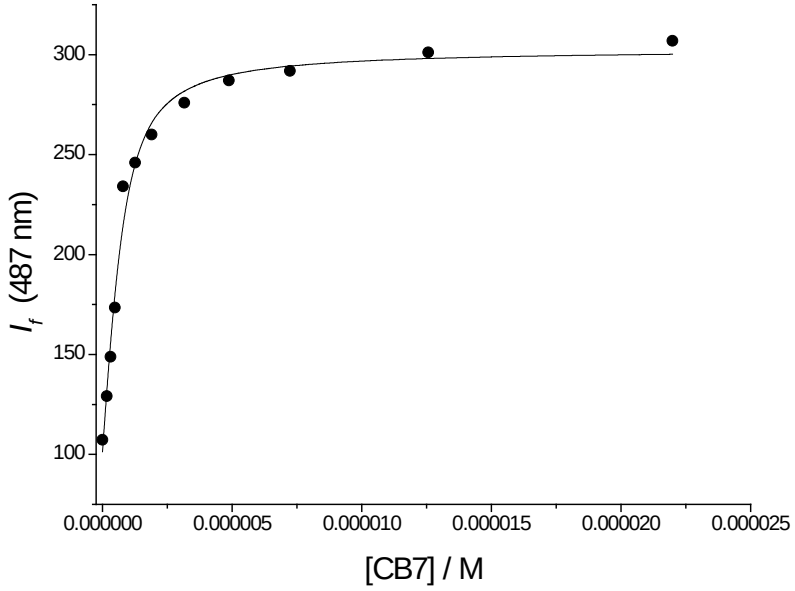

Figure 28 – Fluorescence titration of H33258 dye with CB[7] at pH 4.5. The fluorescence amplitude, in arbitrary units, at 487 nm is plotted *versus* the concentration of CB[7]. The fluorescence measurements were made at λ_{exc} = 295 nm.

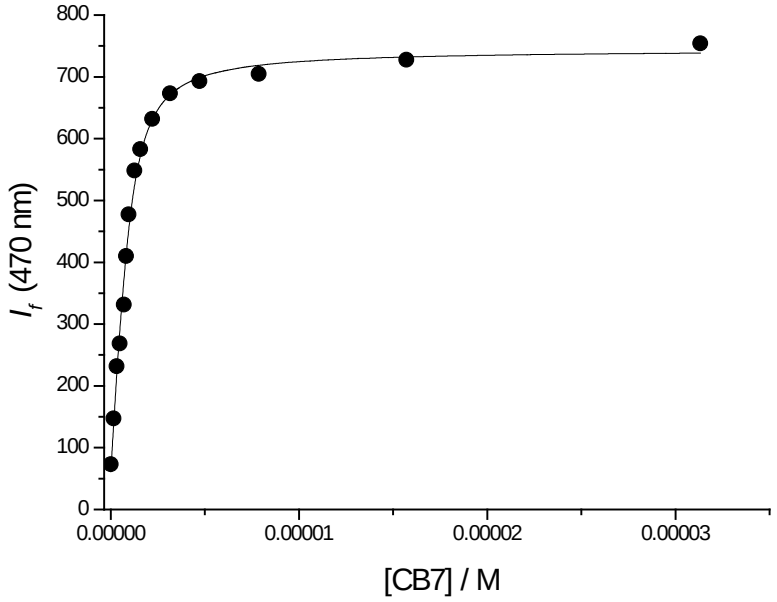

Figure 29 – Fluorescence titration of H33258 dye with CB[7] in 1 mM phosphate buffer at pH 7.2. The fluorescence amplitude, in arbitrary units, at 470 nm is plotted *versus* the concentration of CB[7], and the fluorescence measurements were made at λ_{exc} = 295 nm.

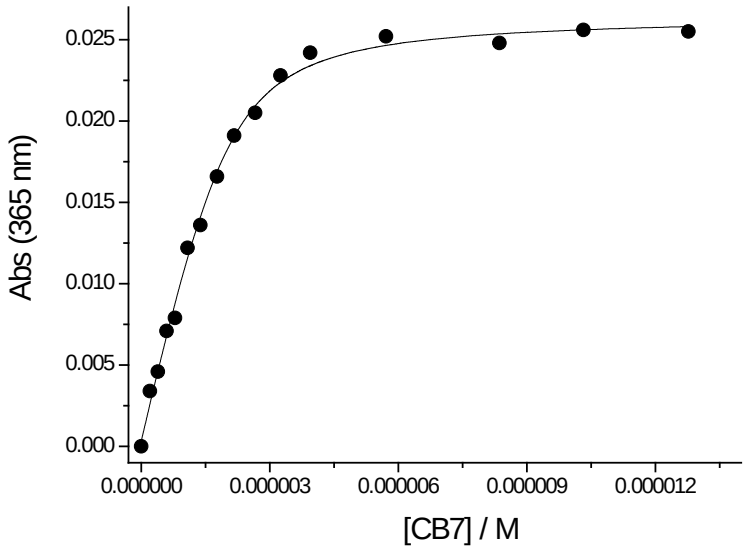

Figure 30 – UV-Vis absorption titration of H33258 dye with CB[7] at pH 7. The absorption amplitude, in arbitrary units, at 365 nm is plotted *versus* the concentration of CB[7].

IV.4 – Job's plot at pH 7 and 4.5

The Job's plot allows the determination of the stoichiometry of the H33258/CB[7] complex. The result for pH 7 and 4.5 is a 1:1 complex, as shown in Figure 31 and 32, respectively. This corresponds to a maximum signal at a mole fraction $\chi_{CB[7]} = 0.5$.

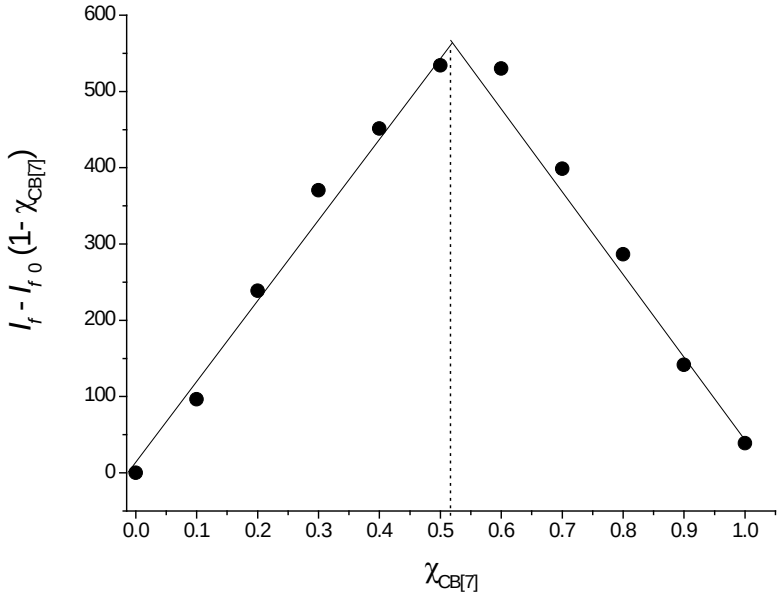

Figure 31 – Job's plot for H33258/CB[7] binding at pH 7. The sum of the concentrations of the two components was kept constant at 10 µM. The λ_{obs} selected for the plot was 471 nm and the fluorescence measurements were made at λ_{exc} = 295 nm.

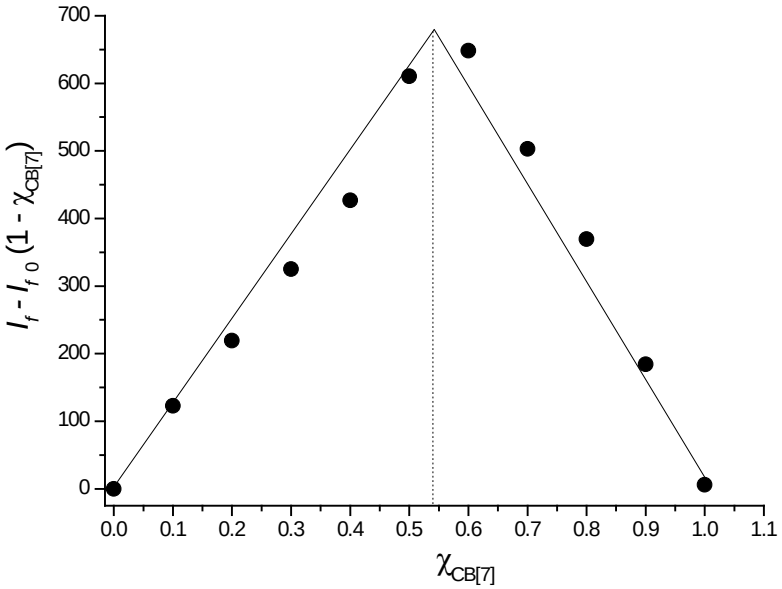

Figure 32 – Job's plot for H33258/CB[7] binding at pH 4.5. The sum of the concentrations of the two components was kept constant at 10 µM. The λ_{obs} selected for the plot was 474 nm and the fluorescence measurements were made at λ_{exc} = 295 nm.

IV.5 - Fluorescence quantum yield of Hoechst 33258, its complex with CB[7] at pH 7 and 4.5, and its complex with CT-DNA in 1 mM phosphate buffer (pH 7.2)

The fluorescence quantum yield is the measurement of the emission efficiency of a determined fluorochrome. In this work, the calculated fluorescence quantum yield of the H33258 dye was 1 % and 29 % at pH 7 and 4.5, respectively, while for the complex with CB[7] the value was 74 % at both pH's. On the other hand, the fluorescence quantum yield, Φ_f, of the H33258/CT-DNA complex was 62 % in 1 mM phosphate buffer at pH 7.2

IV.6 – Fluorescence lifetimes of Hoechst 33258 and its complex with CB[7] at pH 7 and 4.5

The fluorescence lifetime is a kinetic measure for the excited singlet state decay of a photoactive molecule. The fluorescence lifetime results obtained for the H33258 dye and the H33258/CB[7] complex at pH 7 and 4.5 are presented in Table 7. The decay curves are shown in Figure 33. The lifetimes were calculated by deconvolution of the decay from the intrinsic instrument response function (IRF).

Table 7 – Fluorescence lifetime measurements of H33258 dye and H33258/CB[7] complex, at pH 7 and 4.5.

	pH 4.5		pH 7	
	τ_s [ns]	χ^2 *	τ_s [ns]	χ^2 *
H33258 dye	4.03	1.05	0.48**	1.33
H33258 / CB[7]	4.78	1.03	4.47	1.03

* The χ^2 value is a measure for the goodness of the fit.

** Average lifetime (the biexponential fit yields: τ_1 = 4.03 ns (33 %) and τ_2 = 0.34 ns (67 %)).

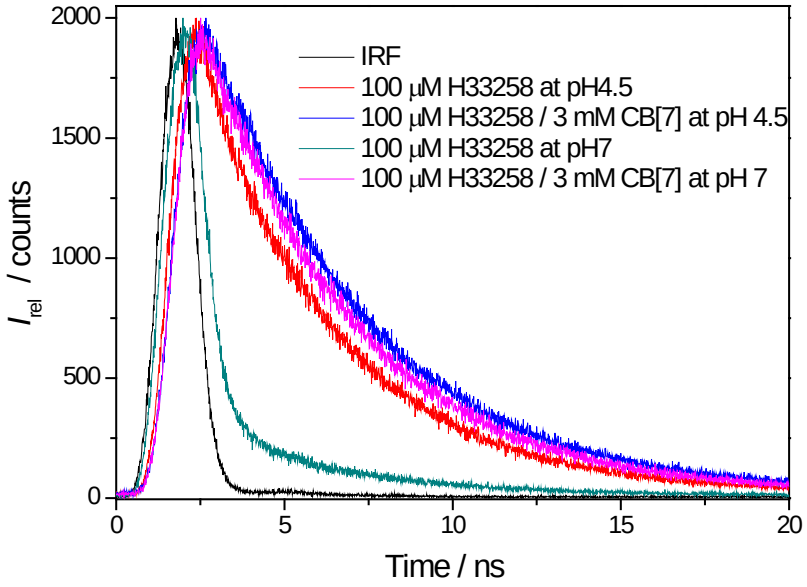

Figure 33 – Fluorescence decays profiles for the H33258 dye and the H33258/CB[7] complex in different pH conditions.

IV.7 – Mass spectrometry of Hoechst 33258, of CB[7] alone, and of the complex at pH 7 and 4.5

Mass spectrometry allows us to obtain information of the stoichiometry of the host-guest complex and its stability in the gas phase.

Figure 34 shows the mass spectrum of a solution of free H33258 dye, at pH 7 and 4.5. The main peak is at m/z 425 is the single charged H33258 dye. At pH 7 another also smaller peak, at m/z = 368 appears, can also be observed. This peak also shows up upon fragmentation MS^2 of the m/z = 425 peak (Figure 60, presented in the annex). This peak was can be a degradation product of the dye (in solution) or in the gas phase.

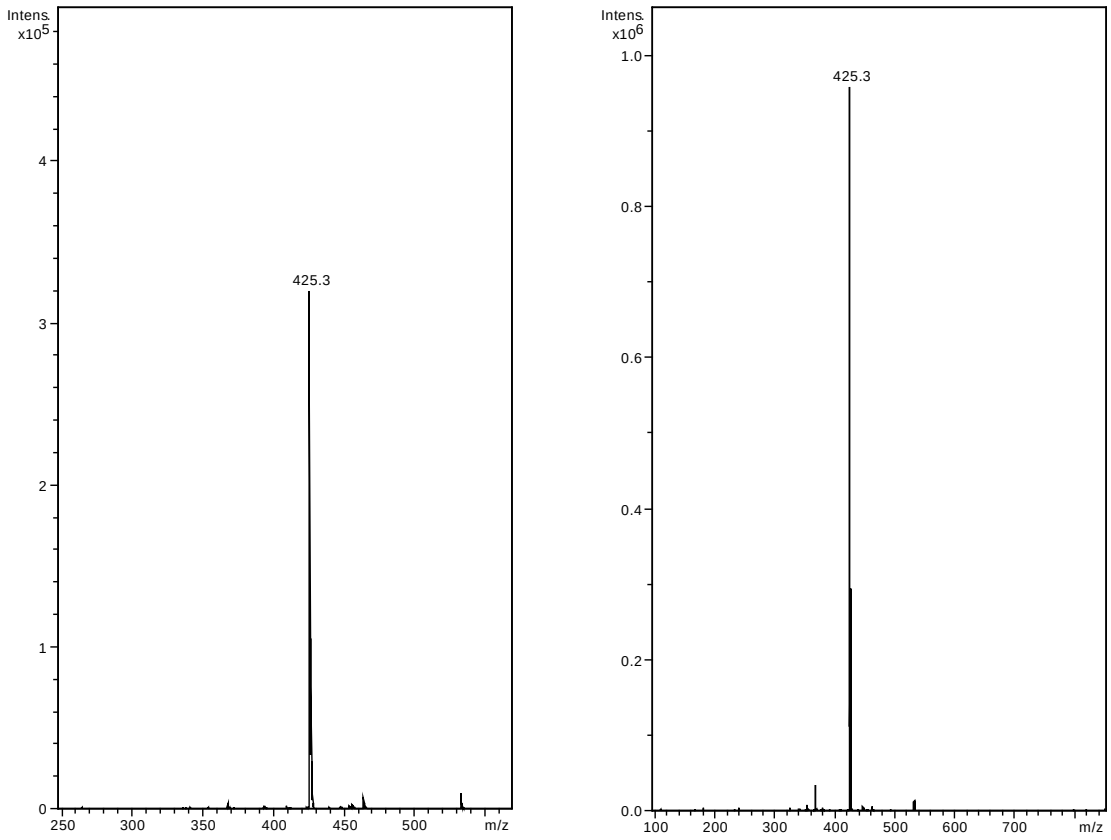

(a) **(b)**

Figure 34 – Mass spectra of the H33258 dye at pH 4.5 (a) and pH 7(b).

Figure 35 a shows the mass spectrum obtained for CB[7] solution, also at pH 7 and 4.5. The main peak is at m/z = 1201, which was assigned to the adduct of CB[7] K^+ {CB[7] + K}$^+$, while the peak at m/z 620 was assigned to the doubly charged CB[7]-K^+ adduct {CB[7] + 2•K}$^{2+}$. The minor peaks at m/z = 869 and 454 are traces of CB[5] (from the synthesis of the CB[7] macrocycle) {CB[5] + K}$^+$ and {CB5 + 2•K}$^{2+}$. An aggregate of CB[7] and CB[5] (m/z 1035) was also observed at pH 4.5 {CB[7] + CB[5] + 2•K}$^{2+}$. (Figure 61, presented in the annex).

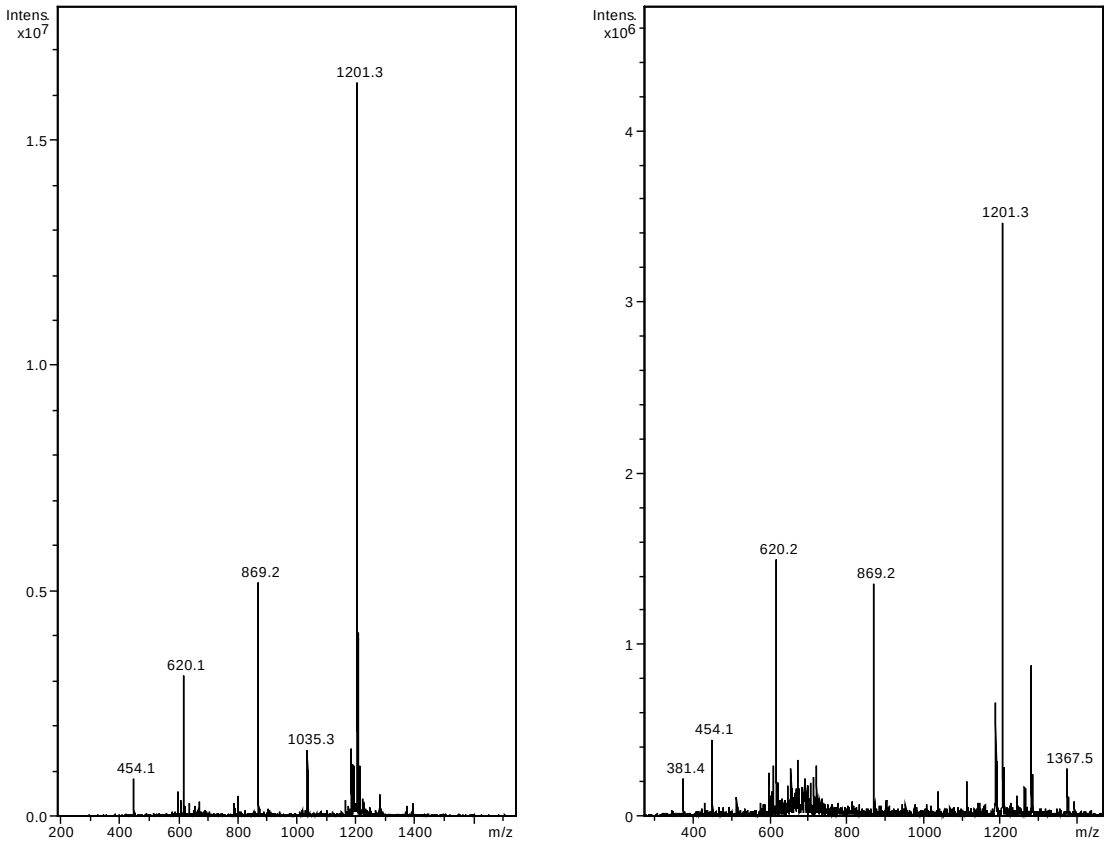

(a) **(b)**

Figure 35 – Mass spectra of CB[7] at pH 4.5 (a) and pH 7 (b).

The ESI-MS spectra of a mixture of 3 µM H33258 dye and 10 µM CB[7] (1 : 3 ratio), at pH 7 and 4.5, are shown in Figure 36. At pH 4.5 the major peaks at m/z 794, 530 and 813 are due to the complex. The structures of the ions are: m/z 794 - {CB[7] + H33258 + 2•K}$^{2+}$; m/z 813 - {CB[7] + H33258 + H + K}$^{2+}$; m/z 530 - {CB[7] + H33258 + 3•H}$^{3+}$ (see Figure 62 in the annex). At pH 7 the main peaks are at m/z 794, 813, and 1201.

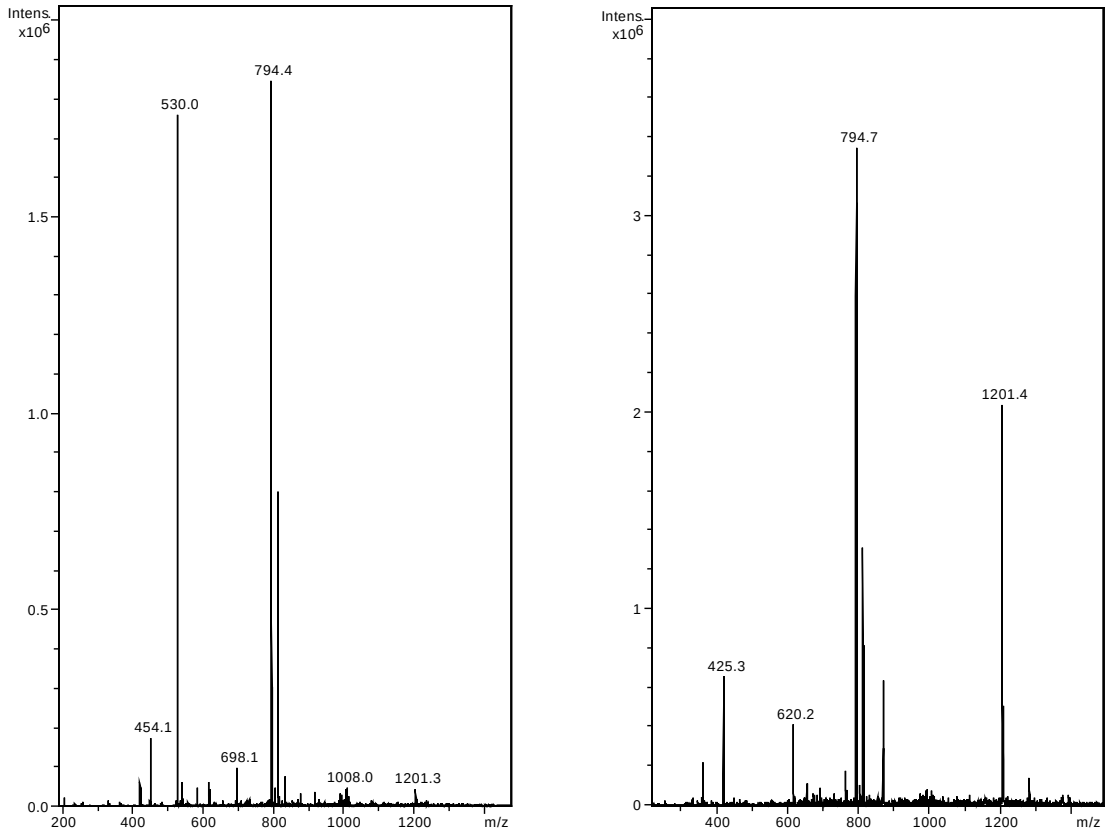

(a) **(b)**

Figure 36 – Mass spectra of H33258/CB[7] (3 µM / 10 µM) at pH 4.5 (a) and pH 7 (b).

IV.8 – NMR

^{1}H-NMR studies were performed in order to confirm the binding mode of H33258 in the complex.

Figures 37 and 38 show the results obtained for the free H33258 dye, while in the Figures 39 and 40 the corresponding data for the H33258/CB[7] complex are shown. The numbers in the figures correspond to the proton assignment of the dye, which was made according to reference[181] and the COSY spectra (Figures 38 and 40).

Noteworthy, the aromatic signals of the uncomplexed dye are rather broad and of relatively low resolution. This may be interpreted as commonly observed dye

aggregation, especially at the relatively high concentrations which had to be used in the NMR spectroscopic experiments (5 mM H33258).

In Figure 39 the ^{1}H-NMR spectra of the uncomplexed and the complexed dye are compared. The most notorious observation is that in the complex the proton signals of the dye are rather shifted (upfield or lowfield) and now a much higher resolution of the signals is observed. The same applies to the methylene protons of the piperazine ring. The for in-cavity complexation typical upfield shift is noted for the protons of the piperazine and the ones of the neighbouring benzimidazole (bz1).

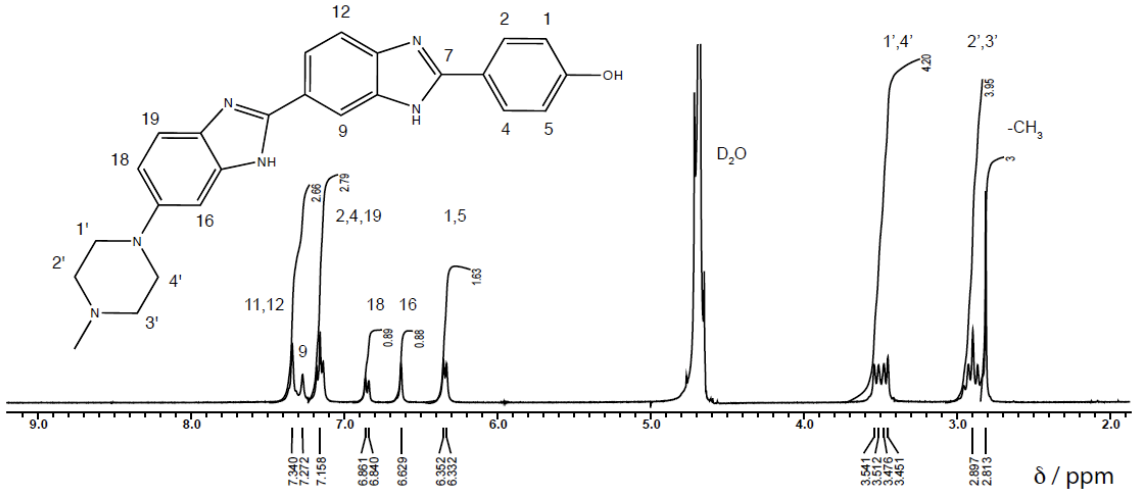

Figure 37 - ^{1}H-NMR spectrum of H33258 dye (5 mM) in 50 mM DCl. Peak assignments were made according to reference [181]

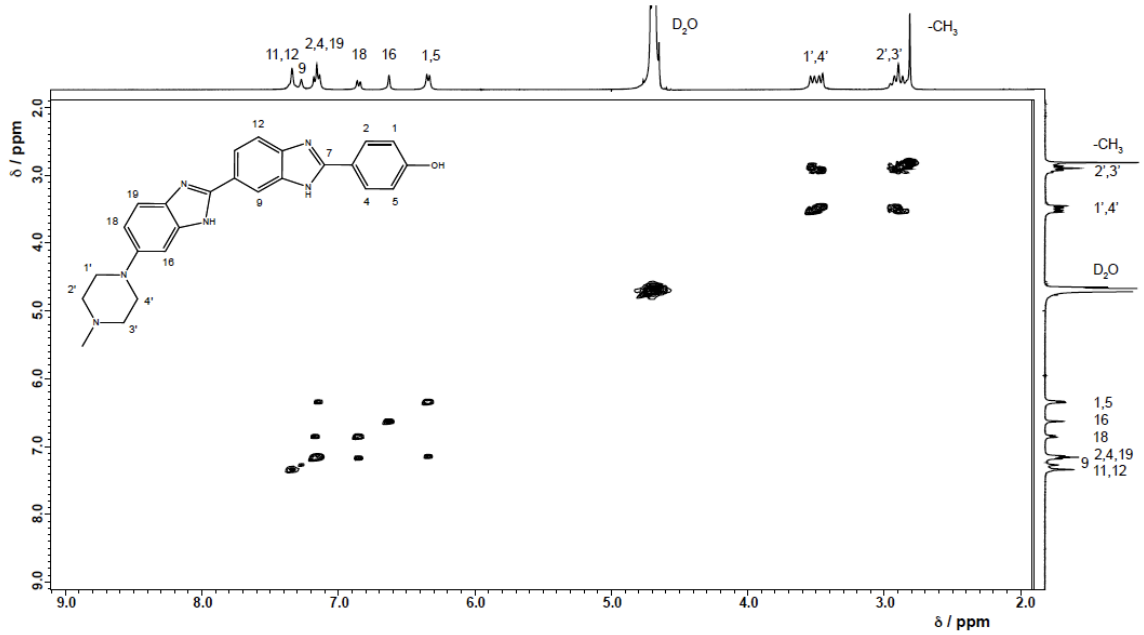

Figure 38 - 2D-NMR: COSY spectrum of H33258 dye (5 mM) in 50 mM DCl.

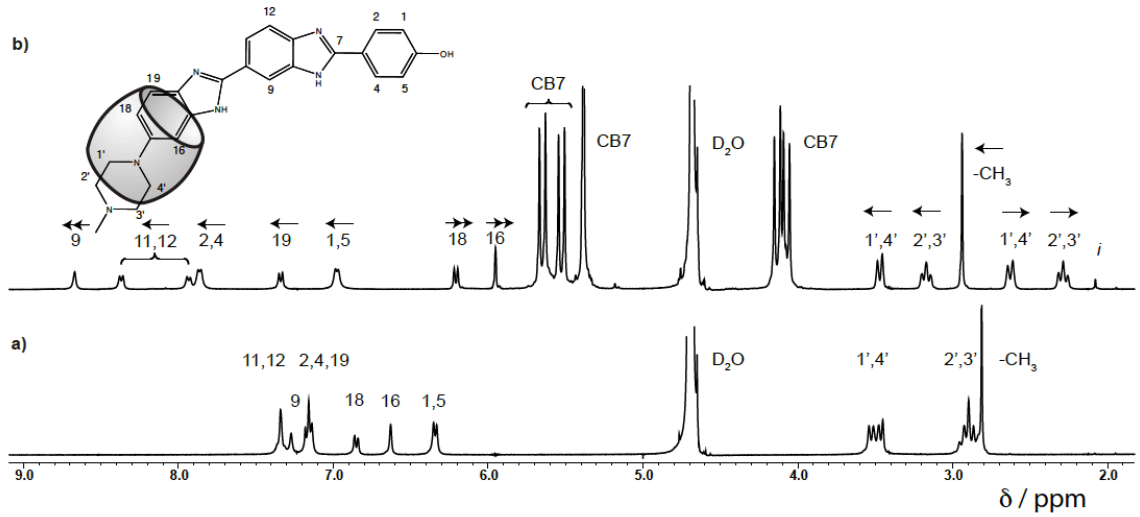

Figure 39 - Comparison of ^{1}H NMR spectra of a) H33258 dye (5 mM) in its free form in 50 mM DCl and b) H33258 dye (3 mM) in presence of CB[7] (3 mM) in 10 mM DCl. Characteristic complexation-induced shifts are represented with arrows. In the proposed structure of the complex, the CB[7] macrocycle is represented as a barrel. "i" marks a minor impurity in the DCl solution.

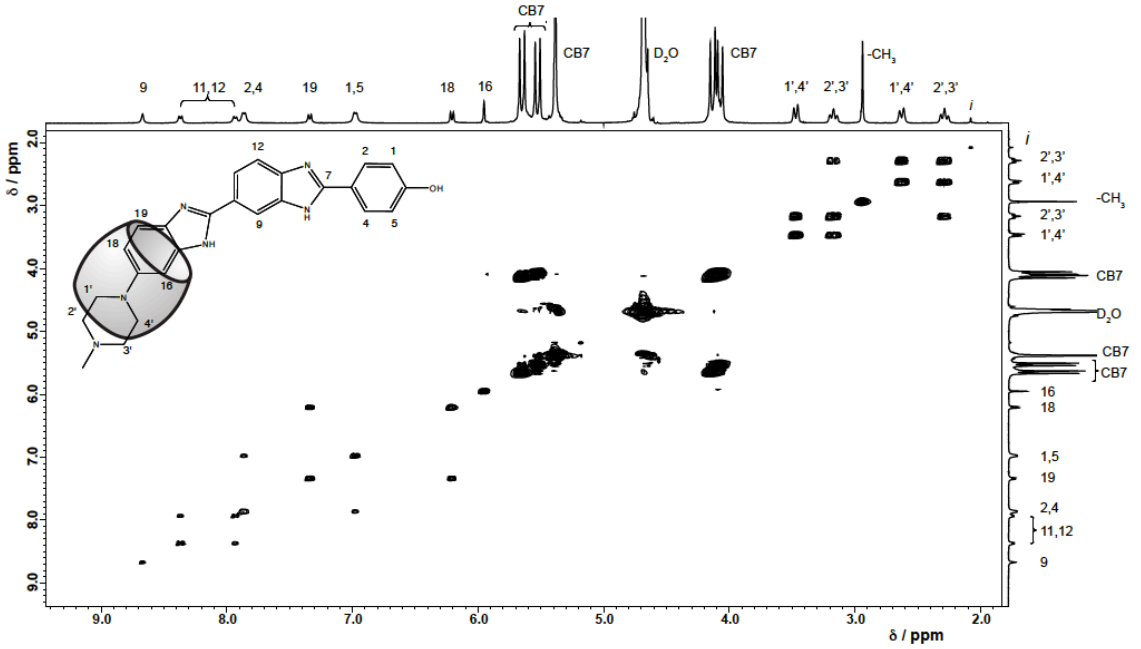

Figure 40 - 2D-NMR: COSY spectrum of H33258 dye (3 mM) in presence of CB[7] (3 mM) 10 mM DCl.

IV.9 – Competitive fluorescence titration with biological polyamines

A competitive fluorescence titration allows the measurement of binding constants of guests that are not fluorescent. In this work, this technique was used to determine the binding constants of various polyamines by CB[7]. For this purpose the highly fluorescent H33258/CB[7] complex (1 µM / 3 µM) was titrated with the respective amines. As a result of the competition between the dye and the amine for CB[7] host, the dye is released and consequently fluorescence quenching is observed (note: the fluorescence quantum yield of the dye in water is *ca.* 70 times lower than in the complex). The thus determined binding constants resulting from the fitting of the titration curves according to a competitive binding mode are summarized in Table 8. The corresponding titration plots are shown in Figures 41-45.

Table 8 – Polyamine structure and binding constant towards CB[7].

Polyamine	**Structure**	***K* (M^{-1})**
Spermine		2.6×10^7
Cadaverine		2.0×10^7
Spermidine		1.2×10^6
Putrescine		1.1×10^5
Histamine	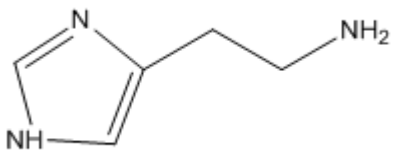	1.7×10^4

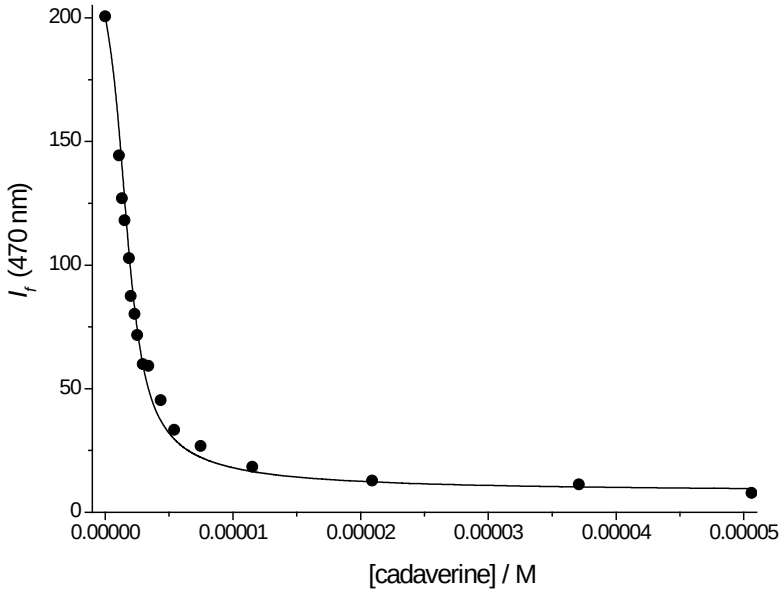

Figure 41 – Competitive fluorescence titration of H33258/CB[7] with cadaverine. The λ_{obs} selected for the plot was 470 nm and the fluorescence measurements were made at λ_{exc} = 295 nm.

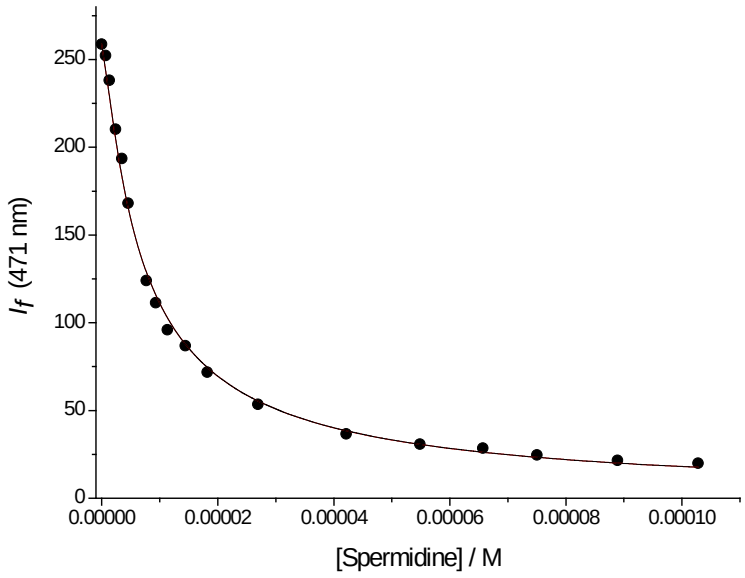

Figure 42 – Competitive fluorescence titration of H33258/CB[7] with spermidine. The λ_{obs} selected for the plot was 471 nm and the fluorescence measurements were made at λ_{exc} = 295 nm.

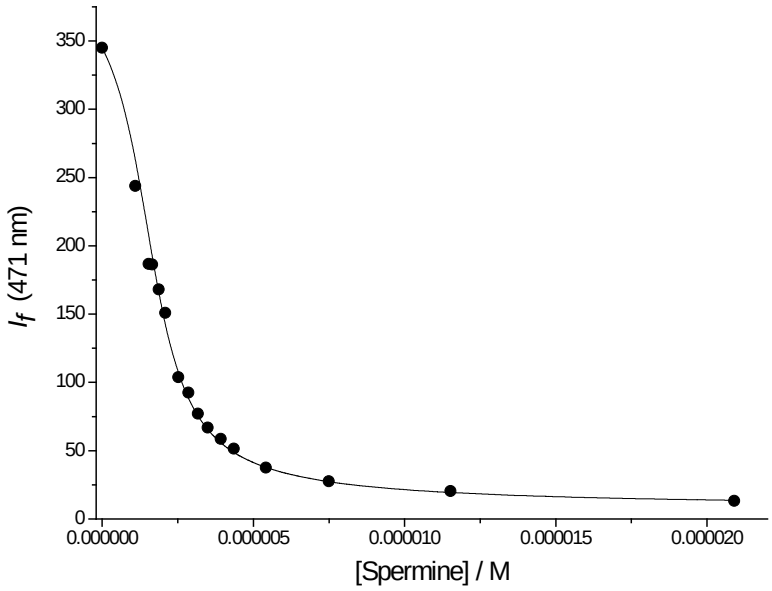

Figure 43 – Competitive fluorescence titration of H33258/CB[7] with spermidine. The λ_{obs} selected for the plot was 471 nm and the fluorescence measurements were made at λ_{exc} = 295 nm.

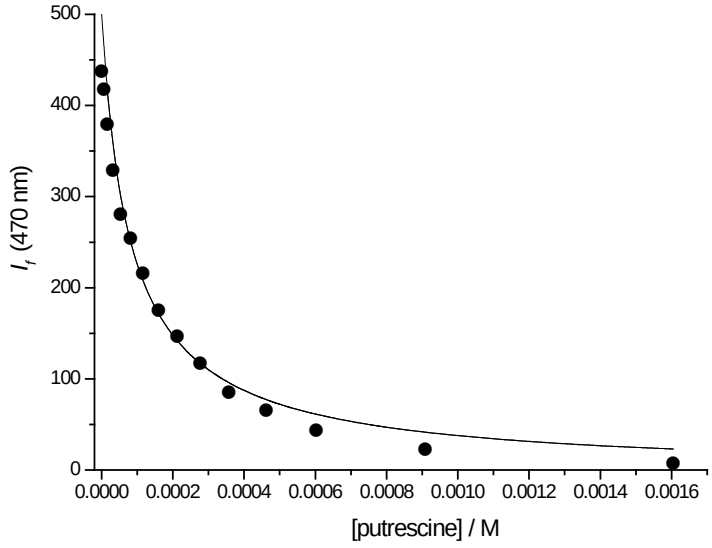

Figure 44 – Competitive fluorescence titration of H33258/CB[7] with putrescine. The λ_{obs} selected for the plot was 470 nm and the fluorescence measurements were made at λ_{exc} = 295 nm.

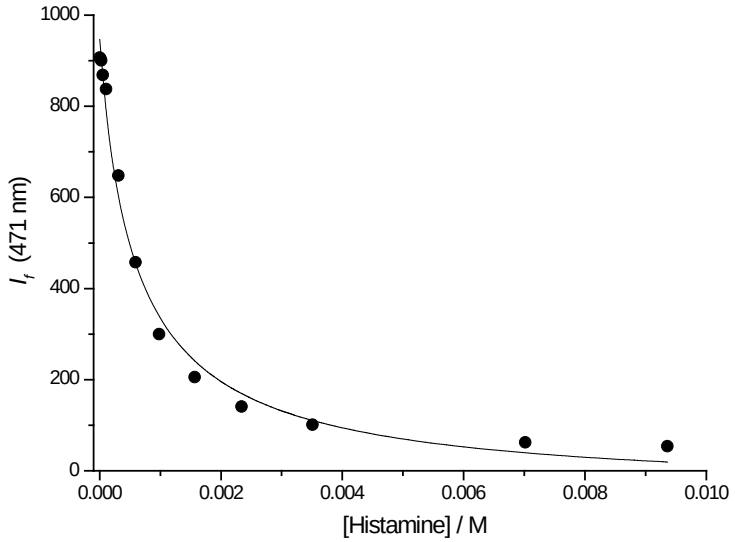

Figure 45 – Competitive fluorescence titration of H33258/CB[7] with histamine. The λ_{obs} selected for the plot was 471 nm and the fluorescence measurements were made at λ_{exc} = 295 nm.

IV.10 – CT-DNA titration in 1 mM phosphate buffer (pH 7.2)

Titrations with CT-DNA were performed by observation of changes in the absorption and fluorescence signals of the dye.

IV.10.1 – Hoechst 33258

Figure 46 shows the UV-Vis absorption titration of 2 µM H33258 dye with CT-DNA. For concentrations until *ca.* 2 µM the addition of CT-DNA caused a decrease of the absorption at 338 nm. Upon further addition of CT-DNA (up to *ca.* 14 µM) a gradual bathochromic shift (to finally 363 nm) and a slight increase of the absorption signal was noted.

The fluorescence titration of 1µM H33258 dye with CT-DNA is shown in Figure 47. For concentrations until *ca.* 1 µM the addition of CT-DNA caused a small decrease of the fluorescence intensity at 472 nm. Upon further addition of CT-DNA (up to *ca.* 7

μM) a gradual increase of the fluorescence intensity signal and a slight bathochromic shift (to finally 475 nm) and was noted.

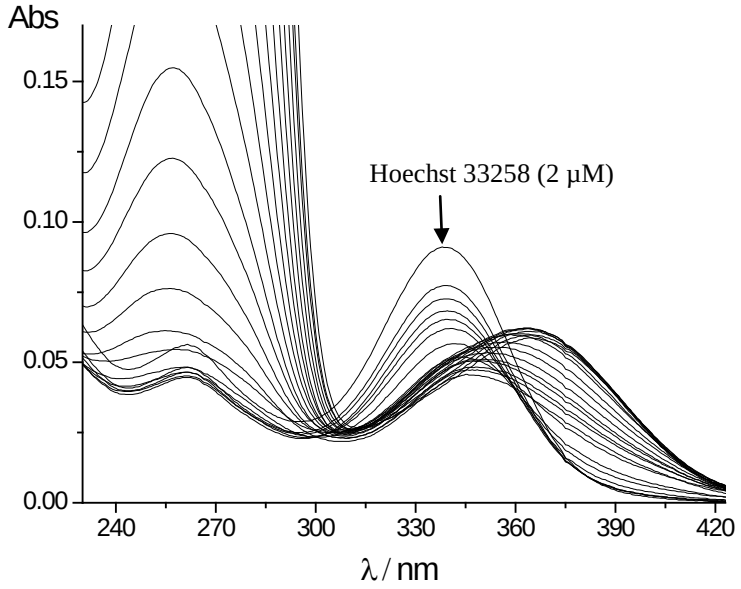

Figure 46 – Absorption titration of 2 μM H33258 dye with CT-DNA in 1 mM phosphate buffer solution at pH 7.2.

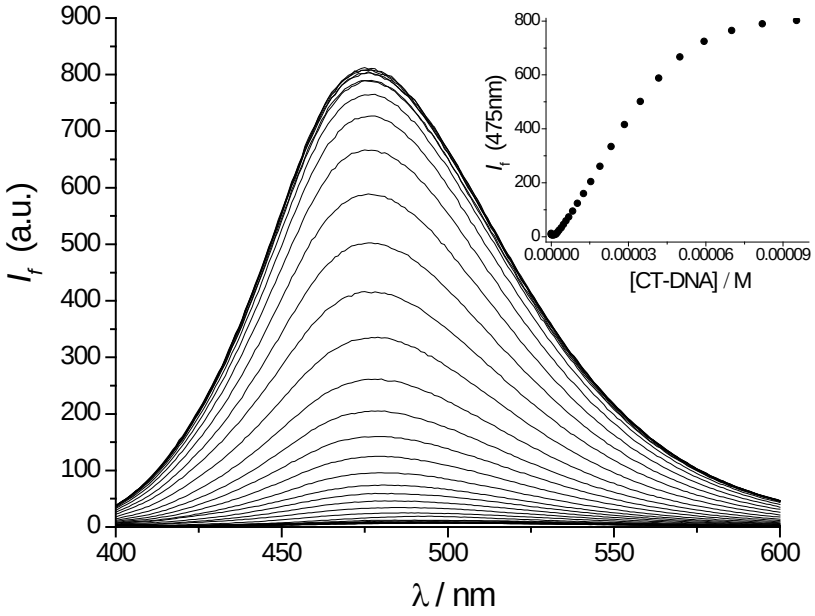

Figure 47 – Fluorescence titration spectra of 1μM H33258 dye with CT-DNA in 1 mM phosphate buffer solution at pH 7.2. The measurement conditions were: λ_{exc} = 354 nm. Inset: The fluorescence amplitude, in arbitrary units, at 475 nm is plotted *versus* the amount of added CT-DNA.

IV.10.2 – H33258/CB[7] complex

Figure 48 shows the UV-Vis absorption titration of the complex H33258/CB[7] (2 µM / 6 µM, respectively) with CT-DNA. For concentrations until *ca.* 13 µM the addition of CT-DNA caused a decrease of the absorption at 348 nm. Upon further addition of CT-DNA (up to *ca.* 60 µM) a gradual bathochromic shift (to finally 363 nm) and a slight increase of the absorption signal, as seen before for the free dye.

The fluorescence titration of H33258/CB[7] complex with CT-DNA is shown in the Figures 49 and 50. For concentrations until *ca.* 7 µM the addition of CT-DNA caused a decrease of the fluorescence intensity at 472 nm. Upon future addition of CT-DNA (up to *ca.* 60 µM) a gradual increase of the fluorescence intensity signal and a slight bathochromic shift (to finally 475 nm) was noted.

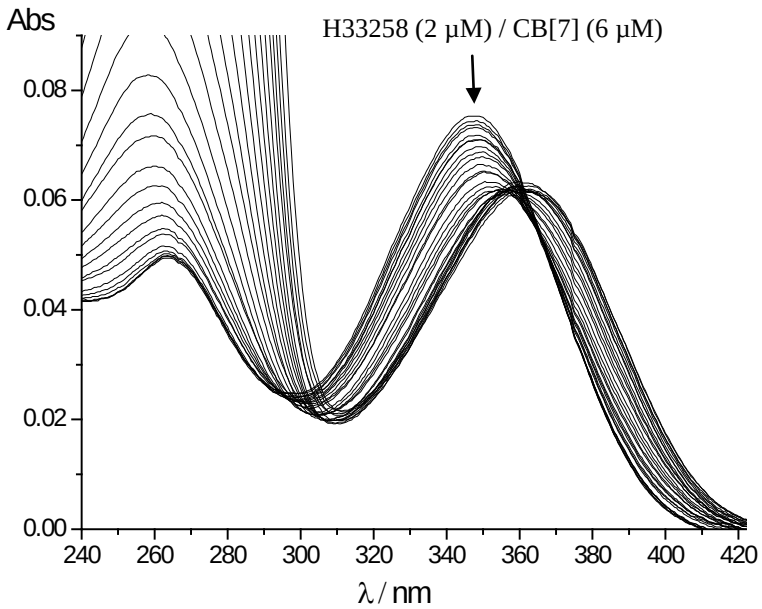

Figure 48 – Absorption titration of H33258/CB[7] complex (2 µM / 6 µM) with CT-DNA in 1 mM phosphate buffer solution at pH 7.2.

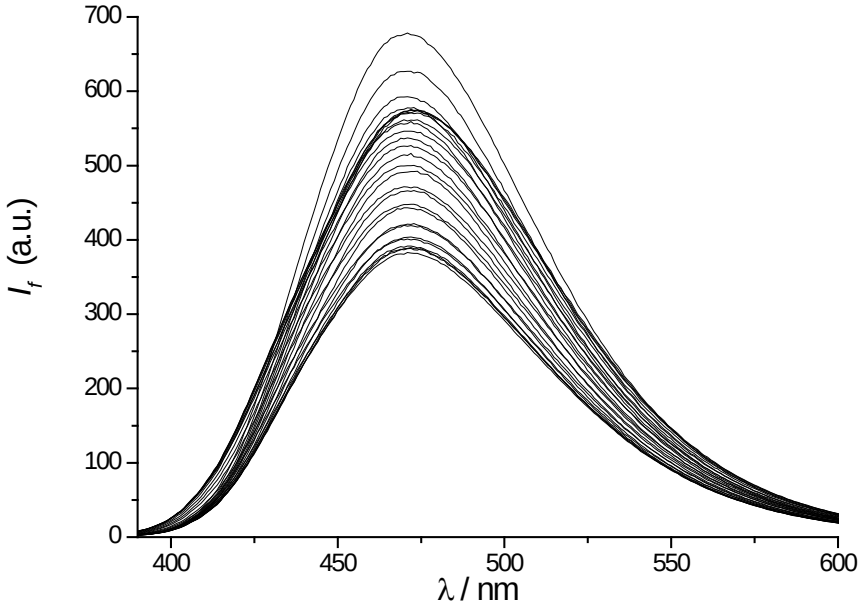

Figure 49 – Fluorescence titration spectra of H33258/CB[7] complex (1 µM / 3 µM) with CT-DNA in 1 mM phosphate buffer solution at pH 7.2. The measurement conditions were: λ_{exc} = 358 nm.

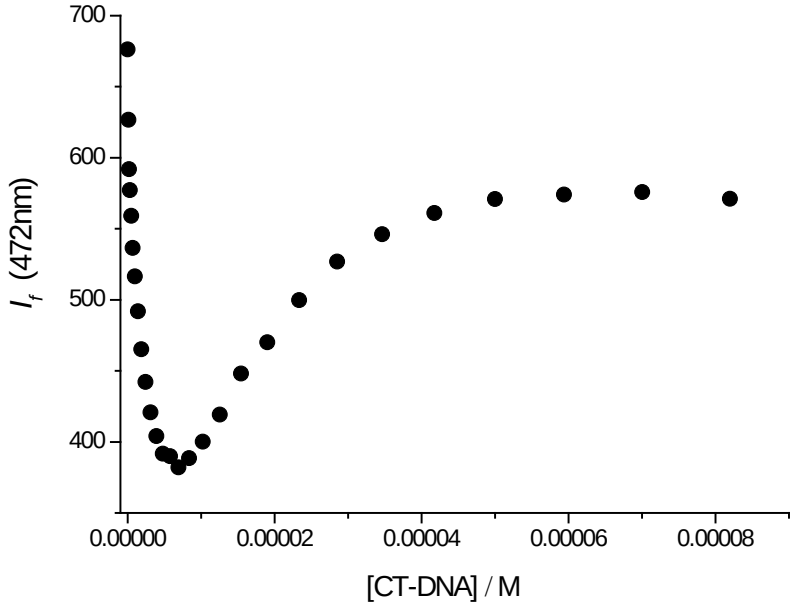

Figure 50 – Fluorescence titration of H33258 dye with CB[7] at pH 7. The fluorescence amplitude, in arbitrary units, at 472 nm is plotted *versus* the concentration of CT-DNA.

IV.11 - Fluorescence titration of the mixture H33258/CB[7]/CT-DNA with CB[7] and amantadine

Two different CT-DNA concentrations of the titration (Figure 50) were strategically chosen (6.9 and 59.3 μM). One corresponds to the lowest fluorescence intensity and the other is the plateau region.

The fluorescence titration of the mixture containing 1μM H33258/ 3μM CB[7]/ 6.9 μM CT-DNA with CB[7] is shown in Figure 51. The consecutive addition of CB[7] led to an increase of the fluorescence intensity at 472 nm until a plateau was reached at *ca.* 20 μM CB[7].

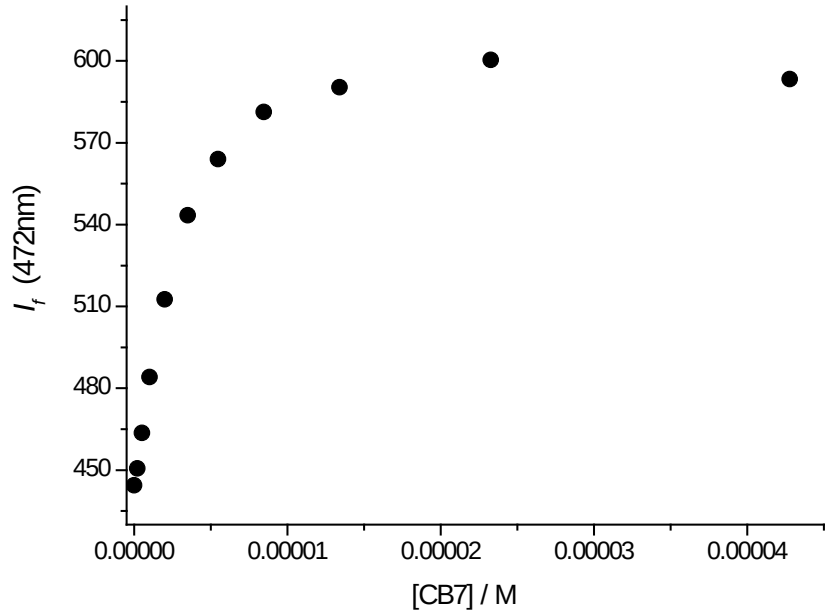

Figure 51 – Fluorescence titration curve of 1μM H33258/3μM CB[7]/6.9 μM CT-DNA mixture with CB[7] in 1 mM phosphate buffer solution at pH 7.2 for λ_{exc} = 358 nm. The fluorescence amplitude, in arbitrary units, at 472 nm is plotted *versus* the concentration of CT-DNA.

The fluorescence titration of the mixture 1μM H33258/ 3μM CB[7]/ 59.3 μM CT-DNA with CB[7] is shown in Figure 52. The consecutive addition of CB[7] led to an increase of the fluorescence intensity at 475 nm until a plateau was reached at *ca.* 31 μM CB[7]. These changes are accompanied by a subtle hypsochromic shift to 472 nm ($\Delta\lambda$ = -3 nm).

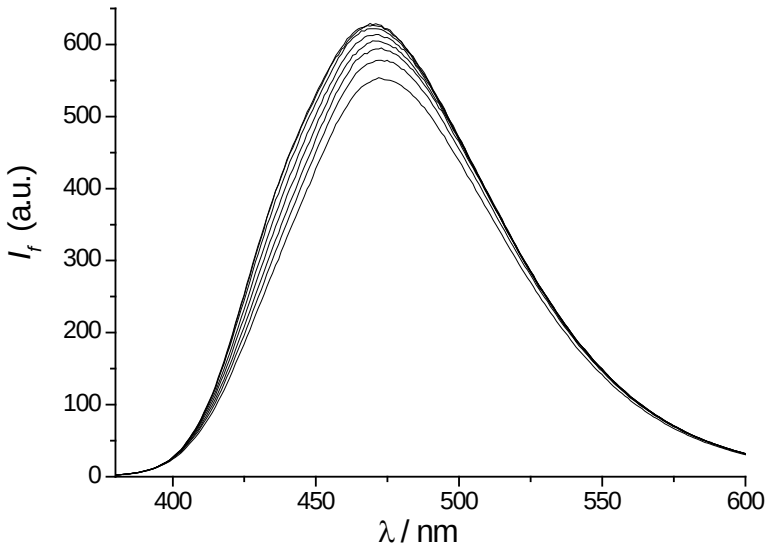

Figure 52 – Fluorescence titration spectra of the mixture 1μM H33258/3μM CB[7]/59.3 μM CT-DNA complex with CB[7] in 1 mM phosphate buffer solution at pH 7.2 and at λ_{exc} = 358 nm.

The competitive experiments with amantadine (see structure below) were performed because it is known that this amine has a high binding affinity to CB[7]. In control experiments it was shown that amantadine has no influence on the fluorescence of the H33258/CT-DNA complex.

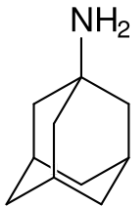

Figure 53 – Structure of amantadine

However, addition of amantadine to the solution of 1μM H33258/ 3μM CB[7]/ 6.9 μM CT-DNA led to a gradual decrease of the fluorescence intensity at 472 nm, (see Figure 54). On the other hand, the addition of amantadine to the solution of 1μM H33258/ 3μM CB[7]/ 59.3 μM CT-DNA did not yield the same result. Here a much higher amine concentration was needed to observe some fluorescence decrease (see Figure 55). Further, these changes were accompanied by a small bathochromic shift from 472 to 475 nm.

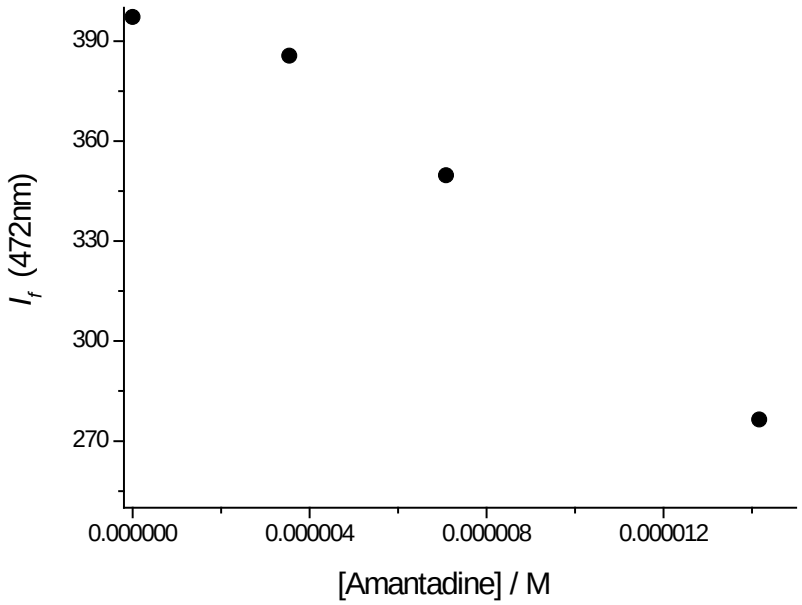

Figure 54 – Addition of amantadine to 1μM H33258/3μM CB[7]/6.9 μM CT-DNA mixture in 1 mM phosphate buffer solution at pH 7.2. The intensity at λ_{obs} = 472 nm is plotted *versus* the amantadine concentration and the λ_{exc} was at 358 nm.

.

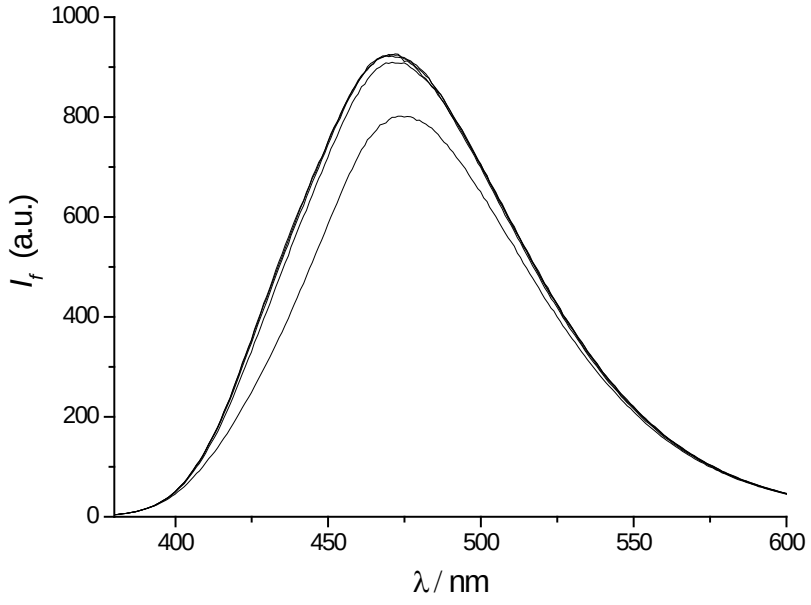

Figure 55 – Addition of amantadine to the mixture 1μM H33258/3μM CB[7]/59.3 μM CT-DNA in 1 mM phosphate buffer solution at pH 7.2. The conditions were: λ_{exc} = 358 nm.

IV.12 – Circular dichroism of Hoechst 33258 with CT-DNA

Circular dichroism (CD) spectroscopy measures differences in the absorption of left-handed polarized light *versus* right-handed polarized light which arise due to chirality. Inherently achiral compounds, like the H33258 dye, show no CD signal. However, when an achiral molecule is integrated in a chiral environment chirality transfer results and induced CD (ICD) can be observed.

The results obtained are presented in Figure 56, were we can see that both the H33258 dye and CB[7] do not exhibit any ICD signals at the wavelength of absorbance of the dye (Figure 56a). On the other hand the 2 µM H33258/ 0.3 µM DNA mixture shows an ICD spectrum with a peak at 348 nm. The 2 µM H33258/ 59 µM DNA mixture showed a spectrum with a peak at 365 nm. The H33258/CB[7]/CT-DNA solution gave similar results.

(a)

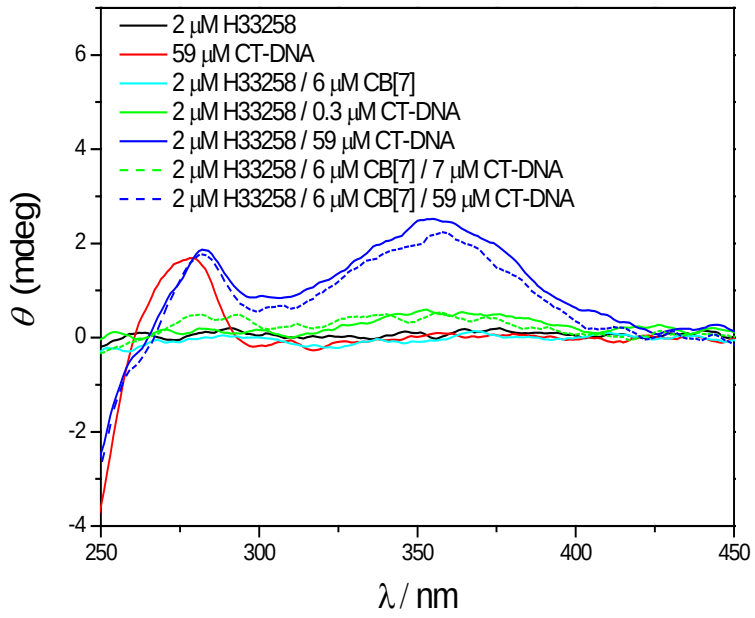

(b)

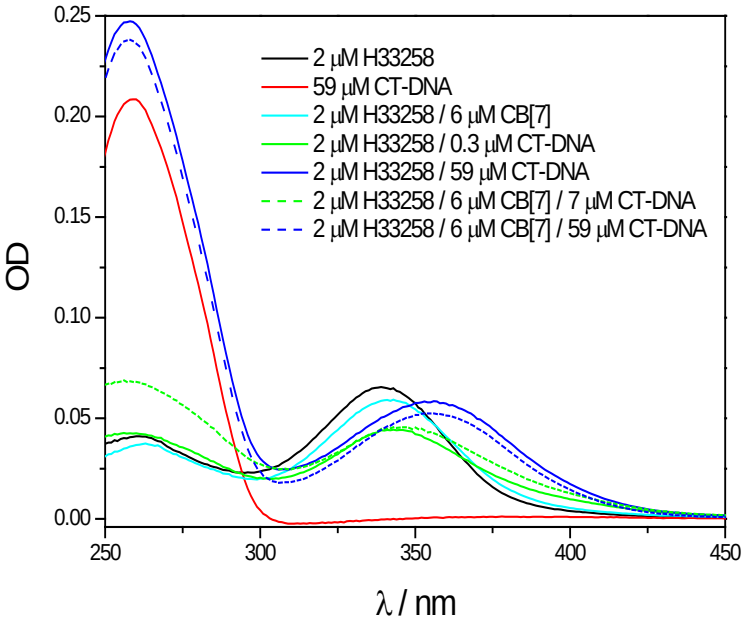

Figure 56 –ICD spectra **(a)** and UV-Vis absorption spectra **(b)** of the H33258 dye (2 μM) alone, CT-DNA (59 μM), and in its respective DNA complex (0.3 and 59 μM), CB[7] complex, and in the DNA complex (7 and 59 μM) in presence of CB[7] (6 μM).

V – Discussion

V.1 – Aggregation

It was safely determined that at pH 7 the dye does not self-aggregate below 30 µM, because the calculated slope of the Lambert-Beer plot (Figure 16) was about 42300 M^{-1} cm^{-1} at 339 nm, which virtually the same as the reported extinction coefficient of H33258 dye (42000 M^{-1} cm^{-1} at 338 nm).[52,53,56,57] At pH 4.5 the extinction coefficient of the dye is not described in the literature and was calculated in this work as 21000 M^{-1} cm^{-1} at 382 nm. The results corroborate that at the H33258 dye concentrations used in this work (1-2 µM) no self-aggregation is to be considered. This is supported by Banerjee and Pal, who verified trough fluorescence transients that at 1 µM the dye does not self-aggregate.[60] Furthermore, Görner observed the for aggregation typical downward curving in the Lambert-beer plots only for dye concentrations above 40 µM.[53]

However, for time-resolved fluorescence measurements and ^{1}H-NMR spectroscopic experiments higher concentrations of the H33258 dye were necessary (0.1-5 mM), at which dye aggregation may play some role. This was verified by the shorter lifetime component in the fluorescence decay curve, that is an expression of aggregation of about one third (33%) at 0.1 mM. On the other hand, the aromatic signals (6.3-7.4 ppm) in the ^{1}H-NMR spectrum of the dye at 5 mM concentration were rather broad, thereby pointing to dye aggregation. Interestingly, the addition of CB[7] caused de-aggregation of the dye, because only one H33258 is accommodated in the macrocycle cavity. Now rather sharp and spectrally well-resolved NMR signals were obtained. The short fluorescence lifetime component also disappeared.

V.2 – Protonation equilibria and photophysical characteristics

From the literature it is known that the H33258 dye has a large Stokes shift and that its photophysical properties changes with pH. In this work it was confirmed that H33258

has a large Stokes shift at pH 7 (*ca*. 130 nm), as shown in Figure 57. The absorption and fluorescence spectra suffer pronounced shifts at different pH values.

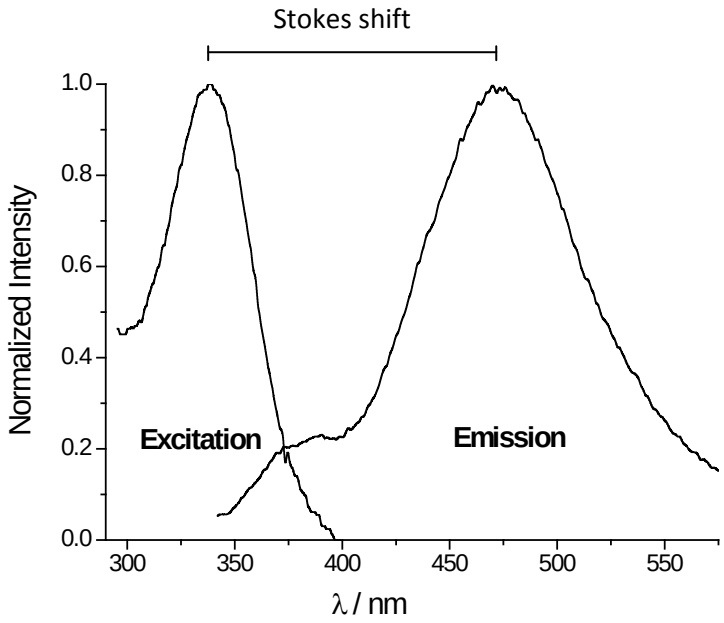

Figure 57 – Stokes shift of H33258 dye in water at pH 7.

The photophysical behaviour and excited deactivation mechanisms of H33258 dye have been subject of some controversial discussion. However, only very few reports, including partially contradictory mechanistic interpretations, are known in the literature.[51,53,54,60] Briefly summarizing, the pH dependence of the dye's fluorescence has been interpreted by invoking excited state intramolecular charge transfer and proton transfer. Noteworthy, no conclusive scheme explaining all observations in a compatible manner seems to exist.

For this purpose in the following paragraphs it is aimed to arrive at an acceptable photophysical fundament, which can explain the corresponding fluorescence properties of the free dye in its different protonation states as well as in the environment of supramolecular hosts like CB[7] or CT-DNA, which have been used in this thesis.

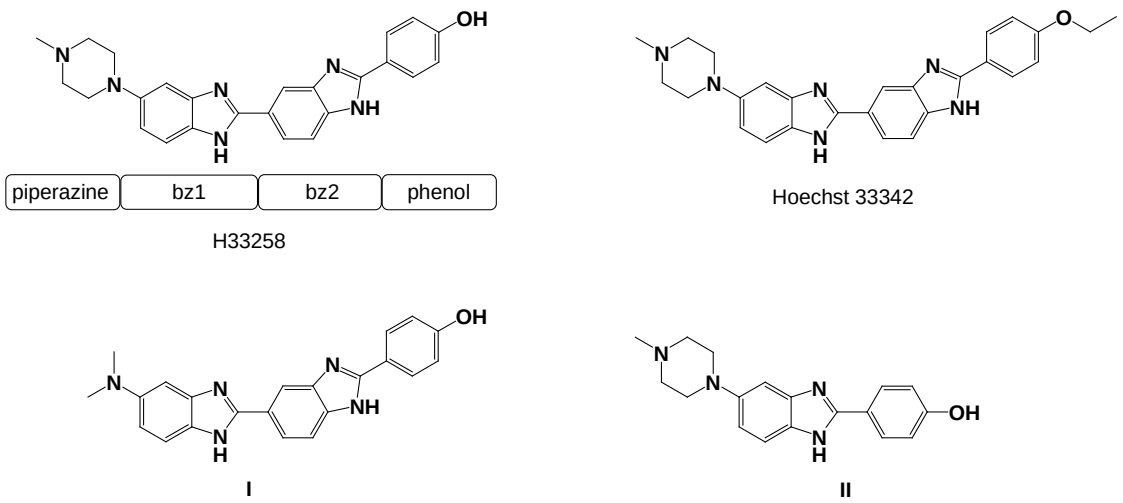

Scheme 2 - The structures of neutral H33258, Hoechst 33342, and the model compounds **I**, **II**.

As a matter of fact, the strong dependence of the Stokes shift and emission maximum on the pH supports the occurrence of charge transfer. While some authors favour charge transfer from the protonated piperazine-bz1 unit to the bz2-phenol unit,[51,54] arguments for the reverse direction may be found as well (see bz1 and bz2 assignment of H33258 in Scheme 2).[60] Intuitively, the amino group, which is conjugated with the aromatic bz1 system, is not a very good electron donor because the proton at the piperazine is shared between both nitrogens *via* hydrogen bonding. Often the work of Kalninsh *et al*. is cited, who reported some semiempirical PM3 calculations of an unprotonated H33258 analogue (see structure **I** in Scheme 2).[51] They found that charge transfer is most likely to proceed from the piperazine-bz1 units to the bz2-phenol unit. However, the electronic situation is completely different for the protonated dye and additionally the calculations refer to the gas phase, not taking into account the pronounced solvent dependence of the excited state behaviour of the dye. Furthermore, at pH 4.5, where the charge transfer fluorescence of the free dye is at its maximum (see discussion below), the bz1 imidazole is protonated as well, which make the complete unit rather an electron acceptor than a donor. The role of the protonated bz1 in the charge transfer process gets even more corroborated by the fact that a simple benzimidazole with corresponding piperazinyl and phenol substitution (see structure **II** in Scheme 2) does not have the same low fluorescence as the H33258 dye in neutral aqueous solution. Furthermore, it

seems very clear is that both benzimidazole units are required for the observation of the peculiar fluorescence behaviour of the dye.

The incidence of proton transfer for the phenolic OH to the bz2 benzimidazole was first argued by Kalninsh *et al.*,[51] but later questioned by Cosa *et al.*[54] However, the occurrence of proton transfer cannot be excluded *ad hoc* and the argument by the latter authors, that the fluorescence lifetimes of H33258 and its *O*-alkylated derivative Hoechst 33342 are similar, is quite empirical. Hence, charge transfer from bz2-phenol to protonated piperazine-bz1 as well as proton transfer from the phenol should be involved to explain the quite peculiar pH dependence of the fluorescence quantum yield of H33258.

It turns out to be of interest to discuss strategic points of the pH titration curve, for which concrete protonation states of H33258 can be assigned. These are: pH < 2 for the triprotonated dye (piperazine, bz1 and bz2); pH = 4.5 for the diprotonated state (piperazine and bz1); pH = 7 for monoprotonation (piperazine); pH 9 for the monoanion (OH deprotonation).[49]

The red-shift of the emission at pH 4.5 and the strong fluorescence (Φ_f = 0.29, this thesis) are coincident with preferential formation of a strongly fluorescent charge transfer state, which has been also described to be accompanied by a planarization of both benzimidazole rings.[51,54] The latter geometrical change counteracts the free rotation around the bz1-bz2 axis and reduces the non-radiative deactivation, thereby contributing at least partially to the increased fluorescence. Upon further protonation of bz2 at pH < 2, the charge transfer with the bz2-phenol unit as electron donor becomes less favourable. On the other hand, at pH 7 the monoprotonated piperazine-bz1 unit is a less strong electron acceptor, thereby lowering the charge transfer probabilities. This goes hand in hand with a dramatic drop of the fluorescence quantum yield (Φ_f = 0.01, this thesis). A lower degree of charge transfer means increased deactivation by internal rotation, as mentioned before. At basic pH, where the piperazine-bz1 unit is completely deprotonated, charge transfer is not anymore a feasible pathway and internal rotation plays a dominant role in non-radiative excited state deactivation.[54,60]

However, proton transfer (see above) should be also discussed, especially at pH 7, which involves an essentially non-fluorescent quinoid structure.[48,51] A similar structure could be formed in the ground state of the deprotonated phenol (pH 9).[54]

In summary, the free dye has its maximum fluorescence quantum yield for the diprotonated form, because this structure accommodates excited charge transfer best. The other forms have lower fluorescence probabilities, because of less favourable electronic conditions for charge transfer, increased non-radiative deactivation via internal rotation, and possibly the impact of proton transfer leading to non-fluorescent quinoid forms. The combined mechanistic interpretation for the fluorescence behaviour of H33258 at different pH values is summarized in Scheme 3.

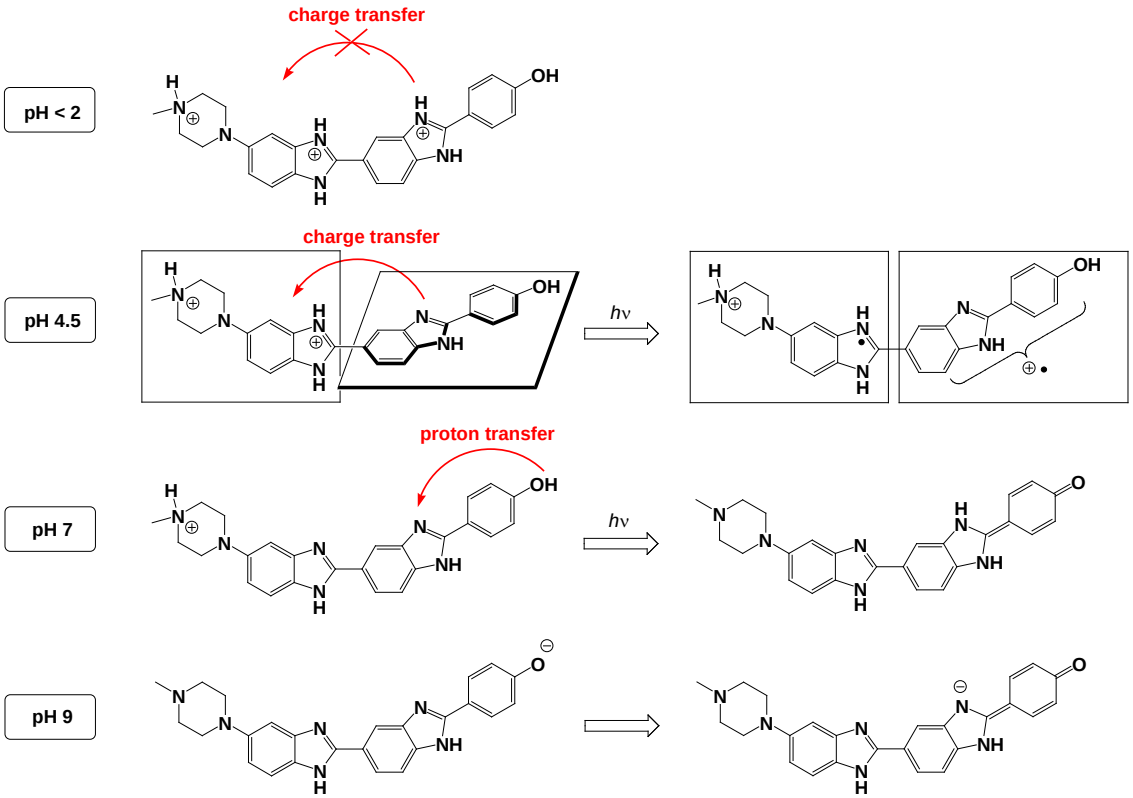

Scheme 3 - The different mechanisms, which modulate the fluorescence of H33258 at different pH values in aqueous solution.

Preliminary semiempirical AM1 calculations (Figure 58) have shown that the HOMO in unprotonated model I, is located at the dimethylamino-bz1 unit, while the LUMO is related to the bz2-phenol moiety. Hence, as expected, charge transfer happens in the bz1

to bz2 direction. However, diprotonated H33258, which prevails at pH 4.5 with the highest fluorescence quantum yield of the free dye, shows expectedly the exactly opposite HOMO-LUMO distribution, which lends additional arguments to the in Scheme 3 presented mechanistic interpretation.

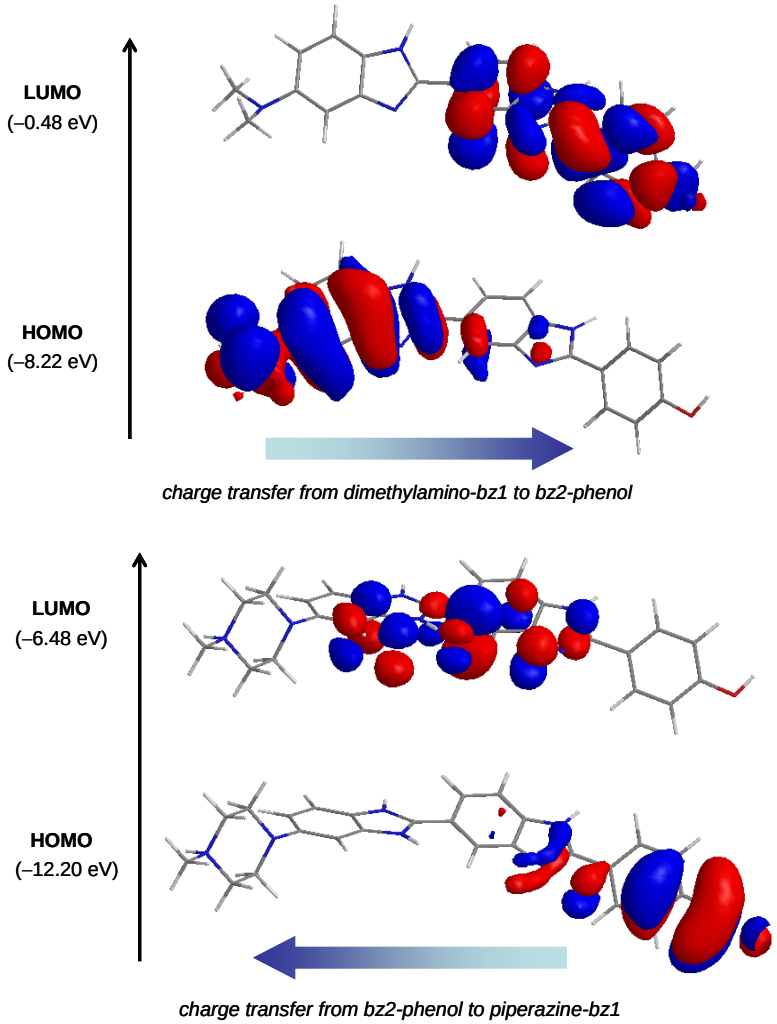

Figure 58 - HOMO-LUMO AM1 calculations for model **I** and H33258.

In non-aqueous solution like polar DMF or less polar alcohols the fluorescence quantum yields of the dye are reported also as very high (Φ_f = 0.4-0.5).[53] This may be explained by the absence of proton transfer in these solvents. However, it is not really clear what is the protonation state of the dye in these organic solvents. If the dye would be in its neutral form, the charge transfer (this time from the non-protonated piperazine-bz1 unit

to the bz2-phenol unit) may lead as well to strong charge transfer fluorescence. What speaks for the latter argumentation is the blue-shifted emission band in these less polar solvents as compared to water.

When the H33258 dye is immersed in the environment of supramolecular hosts, very high fluorescence quantum yields have been observed (Φ_f = 0.74 in CB[7] at pH 7 and Φ_f = 0.62 in CT-DNA at pH 7.2, this thesis). The minor groove of CT-DNA, which is the preferred binding site of H33258, is known to have a polarity close to that of alcohols. It can be assumed that a similar situation as discussed above for alcohols applies here. However, what is decisive for the strongly fluorescent nature of the dye in CT-DNA, is the planarization of the two benzimidazoles due to the confinement effects exerted by the minor groove.[84] This results in a suppression of non-radiative deactivation through internal rotation. Noteworthy, despite the strong charge transfer character of the dye water at pH 4.5, the latter path is still contributing due to the absence of the confinement effects. The higher energy of the fluorescent charge transfer state is expressed by a pronounced blue shift of the emission maximum, akin to the observations made for neat alcohol solvents.

In the case of CB[7] as host, similar dramatic fluorescence enhancements as for CT-DNA were observed. It is more than reasonable to assume that the dye is present in its diprotonated form, stabilized by ion-dipole interactions with the two carbonyl portals of the macrocycle. The formation of a strongly fluorescent charge transfer state, akin to the situation observed for the free dye at pH 4.5, should be favoured. The resulting planar state is stabilized and internal rotation is hindered, which explains the *ca*. 2.5-fold increase in fluorescence quantum yield as compared to the situation of the diprotonated free H33258.

The changes in the absorption and fluorescence spectra provoked by the different pHs allowed the calculation of some pK_a values. Table 9 shows several dissociation constants attributed to the H33258 dye, and the values obtained by fluorescence are similar to the ones determined by the Clegg group.[49]

Table 9 – Dissociation constants of H33258 dye, where D represents the dye.

Protonation equilibrium	Computational estimated[a] pK_a	pK_a from literature[a]	pK_a from literature[b]	pK_a calculated[c]
$D^{3+} \rightarrow D^{2+} + H^+$	3.49 ± 0.03	4.16 ± 0.04	3.5	3.4
$D^{2+} \rightarrow D^{+} + H^+$	5.68 ± 0.03	5.71 ± 0.04	5.5	5.8
$D^{+} \rightarrow D + H^+$	7.94 ± 0.05	7.86 ± 0.02	8.5	9.1
$D \rightarrow D^{-} + H^+$	8.90 ± 0.03	8.77 ± 0.01	9.8	
$D^{-} \rightarrow D^{2-} + H^+$	11.69 ± 0.06	12.45 ± 0.02		

[a] reference [49]; [b] reference [57]; [c] measured by fluorescence.

On the other hand, the calculated pK_a values from UV-Vis absorption pH titration were 4.1 and 8.8 (not shown in Table 9), that are most likely to be assigned to the ones reported by the Zoete group for D^{3+} and D.[49]

Experimental fluorescence quantum yield and fluorescence lifetimes of the dye (Table 10) are also very similar with the ones described in the literature and mentioned in section I.2.2.

The same experiments were performed with the addition of CB[7] to the dye solution, which was never performed before. Not only an inferior Stokes shift (*ca*. 120 nm at pH 7) was found, but also a safe assignment of two pK_a values, that are 5.7 and 8.0, was made. For the assignment of the protonation state to these pK_a values it has to be taken into account that CB[7] leads to a shift of protonation equilibria through host-assisted guest protonation,[12] i.e., the dye becomes protonated easier in the complex causing an increase of the pK_a values, generally by 2-3 units.[12] Accordingly, the pK_a value 5.7 most likely corresponds to the triprotonated form (D^{3+}, ΔpK_a= 2.2), while the 8.0 is tentatively assigned to the diprotonated form (D^{2+}, ΔpK_a= 2.3).

By UV-Vis absorption only one pK_a of 9.0 was calculated. No safe assignment can be made in this case.

As mentioned above in the brief discussion about the photophysical mechanisms of H33258 and their implication in the flurescence of this dye, another striking effect upon addition of cucurbituril is observed in fluorescence quantum yield, that has an increase of Φ_f about 73 times, at pH 7, and 45 times for pH 4.5 (Table 10). In the presence of CB[7] not only the experimental fluorescence quantum increase was verified, but also the fluorescence lifetime at pH 7. This is most likely due to the above discussed de-aggregation upon complexation. Furthermore, the absorption and fluorescence spectra maxima undergo some red- and blue shifts (more pronounced at pH 4.5), respectively. These changes (Table 10, Figures 24 and 25) are induced by the formation of the inclusion complex. The complexation causes a polarity effect (band shifts) and a confinement of the dye (verified by a decrease in nonradiative decay rate (k_{nr})). The most characteristic consequence of the low polarizability experienced by H33258 dye encapsulated inside the CB[7] is the "slower" emission, that translates in an increase in fluorescence lifetime (Table 10).

In order to complete the whole picture it is important to discuss the effect of the CB[7] on the radiative (k_r) and nonradiative (k_{nr}) decay rates of the H33258 dye, which can be directly obtained from the experimental fluorescence quantum yields and the fluorescence lifetimes, see Table 10. Upon complexation with CB[7], the k_r value increased (from 2.1×10^7 s^{-1} to 1.6×10^8 s^{-1}, and 7.2×10^7 s^{-1} to 1.5×10^8 s^{-1} at pH 7 and 4.5, respectively). However, for pH 7 a more important is the effect on the k_{nr}, which decreased strongly upon complexation (from 2.1×10^9 s^{-1} to 5.9×10^7 s^{-1}, and 1.8×10^8 s^{-1} to 5.5×10^7 s^{-1} at pH 7 and 4.5, respectively). The high value for non-radiative decay of free H33258 at pH 7 is most likely due to the aggregation at this pH.

Table 10 – Photophysical parameters of H33258 dye and H33258/CB[7] complex at pH 4.5 and 7.

	System	λ_{abs} (nm)	λ_{em} (nm)	Φ_f	τ_f (ns)	k_r (10^7 s^{-1}) [a]	k_{nr} (10^7 s^{-1}) [b]
pH 7	**H33258**	339	470	0.01	0.48	2.08	206.25
	Complex	349	471	0.74	4.47	16.44	5.93
pH 4.5	**H33258**	346	492	0.29	4.03	7.20	17.62
	Complex	351	486	0.74	4.78	15.38	5.54

[a] $k_r = \Phi_f / \tau_f$; [b] $k_{nr} = (1- \Phi_f)/ \tau_f$

V.3 – Supramolecular charactheristics of the H33258/CB[7] complex

The binding constant of H33258 dye with the CB[7] in water was estimated from the fluorescence and UV-Vis titration by assuming a 1:1 complexation stoichiometry and a substantial binding constant (K = 3.4-3.5 × 10^6 M^{-1}) was obtained, speaking qualitatively for a deep immersion of the dye into the macrocycle cavity. Similar strong binding (K = 10^4-10^6 M^{-1}) has been obtained for other structurally related guests with CB[*n*], e.g. thiabendazole with CB[7]: K = 1.8× 10^6 M^{-1} and a benzimidazole derivative with CB[7]: K = 1.3× 10^5 M^{-1}.[35,41]

The stoichiometry of H33258 dye bounded to CB[7] is 1:1, corresponding to Jobs plots with sharp maxima at 0.51 at pH 7 and 0.54 at pH 4.5. This result is further confirmed by mass spectrometry were the 1:1 complex was clearly identified (peaks at m/z = 813, 794, and 530, presented in Figure 36).

By ^{1}H- and 2D-COSY NMR investigations the binding mode between H33258 and CB[7] was assigned, as shown in Figure 59. This was possible because upon addition of CB[7] to H33258 dye, the aromatic protons which show upfield shifts (Figure 39) are the ones inside the CB[7] cavity. Furthermore, the complex shows fast exchange on the

NMR time-scale accompanied with an apparent symmetry distortion of the CB[7] methylene protons at *ca.* 5.5-5.6 ppm, which align the inside of the portals.[182]

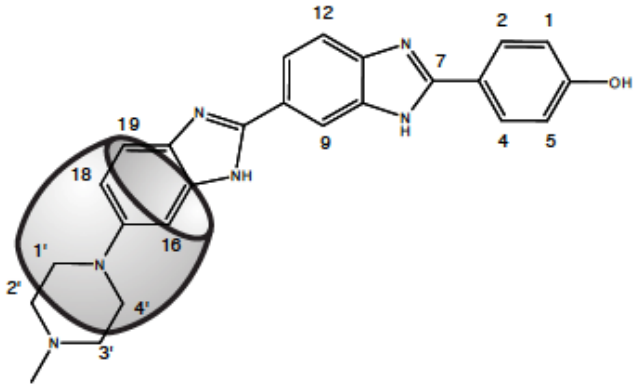

Figure 59 – Proposed structure of the complex H33258/CB[7].

V.4 – Competitive fluorescence titration

The binding constants of the different polyamine/CB[7] complexes are presented in Table 8, section IV.9. The complexation strength follows the sequence spermine > cadaverine > spermidine > putrescine > histamine.

Intuitively, CB[7] probably accommodates preferentially a spacer with five carbons between two amine groups. And indeed, cadverine binds stronger than putrescine (binding constants have a difference of two order of magnitude). However, spermine with shorter spacer units has even a slightly higher *K* than cadaverine. This may be because the former amine has the ability to interact with the CB[7] portals with two additional positive charges of the terminal amine units. Spermidine, on the other hand, can draw only on a total of three charges, and thus, its binding constant falls in between those of cadaverine and putrescine. Histamine has the lowest binding constant, due to its reduced flexibility as compared to the other amine which exclusively contain oligomethylene spacers.

The absolute values of the binding constants of the polyamines with CB[7] are comparable with those reported under comparable conditions by the Rekharsky and Nau

groups (Table 6, section I.3.2).[38,39,176,177] It should be noted that the values for spermine and spermidine are the first ones reported for CB[7] as host. The general trend described here for CB[7] applies also for CB[6].

The rather pronounced selectivity in the interaction of polyamines with CB[7] and the fluorescence quenching of the H33258/CB[7] assembly in the presence of these amines may lead to promising applications as fluorescent switching on-off sensor in aqueous solution under physiological conditions.

V.5 – CT-DNA assays

The binding affinity between H33258 and CB[7] in the chosen phosphate buffer (K = 3.7×10^6 M^{-1}) was very similar with the one obtained in water at pH 7.

The absorption and fluorescence titration spectra of H33258 with CT-DNA are very similar with the ones already described in the literature, for example by Latt *et al*.[99] Increments of CT-DNA added to a fixed amount of dye caused changes in both maxima and intensity of dye absorption and emission, being more pronounced for fluorescence. The fluorescence intensity change was biphasic, with some quenching at low DNA/dye ratios, followed by a gradual enhancement at higher ratios. This effect is accompanied by gradual red-shift of the absorption wavelength maximum from 338 nm to 363 nm. These shifts happen because the dye passes from a polar aqueous buffer environment to a non-polar DNA minor groove environment.[54,56,79,95] The significant increase of the fluorescence intensity upon supramolecular interaction between H33258 and CT-DNA at higher DNA/dye ratios is consistent with the determined fluorescence quantum yield of the minor groove bound dye (Φ_f = 62%).[56,79]

Similar effects are noted in absorption and fluorescence titration spectra of H33258/CB[7] complex with CT-DNA. However, the biphasic behavior (quenching for low DNA/dye ratios and enhancement for high DNA/dye ratios) is now even much more pronounced. As can be seen from Figure 50, the H332258/DNA assembly has a slightly lower fluorescence than the H33258/CB[7] complex, which is consistent with the determined fluorescence quantum yields (62% *versus* 74%, respectively).

Clearly, the results obtained from the CT-DNA titrations point to the existence of two modes of dye interaction, depending on the DNA/dye concentration ratio: a specific (minor groove) mode and an unspecific mode (e.g., by electrostatic interaction and loose binding), as described before in the literature.[53,57,76,79,95,99-101] It has been speculated that the unspecific binding will lead to lower fluorescence for presumably two reasons. First, the dye is not fully subjected to the confinement effect, as it is the case for minor groove binding. This enhances efficient deactivation by internal rotation. Second, there might be an energy transfer from the specific bound dye (always present also at low DNA/dye ratios) to the unspecific bound dye, leading to effective fluorescence quenching of the minor groove bound dye.

The idea is that at the lowest I_f point (*ca.* 1 μM of CT-DNA) unspecific binding is happening between H33258/CT-DNA (because there are an excess of H33258 molecules that binds in a specific and unspecific way) and that the continuous addition of CT-DNA promotes a translation to exclusively specific dye binding (*ca.* 7 μM of CT-DNA). The same is happening when for the H33258/CB[7] complex, but due to the competition between CB[7] and CT-DNA for the H33258 dye, the amount of required CT-DNA is *ca.* 9 time higher (*ca*. 7 *versus ca*. 60 μM).

Furthermore, CB[7] and amantadine titrations with mixtures of H33258/CB[7]/6.9 μM CT-DNA and H33258/CB[7]/59.3 μM CT-DNA were performed in order to confirm these hypotheses. Amantadine is a very strong competitor for the CB[7] macrocycle, leading to a shift of the equilibria towards the formation of the H33258/CT-DNA complex. The addition of amantadine to the complexes caused a lowering in the fluorescence intensity. This was predictable, because it is occupying the CB[7] cavity and the fluorescence will eventually be the one correspondent to H33257/CT-DNA. For the H33258/CB[7]/6.9 μM CT-DNA complex a more pronounced fluorescence decrease (note the slightly lower fluorescence of the dye in any binding situation as compared to CB[7]) at a comparably smaller amantadine concentration (Figure 54) than for the H33258/CB[7]/59.3 μM CT-DNA mixture (Figure 55) was noted. This provides some proof that at the lower CT-DNA concentration some dye is still complexed by CB[7].

Finally, circular dichroism (CD) spectra (Figure 56a) were undertaken to confirm the the existence of two binding modes of the H33258/CT-DNA complex. Only for the higher CT-DNA concentration, corresponding to specific binding a clear CD signal was

obtained. Most likely, the CT-DNA concentration for the unspecific binding situation was too low to allow the observation of an appreciable signal. Although the induced CD of the H33258 dye in complexes with DNA is well-reported in the literature,[90,99] herein the H33258/CT-DNA complex in presence of CB[7] is presented for the first time. The introduction of CB[7] to the H33258/DNA system gave similar results for nonspecific H33258 binding at low CT-DNA concentration and specific binding for high concentrations. Additionally, these observations are well-corroborated by the parallel effects in the UV-Vis absorption spectra (Figure 56b).

Finally, it should be mentioned that although the formation of ternary complexes involving CB[7] and DNA was reported occasionally,[32] our results seem to be much more in agreement with the well established-balance between specific and unspecific bind of H33258 by CT-DNA. It may be speculated that the inclusion of the dye in the protective surrounding of two supramolecular hosts (CB[7] and CT-DNA) at the same time would be certainly accompanied by fluorescence enhancement, as observed for other ternary complexes with CB[7].[183] We have no evidence for such scenario at low DNA/dye ratios.

VI – Conclusions and perspectives

It was discovered that the addition of CB[7] to H33258 dye leads to a formation of a strong 1:1 supramolecular complex with clear biomimetic features and an extraordinary fluorescence quantum yield. The modulation of the photophysical properties of the dye through the formation of the H33258/CB[7] complex makes this pair an interesting platform to evaluate the binding constants of other non-fluorescent compounds (such as polyamines) with the CB[7] macrocycle.

Furthermore, the underlying photophysical reasons for the observed modulation of the dye fluorescence under different pH conditions and in presence of CB[7] and CT-DNA as supramolecular hosts have been re-evaluated, leading to some considerable changes with respect to so far presented interpretations. This new view is a working hypothesis, which will need further theoretical and experimental confirmation in the future.

It was demonstrated that the beforehand in the literature discussed formation of a CT-DNA/H33258 dye complex with two different binding modes, a specific (high CT-DNA/H33258 ratio) and an unspecific (low CT-DNA/H33258 ratio) mode, applies also to the competitive binding of the dye by two hosts (CB[7] and CT-DNA).

Perspectives:

Based on the results of this work it is planned to proceed towards applications of the H33258/CB[7] platform for the development of:

- Assays for coupled enzymatic reactions; *spermidine synthase* and *spermine synthase* as consecutive reactions starting initially from putrescine
- Assays for enzymatic activity of diamine oxidases
- Artificial systems for supramolecular activation of DNA by competitive binding of H33258 by CB[7]

Furthermore, it is desirable to study the photophysical mechanisms, which lead to the efficient fluorescence quenching at pH 7, in more detail. This could be done by application of high-level quantum-chemical calculations.

VII – Bibliography

[1] R. Behrend, E. Meyer, F. Rusche, *.Liebigs Ann. Chem.* **1905**, *339*, 1.

[2] W. A. Freeman, W. L. Mock, N. Y. Shih, *J. Am. Chem. Soc.* **1981**, *103*, 7367.

[3] K. Kim, N. Selvapalam, Y. H. Ko, K. M. Park, D. Kim, J. Kim, *Chem. Soc. Rev.* **2007**, *36*, 267.

[4] K. Kim, N. Selvapalam, D. H. Oh, *J. Incl. Phenom. Macrocycl. Chem.* **2004**, *50*, 31.

[5] J. Lagona, P. Mukhopadhyay, S. Chakrabarti, L. Isaacs, *Angew. Chem. Int. Ed.* **2005**, *44*, 4844.

[6] J. W. Lee, S. Samal, N. Selvapalam, H. J. Kim, K. Kim, *Acc. Chem. Res.* **2003**, *36*, 621.

[7] S. Gadde, E. K. Batchelor, J. P. Weiss, Y. Ling, A. E. Kaifer, *J. Am. Chem. Soc.* **2008**, *130*, 17114.

[8] A. Day, A. P. Arnold, R. J. Blanch, B. Snushall, *J. Org. Chem.* **2001**, *66*, 8094.

[9] A. I. Day, R. J. Blanch, A. P. Arnold, S. Lorenzo, G. R. Lewis, I. Dance, *Angew. Chem. Int. Ed.* **2002**, *41*, 275.

[10] C. Marquez, F. Huang, W. M. Nau, *IEEE Trans. Nanobiosci.* **2004**, *3*, 39.

[11] W. S. Jeon, K. Moon, S. H. Park, H. Chun, Y. H. Ko, J. Y. Lee, E. S. Lee, S. Samal, N. Selvapalam, M. V. Rekharsky, V. Sindelar, D. Sobransingh, Y. Inoue, A. E. Kaifer, K. Kim, *J. Am. Chem. Soc.* **2005**, *127*, 12984.

[12] A. L. Koner, W. M. Nau, *Supramol. Chem.* **2007**, *19*, 55.

[13] C. Marquez, R. R. Hudgins, W. M. Nau, *J. Am. Chem. Soc.* **2004**, *126*, 5806.

[14] J. Kim, I. S. Jung, S. Y. Kim, E. Lee, J. K. Kang, S. Sakamoto, K. Yamaguchi, K. Kim, *J. Am. Chem. Soc.* **2000**, *122*, 540.

[15] P. Germain, J. M. Letoffe, M. P. Merlin, H.-J. Buschmann, *Thermochim. Acta* **1998**, *315*, 87

[16] K. Jansen, H. J. Buschmann, A. Wego, D. Dopp, C. Mayer, H. J. Drexler, H. J. Holdt, E. Schollmeyer, *J. Incl. Phenom. Macrocycl. Chem.* **2001**, *39*.

[17] W. L. Mock, N. Y. Shih, *J. Am. Chem. Soc.* **1989**, *111*, 2697.

[18] M. D. Pluth, K. N. Raymond, *Chem. Soc. Rev.* **2007**, *36*, 161.

[19] J. Szejtli, *Chem. Rev.* **1998**, *98*, 1743.

[20] S. M. Liu, C. Ruspic, P. Mukhopadhyay, S. Chakrabarti, P. Y. Zavalij, L. Isaacs, *J. Am. Chem. Soc.* **2005**, *127*, 15959.

[21] T. W. Mu, L. Liu, K. C. Zhang, Q. X. Guo, *Chin. Chem. Lett.* **2001**, *12*, 783

[22] S. Y. Kim, I. S. Jung, E. Lee, J. Kim, S. Sakamoto, K. Yamaguchi, K. Kim, *Angew. Chem. Int. Ed.* **2001**, *40*, 2119.

[23] Y. J. Jeon, P. K. Bharadwaj, S. Choi, J. W. Lee, K. Kim, *Angew. Chem. Int. Ed.* **2002**, *41*, 4474.

[24] S. Y. Jon, Y. H. Ko, S. H. Park, H. J. Kim, K. Kim, *Chem. Commun.* **2001**, 1938.

[25] I. Hwang, W. S. Jeon, H. J. Kim, D. Kim, H. Kim, N. Selvapalam, N. Fujita, S. Shinkai, K. Kim, *Angew. Chem. Int. Ed.* **2007**, *46*, 210.

[26] T. Robinson, G. McMullan, R. Marchant, P. Nigam, *Bioresour. Technol.* **2001**, *77*, 247.

[27] H. J. Buschmann, *Biologische Abwasserreinigung* **1997**, *9*, 101.

[28] A. Kornmuller, S. Karcher, M. Jekel, *Water Res.* **2001**, *35*, 3317.

[29] J. Mohanty, W. M. Nau, *Angew. Chem. Int. Ed.* **2005**, *44*, 3750.

[30] W. L. Mock, N. Y. Shih, *J. Org. Chem.* **1983**, *48*, 3618.

[31] H. C. Kolb, M. G. Finn, K. B. Sharpless, *Angew. Chem. Int. Ed.* **2001**, *40*, 2004.

[32] H. Isobe, N. Tomita, J. W. Lee, H. J. Kim, K. Kim, E. Nakamura, *Angew. Chem. Int. Ed.* **2000**, *39*, 4257.

[33] Y. B. Lim, T. Kim, J. W. Lee, S. M. Kim, H. J. Kim, K. Kim, J. S. Park, *Bioconjug. Chem.* **2002**, *13*, 1181.

[34] Y. J. Jeon, S. Y. Kim, Y. H. Ko, S. Sakamoto, K. Yamaguchi, K. Kim, *Org. Biomol. Chem.* **2005**, *3*, 2122.

[35] N. Saleh, A. L. Koner, W. M. Nau, *Angew. Chem. Int. Ed.* **2008**, *47*, 5398.

[36] K. Kim, *Chem. Soc. Rev.* **2002**, *31*, 96.

[37] D. M. Bailey, A. Hennig, V. D. Uzunova, W. M. Nau, *Chem. Eur. J.* **2008**, *14*, 6069.

[38] A. Praetorius, D. M. Bailey, T. Schwarzlose, W. M. Nau, *Org. Lett.* **2008**, *10*, 4089.

[39] A. Hennig, H. Bakirci, W. M. Nau, *Nat. Methods* **2007**, *4*, 629.

[40] U. Pischel, *Angew. Chem. Int. Ed.* **2007**, *46*, 4026.

[41] U. Pischel, V. D. Uzunova, P. Remon, W. M. Nau, *Chem. Commun.* **2010**, *46*, 2635.

[42] J. M. Lehn, *Proc. Ind. Acad. Sci. - Chem. Sci.* **1994**, *106*, 915.

[43] W. S. Jeon, A. Y. Ziganshina, J. W. Lee, Y. H. Ko, J. K. Kang, C. Lee, K. Kim, *Angew. Chem. Int. Ed.* **2003**, *42*, 4097.

[44] B. D. Wagner, S. J. Fitzpatrick, M. A. Gill, A. I. MacRae, N. Stojanovic, *Can. J. Chem.* **2001**, *79*, 1101.

[45] B. D. Wagner, N. Stojanovic, A. I. Day, R. J. Blanch, *J. Phys. Chem. B* **2003**, *107*, 10741.

[46] M. A. Rankin, B. D. Wagner, *Supramol. Chem.* **2004**, *16*, 513.

[47] C. Aleman, A. Adhikary, D. Zanuy, J. Casanovas, *J. Biomol. Struct. Dyn.* **2002**, *20*, 301.

[48] R. Kakkar, R. Garg, Suruchi, *J. Mol. Struct. - Theochem.* **2002**, *579*, 109.

[49] M. Ladinig, W. Leupin, M. Meuwly, M. Respondek, J. Wirz, V. Zoete, *Helv.Chim. Acta* **2005**, *88*, 53.

[50] D. J. Arndt-Jovin, T. M. Jovin, *Methods Cell Biol.* **1989**, *30*, 417.

[51] K. K. Kalninsh, D. V. Pestov, Y. K. Roshchina, *J. Photochem. Photobiol. A: Chem.* **1994**, *83*, 39.

[52] V. N. Umetskaya, J. M. Rosanov, *Biofizika* **1990**, *35*, 399.

[53] H. Görner, *Photochem. Photobiol.* **2001**, *73*, 339.

[54] G. Cosa, K. S. Focsaneanu, J. R. N. McLean, J. P. McNamee, J. C. Scaiano, *Photochem. Photobiol.* **2001**, *73*, 585.

[55] K. D. Harshman, P. B. Dervan, *Nucleic Acids Res.* **1985**, *13*, 4825.

[56] R. Jin, K. J. Breslauer, *Proc. Natl. Acad. Sci. USA* **1988**, *85*, 8939.

[57] F. G. Loontiens, P. Regenfuss, A. Zechel, L. Dumortier, R. M. Clegg, *Biochemistry* **1990**, *29*, 9029.

[58] H. Ojha, B. M. Murari, S. Anand, M. I. Hassan, F. Ahmad, N. K. Chaudhury, *Chem. Pharm. Bull.* **2009**, *57*, 481.

[59] Y. Guan, W. Zhou, X. H. Yao, M. P. Zhao, Y. Z. Li, *Anal. Chim. Acta* **2006**, *570*, 21.

[60] D. Banerjee, S. K. Pal, *Chem. Phys. Lett.* **2006**, *432*, 257.

[61] T. Araki, A. Yamamoto, M. Yamada, *Histochem.* **1987**, *87*, 331.

[62] Y. Bathini, K. E. Rao, R. G. Shea, J. W. Lown, *Chem. Res. Toxicol.* **1990**, *3*, 268.

[63] S. Y. Breusegem, R. M. Clegg, F. G. Loontiens, *J. Mol. Biol.* **2002**, *315*, 1049.

[64] S. Y. Breusegem, F. G. Loontiens, P. Regenfuss, R. M. Clegg, *Methods Enzymol.* **2001**, *340*, 212.

[65] M. A. Carrondo, M. Coll, J. Aymami, A. H. Wang, G. A. van der Marel, J. H. van Boom, A. Rich, *Biochemistry* **1989**, *28*, 7849.

[66] L. Denison, A. Haigh, G. D'Cunha, R. F. Martin, *Int. J. Radiat. Biol.* **1992**, *61*, 561.

[67] H. Loewe, J. Urbanietz, *Arzneimittelforschung* **1974**, *24*, 1927.

[68] F. G. Loontiens, L. W. Mclaughlin, S. Diekmann, R. M. Clegg, *Biochemistry* **1991**, *30*, 182.

[69] R. F. Martin, N. Holmes, *Nature* **1983**, *302*, 452.

[70] P. E. Pjura, K. Grzeskowiak, R. E. Dickerson, *J. Mol. Biol.* **1987**, *197*, 257.

[71] J. Portugal, M. J. Waring, *Biochim. Biophys. Acta* **1988**, *949*, 158.

[72] J. R. Quintana, A. A. Lipanov, R. E. Dickerson, *Biochemistry* **1991**, *30*, 10294.

[73] N. Spink, D. G. Brown, J. V. Skelly, S. Neidle, *Nucleic Acids Res.* **1994**, *22*, 1607.

[74] M. Sriram, G. A. van der Marel, H. L. Roelen, J. H. van Boom, A. H. Wang, *EMBO J.* **1992**, *11*, 225.

[75] K. Steinmetzer, K. E. Reinert, *J. Biomol. Struct. Dyn.* **1998**, *15*, 779.

[76] T. Stokke, H. B. Steen, *J. Histochem. Cytochem.* **1985**, *33*, 333.

[77] M. K. Teng, N. Usman, C. A. Frederick, A. H. Wang, *Nucleic Acids Res.* **1988**, *16*, 2671.

[78] M. C. Vega, I. G. Saez, J. Aymami, R. Eritja, G. A. Vandermarel, J. H. Vanboom, A. Rich, M. Coll, *Eur. J. Biochem.* **1994**, *222*, 721.

[79] A. Adhikary, V. Buschmann, C. Müller, M. Sauer, *Nucleic Acids Res.* **2003**, *31*, 2178.

[80] S. E. S. Ebrahimi, J. A. Parkinson, K. R. Fox, J. H. Mckie, J. Barber, K. T. Douglas, *Chem. Commun.* **1992**, 1398.

[81] K. J. Embrey, M. S. Searle, D. J. Craik, *Biochem. Int.* **1991**, *24*, 567.

[82] K. J. Embrey, M. S. Searle, D. J. Craik, *Eur. J. Biochem.* **1993**, *211*, 437.

[83] A. Fede, M. Billeter, W. Leupin, K. Wüthrich, *Structure* **1993**, *1*, 177.

[84] A. Fede, A. Labhardt, W. Bannwarth, W. Leupin, *Biochemistry* **1991**, *30*, 11377.

[85] J. A. Parkinson, J. Barber, B. A. Buckingham, K. T. Douglas, G. A. Morris, *Magn. Reson. Chem.* **1992**, *30*, 1064.

[86] J. A. Parkinson, J. Barber, K. T. Douglas, J. Rosamond, D. Sharples, *Biochemistry* **1990**, *29*, 10181.

[87] M. S. Searle, K. J. Embrey, *Nucleic Acids Res.* **1990**, *18*, 3753.

[88] E. Gavathiotis, G. J. Sharman, M. S. Searle, *Nucleic Acids Res.* **2000**, *28*, 728.

[89] W. Sufen, P. Tuzhi, C. F. Yang, *Electroanalysis* **2002**, *14*, 1648.

[90] C. Canzonetta, R. Caneva, M. Savino, A. Scipioni, B. Catalanotti, A. Galeone, *Biochim. Biophys. Acta* **2002**, *1576*, 136.

[91] L. D. Higgins, M. S. Searle, *Chem. Commun.* **1999**, 1861.

[92] B. Jerkovic, P. H. Bolton, *Biochemistry* **2000**, *39*, 12121.

[93] I. Haq, J. E. Ladbury, B. Z. Chowdhry, T. C. Jenkins, J. B. Chaires, *J. Mol. Biol.* **1997**, *271*, 244.

[94] C. E. Bostock-Smith, M. S. Searle, *Nucleic Acids Res.* **1999**, *27*, 1619.

[95] K. Utsuno, Y. Maeda, M. Tsuboi, *Chem. Pharm. Bull.* **1999**, *47*, 1363.

[96] Y. Kubota, S. Murashige, Y. Fujisaki, *Nucleic Acids Symp. Ser.* **1986**, 219.

[97] T. Hard, P. Fan, D. R. Kearns, *Photochem. Photobiol.* **1990**, *51*, 77.

[98] R. F. Steiner, H. Sternberg, *Arch. Biochem. Biophys.* **1979**, *197*, 580.

[99] S. A. Latt, G. Stetten, *J. Histochem. Cytochem.* **1976**, *24*, 24.

[100] S. A. Latt, J. C. Wohlleb, *Chromosoma* **1975**, *52*, 297.

[101] P. Colson, C. Houssier, C. Bailly, *J. Biomol. Struct. Dyn.* **1995**, *13*, 351.

[102] J. W. Ellwart, P. Dormer, *Cytometry* **1990**, *11*, 239.

[103] G. Lammler, H. Herzog, E. Saupe, H. R. Schutze, *Bull. World Health Organ.* **1971**, *44*, 751.

[104] D. A. Denham, R. R. Suswillo, R. Rogers, P. B. McGreevy, B. J. Andrews, *J. Helminthol.* **1976**, *50*, 243.

[105] W. Raether, G. Lammler, *Ann. Trop. Med. Parasitol.* **1971**, *65*, 107.

[106] C. Bailly, *Curr. Med. Chem.* **2000**, *7*, 39.

[107] K. J. Soderlind, B. Gorodetsky, A. K. Singh, N. R. Bachur, G. G. Miller, J. W. Lown, *Anticancer Drug Des.* **1999**, *14*, 19.

[108] M. M. McHugh, J. M. Woynarowski, R. D. Sigmund, T. A. Beerman, *Biochem. Pharmacol.* **1989**, *38*, 2323.

[109] J. M. Woynarowski, R. D. Sigmund, T. A. Beerman, *Biochemistry* **1989**, *28*, 3850.

[110] A. Y. Chen, C. Yu, B. Gatto, L. F. Liu, *Proc. Natl. Acad. Sci. USA* **1993**, *90*, 8131.

[111] A. Adhikary, E. Bothe, V. Jain, C. Von Sonntag, *Int. J. Radiat. Biol.* **2000**, *76*, 1157.

[112] N. K. Chaudhury, R. Bhardwaj, *Curr. Sci.* **2004**, *87*, 1256.

[113] R. Kakkar, R. Garg, Suruchi, *J. Mol. Struct. - Theochem.* **2004**, *668*, 243.

[114] H. Mohan, A. Adhikary, V. Jain, J. P. Mittal, *Proc. Ind. Acad. Sci. - Chem. Sci.* **2000**, *112*, 487.

[115] J. S. Adhikari, D. Khaitan, M. B. Arya, B. S. Dwarakanath, *J. Cancer Res. Ther.* **2005**, *1*, 151.

[116] P. J. Smith, C. O. Anderson, *Int. J. Radiat .Biol. Relat. Stud. Phys. Chem. Med.* **1984**, *46*, 331.

[117] S. D. Young, R. P. Hill, *Br. J. Cancer* **1989**, *60*, 715.

[118] R. Montanez, F. Sanchez-Jimenez, J. F. Aldana-Montes, M. A. Medina, *Amino Acids* **2007**, *33*, 283.

[119] S. S. Cohen, *Introduction to the polyamines*, Prentice-Hall, Englewood Cliffs, N.J.,, **1971**.

[120] E. Agostinelli, M. P. M. Marques, R. Calheiros, F. P. S. C. Gil, G. Tempera, N. Viceconte, V. Battaglia, S. Grancara, A. Toninello, *Amino Acids* **2010**, *38*, 393.

[121] C. Moinard, L. Cynober, J. P. de Bandt, *Clin. Nutr.* **2005**, *24*, 184.

[122] H. M. Wallace, *Biochem. Soc. Trans.* **2003**, *31*, 354.

[123] E. Larque, M. Sabater-Molina, S. Zamora, *Nutrition* **2007**, *23*, 87.

[124] N. Seiler, J. G. Delcros, J. P. Moulinoux, *Int. J. Biochem. Cell Biol.* **1996**, *28*, 843.

[125] T. B. Paiva, M. Tominaga, A. C. Paiva, *J. Med. Chem.* **1970**, *13*, 689.

[126] Q. Yuan, R. M. Ray, M. J. Viar, L. R. Johnson, *Am. J. Physiol. Gastrointest. Liver Physiol.* **2001**, *280*, G130.

[127] J. L. Bueb, A. Da Silva, M. Mousli, Y. Landry, *Biochem. J.* **1992**, *282 (Pt 2)*, 545.

[128] N. Shah, T. Thomas, A. Shirahata, L. H. Sigal, T. J. Thomas, *Biochemistry* **1999**, *38*, 14763.

[129] C. Stefanelli, F. Bonavita, I. Stanic, M. Mignani, A. Facchini, C. Pignatti, F. Flamigni, C. M. Caldarera, *FEBS Lett.* **1998**, *437*, 233.

[130] S. A. McCormack, M. J. Viar, L. R. Johnson, *Am. J. Physiol.* **1993**, *264*, G367.

[131] A. E. Pegg, P. P. McCann, *Am. J. Physiol.* **1982**, *243*, C212.

[132] P. Pohjanpelto, E. Holtta, O. A. Janne, *Mol. Cell Biol.* **1985**, *5*, 1385.

[133] C. W. Tabor, H. Tabor, *Annu. Rev. Biochem.* **1984**, *53*, 749.

[134] V. Gentile, V. Thomazy, M. Piacentini, L. Fesus, P. J. Davies, *J. Cell Biol.* **1992**, *119*, 463.

[135] M. F. Santos, M. J. Viar, S. A. McCormack, L. R. Johnson, *Am. J. Physiol.* **1997**, *273*, G175.

[136] G. D. Lux, L. J. Marton, S. B. Baylin, *Science* **1980**, *210*, 195.

[137] S. A. McCormack, M. J. Viar, L. R. Johnson, *Am. J. Physiol.* **1992**, *263*, G426.

[138] C. S. Melendrez, J. L. Ruttle, D. M. Hallford, P. S. Chaudhry, E. R. Casillas, *J. Androl.* **1992**, *13*, 293.

[139] R. M. Ray, B. J. Zimmerman, S. A. McCormack, T. B. Patel, L. R. Johnson, *Am. J. Physiol.* **1999**, *276*, C684.

[140] H. Ruan, J. R. Hill, S. Fatemie-Nainie, D. R. Morris, *J. Biol. Chem.* **1994**, *269*, 17905.

[141] M. Schindler, D. E. Koppel, M. P. Sheetz, *Proc. Natl. Acad. Sci. USA* **1980**, *77*, 1457.

[142] F. Schuber, *Biochem. J.* **1989**, *260*, 1.

[143] D. Balasundaram, A. K. Tyagi, *Mol. Cell Biochem.* **1991**, *100*, 129.

[144] H. R. Matthews, *Bioessays* **1993**, *15*, 561.

[145] J. E. Morgan, J. W. Blankenship, H. R. Matthews, *Biochemistry* **1987**, *26*, 3643.

[146] S. A. McCormack, R. M. Ray, P. M. Blanner, L. R. Johnson, *Am. J. Physiol.* **1999**, *276*, C459.

[147] S. Wallis, S. Lloyd, I. Wise, G. Ireland, T. P. Fleming, D. Garrod, *Mol. Biol. Cell* **2000**, *11*, 1077.

[148] J. Y. Wang, J. Wang, V. A. Golovina, L. Li, O. Platoshyn, J. X. Yuan, *Am. J. Physiol. Cell. Physiol.* **2000**, *278*, C303.

[149] K. Williams, *Biochem. J.* **1997**, *325 (Pt 2)*, 289.

[150] A. C. Childs, D. J. Mehta, E. W. Gerner, *Cell Mol. Life Sci.* **2003**, *60*, 1394.

[151] V. G. Brunton, M. H. Grant, H. M. Wallace, *Biochem. Pharmacol.* **1990**, *40*, 1893.

[152] D. M. Morgan, *Biochem. Soc. Trans.* **1990**, *18*, 1080.

[153] A. T. Maurelli, R. E. Fernandez, C. A. Bloch, C. K. Rode, A. Fasano, *Proc. Natl. Acad. Sci. USA* **1998**, *95*, 3943.

[154] A. D. Sunil, R. Silverstein, C. R. Amura, T. Kielian, D. C. Morrison, *Antimicrob. Agents Chemother.* **1999**, *43*.

[155] G. G. Krueger, P. R. Bergstresser, N. J. Lowe, J. J. Voorhees, G. D. Weinstein, *J. Am. Acad. Dermatol.* **1984**, *11*, 937.

[156] N. Martinet, S. Beninati, T. P. Nigra, J. E. Folk, *Biochem. J.* **1990**, *271*, 305.

[157] H. Desser, P. Hocker, M. Weiser, J. Bohnel, *Clin. Chim. Acta* **1975**, *63*, 243.

[158] W. H. Brooks, *Med. Hypotheses* **1994**, *43*, 403.

[159] U. B. Gunnia, P. S. Amenta, J. R. Seibold, T. J. Thomas, *Kidney Int. Suppl.* **1991**, *39*, 882.

[160] H. C. Hsu, T. Thomas, J. R. Seibold, T. J. Thomas, *Agents Actions* **1993**, *39 Spec No*, C204.

[161] H. C. Hsu, T. Thomas, L. H. Sigal, T. J. Thomas, *Autoimmunity* **1999**, *29*, 299.

[162] T. J. Thomas, U. B. Gunnia, J. R. Seibold, T. Thomas, *Biochem. J.* **1995**, *311 (Pt 1)*, 175.

[163] F. Galli, S. Beninati, S. Benedetti, A. Lentini, F. Canestrari, A. Tabilio, U. Buoncristiani, *Kidney Int. Suppl.* **2001**, *78*, S73.

[164] G. Stabellini, G. Mariani, F. Pezzetti, C. Calastrini, *Exp. Mol. Pathol.* **1997**, *64*, 147.

[165] M. E. Swendseid, M. Panaqua, J. D. Kopple, *Life Sci.* **1980**, *26*, 533.

[166] L. Cecco, S. Antoniello, M. Auletta, M. Cerra, P. Bonelli, *Int. J. Biol. Markers* **1992**, *7*, 52.

[167] H. Sugimoto, S. Sakurai, T. Abe, H. Takagi, H. Takahashi, J. Takezawa, T. Nagamine, S. Matsuzaki, *J. Gastroenterol.* **1994**, *29*, 159.

[168] D. W. Lundgren, P. M. Farrell, P. A. Di Sant'Agnese, *Clin. Chim. Acta* **1975**, *62*, 357.

[169] D. H. Russell, M. G. Rosenblum, R. C. Beckerman, B. G. Durie, L. M. Taussig, D. R. Barnett, *Pediatr. Res.* **1979**, *13*, 1137.

[170] L. Alhonen, J. J. Parkkinen, T. Keinanen, R. Sinervirta, K. H. Herzig, J. Janne, *Proc. Natl. Acad. Sci. USA* **2000**, *97*, 8290.

[171] D. H. Russell, L. Z. Stern, *Neurology* **1981**, *31*, 80.

[172] L. D. Morrison, S. J. Kish, *Neurosci. Lett.* **1995**, *197*, 5.

[173] V. S. Sauro, H. J. Klamut, W. F. Dick, D. N. Oey, K. P. Strickland, *Biochem. Cell Biol.* **1990**, *68*, 1402.

[174] D. H. Russell, *Clin. Chem.* **1977**, *23*, 22.

[175] H. Isobe, S. Sato, J. W. Lee, H. J. Kim, K. Kim, E. Nakamura, *Chem. Commun.* **2005**, 1549.

[176] M. V. Rekharsky, Y. H. Ko, N. Selvapalam, K. Kim, Y. Inoue, *Supramol. Chem.* **2007**, *19*, 39.

[177] W. M. Nau, G. Ghale, A. Hennig, H. Bakirci, D. M. Bailey, *J. Am. Chem. Soc.* **2009**, *131*, 11558.

[178] S. R. Gallagher, in *In Current Protocols in Molecular Biology* (Eds.: F. M. Ausubel, R. Brent, R. E. Kingston, D. D. Moore, J. G. Seidman, J. A. Smith, K. Struhl), Greene and Wiley-Interscience, New York, **1994**.

[179] P. Job, *Ann. Chim. (Paris)* **1928**, 113.

[180] B. Valeur, *Molecular fluorescence : principles and applications*, Wiley-VCH, Weinheim ; New York, **2002**.

[181] J. A. Parkinson, J. Barber, B. A. Buckingham, K. T. Douglas, G. A. Morris, *Magn. Reson. Chem.* **2005**, *30*, 1064

[182] H. J. Buschmann, A. Wego, A. Zielesny, E. Schollmeyer, *J. Incl. Phenom. Macrocycl. Chem.* **2006**, 85.

[183] A. C. Bhasikuttan, J. Mohanty, W. M. Nau, H. Pal, *Angew. Chem. Int. Ed.* **2007**, *46*, 4120.

VIII – Annex

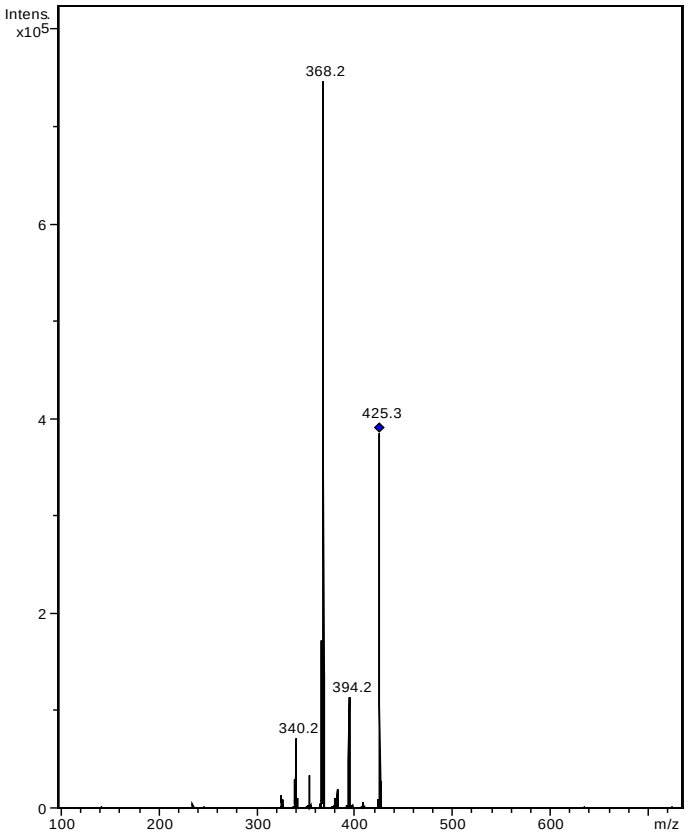

Figure 60 – MS^2 of the H33258 dye peak (m/z = 425).

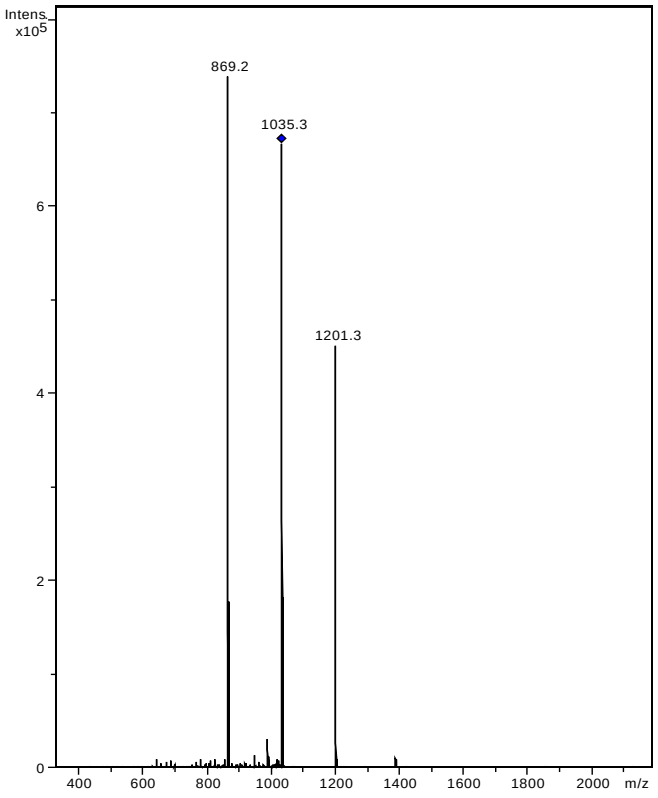

Figure 61 – MS^2 of the peak m/z = 1035.

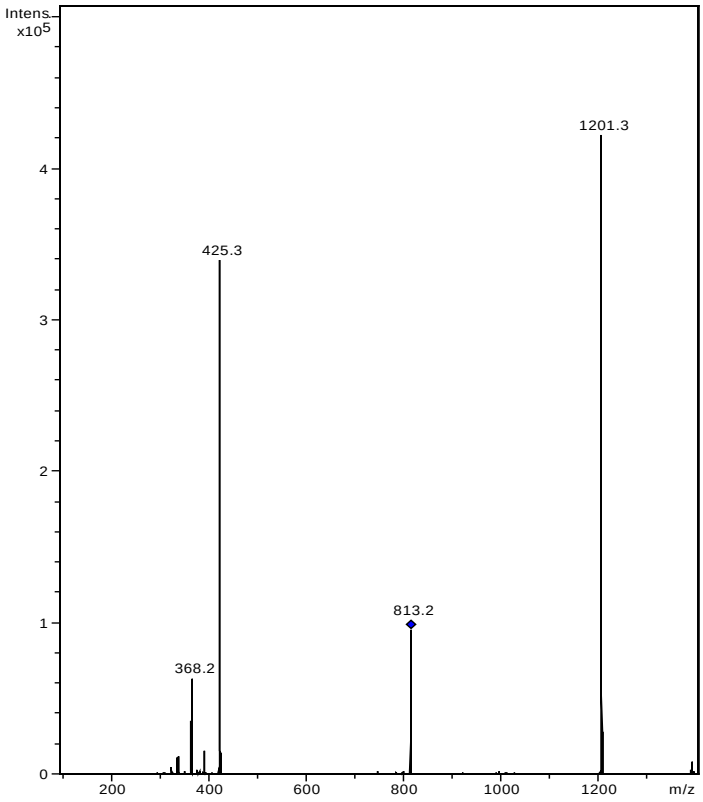

Figure 62 – MS^2 of the peak m/z = 813.